Technical University of Munich

Biotechnology of Natural Products

Functional and Comparative Analysis of Small Molecule Glycosyltransferases from Plants by High-Throughput Assays

Kate McGraphery

Vollständiger Abdruck der von der TUM School of Life Sciences der Technischen Universität München zur Erlangung des akademischen Grades eines

Doktors der Naturwissenschaften (Dr. rer. nat.)

genehmigten Dissertation.

Vorsitzender:	Prof. Dr. Wolfgang Liebl
Prüfer der Dissertation:	1. Prof. Dr. Wilfried Schwab
	2. Prof. Dr. Corinna Dawid

Die Dissertation wurde am 03.02.2021 bei der Technischen Universität München eingereicht und durch die TUM School of Life Sciences am 11.05.2021 angenommen.

This dissertation is dedicated to my sons – Nicholas and Anthony.

Having you during my doctoral was the best thing that could have happened to me. The both of you have given my life a new meaning and a new dimension. Thank you for filling my life with more love, depth, and pure bliss. Life is a wonderful journey – and yours is only beginning – I will always be by your side guiding you along your path supporting you unconditionally.

Acknowledgements

"Your PhD is the best time of your life" said to me Prof. Dr. Wilfried Schwab on the first day of my doctorate. This has stuck by me throughout my whole doctoral journey. Not only because it really was the best 5 years of my life – but because Willi made sure it was. Therefore, I would like to explicitly thank and portray my ultimate gratitude to Willi for the guidance, constant support, unconditional positivity, and supreme understanding throughout this journey.

Thank you for facilitating an environment where my scientific thought process and ultimately my understanding would only prosper. The patience that you have for your students and those around you is yet to be learned by many. The freedom you enable for brainstorming whilst motivating and encouraging to overcome research obstacles, as well as your perpetual optimism and support has truly contributed to the success of my PhD. The environment you fostered for me during these 5 years has changed the person I am today – both professionally and personally.

I often thought "how did I get so lucky?" – not only with Willi but to also be surrounded by such amazing colleagues whom I can easily refer to as friends. My deepest gratitude to Elisabeth Kurze, Katja Haertl, Guangxin Sun, Annika Haugeneder, Emilia Romer, Soraya Chebib, Johanna Trinkl, Julian Ruediger, and Martina Kolarek for all the laughs and great times we spent together. Not to mention all the wise advice and help you have provided me to bring my project to its completion. Further appreciation to Jieren Liao, Nicolas Figueroa, and Shuai Zhao for the daily chit-chat and pleasant working environment. Moreover, thank you to Ruth Habegger, Anja Forstner, Mechthild Mayershofer, and Hannelore Meckl for the help and support regarding lab safety and general laboratory techniques. Heartfelt thanks to Thomas Hoffmann and Rafal Jonczyk for the LC-MS mentoring and advising - not a single measurement would be the same without you. Profound gratitude to Heike

Adamski for all the administrative and bureaucratic assistance - whether work-related or 'Elternzeit' related – you were always there to answer any of my questions and to translate complicated German documents.

Warmest and deepest gratitude to everyone at the BiNA team whom supported me throughout this incredible doctoral and motherhood journey. There are not enough words to express the profound thankfulness I feel – Vielen Dank!

Warmest gratitude and indescribable appreciation to my best friend and husband – Peter Egorov. The one who has been with me through every single milestone in the last 13 years of my life. Not only was he there for me physically and emotionally – but the unconditional love, deep understanding, true friendship, and eternal positivity he has instilled on me has led me through my doctoral with more success than ever imaginable. I feel lucky and proud to have shared my educational journey with you by my side – high school, Bachelor, Master and now PhD. All the laughs we have shared, the countries we have visited, the successes we have achieved, the family we have built – I would do it all again and would not change a thing. I am excited for the next chapter of my life and the journey I am about to embark upon with you right by my side. I love you and appreciate you more than words can ever describe.

Deepest gratitude to all my family and friends in Canada and other parts of the world.

My dearest parents and beautiful sisters who have raised me and taught me to follow my dreams and never give up. Ever since I was a young girl, I was brought up with confidence and protected from harm. I have always looked up to my sisters - the wise and honest advice in all aspects of my life has guided me in the right direction. The love and support I was encompassed with in my childhood and adolescence has shaped the adult I am today and I am forever grateful. The comfort and love I have from my family, motivates me every day to do better and be the best version of myself. Not a day goes by that I do not think of you – even though we are now miles away – I love you with all that I have.

My sweetest friends who are still waiting for me to move back to Canada – I could have never done any of this without you. In particular, Katarina Stevanovic, Monica Monchis, and Anna Pelleboer – I am sorry to say this but our all-nighters studying for exams are officially over! Katarina and I moved to Germany together to start our Masters – it was a dream come true. Our endless conversations, visits, and sweet memories have made this journey that much better and bearable. Big thanks to all of my friends and classmates for the constant support – I miss you all so much.

Thank you to Deutsche Forschungsgemeinschaft (DFG) for the funding of this project. I am honored to have completed my Doctoral studies at Technical University of Munich (TUM) – all the facilities and student matters were always dealt with ease, understanding, and great efficiency. I am proud to officially be a TUM alumnus – thank you for facilitating this beautiful journey of mine. Last but not least, deepest gratitude to Prof. Dr. Corinna Dawid and Prof. Dr. Wolfgang Liebl for taking the time and your effort in facilitating and conducting my final examination.

Table of Contents

Abstract

Enzymes are a vital part in all biological systems as they catalyze the majority of chemical reactions that occur in nature. Glycosyltransferases (GTs) specifically have the ability to modify volatility, solubility, and hydrophobicity of small molecules through an enzymatic reaction – glycosylation. Over the years, this has attracted immense attention in pharmaceutical, nutraceutical, and cosmeceutical industries. However, the lack of known GTs and the scarcity of high-throughput (HTP) methods of quantification hinders the further discovery of novel applications in various fields of research. Moreover, due to GTs natural promiscuity some plant secondary metabolites have the potential to act as allosteric activators or inhibitors in competitive or non-competitive fashion. The ability to be able to drive desired glycosylation of plant secondary metabolites or hinder others can reveal and be applied to various novel applications.

In this doctoral thesis, new commercially available HTP methods are compared and tailored to suit family-1 plant GTs. The aim was to provide a fast, non-hazardous, robust, costs-effective, and reproducible assay for uridine diphosphate (UDP)-glucose dependent plant GTs. A pH-sensitive assay, UDP-Glo™ GT assay, phosphate GT activity assay, and UDP^2 TR-FRET assay were compared and tailored to suit family-1 plant GTs. *Vitis vinifera* (UGT72B27) GT was subjected to glycosylation reactions with a range of various phenolic plant secondary metabolites. Each method was carefully adapted to function with the characteristics of the family-1 GT taking into consideration their metal-independent catalytic active site. Substrate screening and kinetic parameters (K_M, V_{max}, and k_{cat}) were evaluated and compared via the four methods. Upon comparison, the pH-sensitive assay and the UDP^2 TR-FRET assay yielded incomparable results and were deemed unsuitable for HTP family-1 plant GT kinetic quantification. Although the pH-sensitive assay could be utilized to perform an initial screen in a quick manner, the results should be confirmed with an alternate

method to ensure feasibility. The UDP[2] TR-FRET assay is incompatible and was eliminated from any further evaluation and experimentation with family-1 plant GTs. Furthermore, the UDP-Glo™ GT assay and phosphate GT activity assay yielded closely similar and reproducible kinetic parameters. Therefore, with the easy experimental set-up and rapid readout rate the two assays are suitable for HTP screening and quantitative kinetic analysis of family-1 plant GTs. These findings shed a light on new and emerging HTP assays, which will allow for fast, robust, and non-hazardous analysis and discovery of new GTs with the great potential to uncover further applications.

The tailored UDP-Glo™ GT assay was utilized in enhancement and inhibition of UDP-glucose hydrolase and glycosylation reactions of family-1 plant GTs. The amount of UDP detected by this assay is directly proportional to the amount of glycoside formed and the amount of UDP-glucose consumed. Utilizing the tailored UDP-Glo™ GT assay resulted in the discovery of inherent UDP-glucose hydrolase activity of some family-1 GTs. Several family-1 GTs were selected and subjected to hydrolase activity experimentation as well as, directing this hydrolase activity towards enhancement or inhibition. UGT72B46 from *Malus x domestica*, UGT72B50, and UGT72B51, both from *Pyrus communis* showed pronounced hydrolase activity when only the donor substrate (UDP-glucose) was present. UGT72AY1 from *Nicotiana benthamiana* also showed a hydrolase activity, which was inhibited upon the addition of apocarotenoid substrates – retinol and β-carotene. These two substrates are not glycosylated by UGT72AY1 but have the ability to allosterically inhibit the GTs inherent hydrolase activity. These findings further set the stage to quantitatively analyze the enhancement and/or inhibition of scopoletin glycosylation of UGT72AY1 via Liquid Chromatography Mass Spectrometry (LC-MS). It was successfully determined that (apo)carotenoids – β-carotene, retinol, and apocarotenal – are able to enhance and drive glucoside formation. Therefore, this demonstrates the novel

physiological function of (apo)carotenoids and their ability to act as allosteric activators of family-1 plant GTs.

The findings accrued in this doctoral research unravel new and robust HTP methods, which could be applied towards a vast range of family-1 plant GTs. Not only to be able to discover new potential plant secondary metabolites or novel GTs, but to manipulate known GTs and uncover their full potential and vast range of acceptor substrates. Moreover, to be able to direct glycosylation and other side-activities towards activation or inhibition. These novel properties will allow to improve known processes and elucidate further applications in agricultural, pharmaceutical, cosmeceutical, and nutraceutical industries.

Zusammenfassung

Enzyme sind ein lebenswichtiger Bestandteil aller biologischen Systemen, da sie die Mehrzahl der in der Natur vorkommenden chemischen Reaktionen katalysieren. Glykosyltransferasen (GTs) haben insbesondere die Fähigkeit, die Flüchtigkeit, Löslichkeit und Hydrophobie kleiner Moleküle durch eine enzymatische Reaktion - die Glykosylierung - zu modifizieren. Im Laufe der Jahre hat dies in der pharmazeutischen, kosmetischen und Lebensmittelindustrie immense Aufmerksamkeit erregt. Die geringe Anzahl von charakterisierten GTs und die Knappheit von Hochdurchsatz-(HTP)-Quantifizierungsmethoden behindern jedoch die weitere Entdeckung neuer Anwendungen in verschiedenen Forschungsbereichen. Darüber hinaus haben einige pflanzliche Sekundärmetabolite aufgrund der natürlichen Promiskuität der GTs das Potenzial, als allosterische Aktivatoren oder Inhibitoren in kompetitiver oder nicht kompetitiver Weise zu wirken. Die Fähigkeit, die erwünschte Glykosylierung pflanzlicher Sekundärmetabolite zu verstärken oder anderer Sekundärmetabolite zu hemmen, kann verschiedene neue Anwendungen aufdecken und auf diese angewendet werden.

In dieser Doktorarbeit wurden neue kommerziell verfügbare HTP-Methoden verglichen und auf pflanzliches GTs der Familie 1 zugeschnitten. Ziel war es, einen schnellen, ungefährlichen, robusten, kostengünstigen und reproduzierbaren Test für Uridindiphosphat (UDP)-Glucose abhängige Pflanzen-GTs bereitzustellen. Ein pH-sensitiver Assay, ein UDP-Glo™-GT-Assay, ein Phosphat-GT-Aktivitäts-Assay und ein UDP² TR-FRET-Assay wurden verglichen und auf Pflanzen-GTs der Familie 1 angepasst. *Vitis vinifera* (UGT72B27) GT wurde für Glykosylierungsreaktionen mit einer Reihe verschiedener phenolischer pflanzlicher Sekundärmetaboliten verwendet. Jede Methode wurde sorgfältig angepasst, um mit den Enzymen der Familie-1-GTs, unter Berücksichtigung ihres metallunabhängigen katalytisch aktiven Zentrums, zu funktionieren. Substratscreening und kinetische Parameter (K_M, V_{max} und k_{cat}) wurden

mit den vier Methoden durchgeführt, ausgewertet und verglichen. Der pH-sensitive Assay und der UDP² TR-FRET-Assay ergaben im Vergleich widersprüchliche Ergebnisse und wurden als ungeeignet für die Quantifizierung der kinetischen Parameter mittels HTP von pflanzlichen GTs der Familie 1 erachtet. Obwohl der pH-empfindliche Assay zur schnellen Durchführung eines ersten Screenings verwendet werden konnte, sollten die Ergebnisse mit einer alternativen Methode bestätigt werden, um die Ergebnisse zu validieren. Der UDP² TR-FRET-Assay ist inkompatibel und wurde von jeder weiteren Evaluierung und jedem weiteren Experiment mit pflanzlichen GTs der Familie-1 ausgeschlossen. Darüber hinaus lieferten der UDP-Glo™ GT-Assay und der Phosphat GT-Aktivitäts-Assay sehr ähnliche und reproduzierbare kinetische Parameter. Mit dem einfachen Versuchsaufbau und der schnellen Leserate eignen sich die beiden Assays daher für das HTP-Screening und die quantitative kinetische Analyse von pflanzlichen GTs der Familie 1. Diese Ergebnisse verdeutlichen, dass beide HTP-Assays, eine schnelle, robuste und ungefährliche Analyse von pflanzlichen GTs ermöglichen sowie zur Entdeckung neuer GTs mit dem Potenzial zur Auffindung weiterer Anwendungen verwendet werden können.

Der angepasste UDP-Glo™ GT-Assay wurde zur Verbesserung und Hemmung der UDP-Glucose-Hydrolase und der Glykosylierungsreaktionen von pflanzlichen GTs der Familie 1 eingesetzt. Die Menge an UDP, die mit diesem Assay nachgewiesen wurde, ist direkt proportional zur Menge des gebildeten Glykosids und der Menge des verbrauchten UDP-glucose. Die Verwendung des maßgeschneiderten UDP-Glo™ GT-Tests führte zur Entdeckung der manchen GTs innewohnenden UDP-Glukosehydrolase-Aktivität. Mehrere GTs der Familie-1 wurden ausgewählt und einem Experiment zur Hydrolase-Aktivität unterzogen, wobei diese Hydrolase-aktivität modifiziert wurde. UGT72B46 aus *Malus x domestica*, UGT72B50 und UGT72B51, beide aus *Pyrus communis*, zeigten eine ausgeprägte Hydrolase-Aktivität, wenn nur das Spendersubstrat (UDP-Glucose) vorhanden war. UGT72AY1 aus

Nicotiana benthamiana zeigte ebenfalls eine Hydrolase-Aktivität, die durch die Zugabe von (Apo)carotinoiden - Retinol und β-Carotin - gehemmt wurde. Diese beiden Substrate werden von UGT72AY1 nicht glykosyliert, haben jedoch die Fähigkeit, die einigen GTs innewohnenden Hydrolaseaktivität allosterisch zu hemmen. Diese Ergebnisse führten dazu die Scopoletin-Glykosylierung von UGT72AY1 in Gegenwart der (Apo)carotinoiden durchzuführen. Es wurde mittels Flüssig-Chromatographie Massen-Spektrometrie (LC-MS) erfolgreich nachgewiesen, dass die (Apo)Carotinoide - β-Carotin, Retinol und Apocarotenal - in der Lage sind, die Bildung von Glukosiden zu steigern. Dies zeigt erstmals die Fähigkeit von (Apo)Carotinoiden als allosterische Aktivatoren pflanzlicher GTs der Familie 1 zu wirken.

Die im Rahmen dieser Doktorarbeit gewonnenen Erkenntnisse zeigen neue und robuste HTP-Methoden auf, die auf eine breite Palette von GTs der Familie-1-Pflanze angewendet werden können. Nicht nur, um neue potentielle sekundäre Pflanzenmetaboliten oder neuartige GTs zu entdecken, sondern auch, um bekannte GTs zu manipulieren und ihr volles Potential und eine breite Palette von Akzeptorsubstraten aufzudecken. Darüber hinaus kann die Glykosylierung und andere Nebenaktivitäten in Richtung Aktivierung oder Hemmung gelenkt werden. Diese neuartigen Eigenschaften werden es ermöglichen, bekannte Prozesse zu verbessern und weitere Anwendungen in der landwirtschaftlichen, pharmazeutischen, kosmetischen und Lebensmittelindustrie aufzuklären.

List of Figures

List of Tables

Acronyms

ABA	Abscisic acid
APS	Ammonium persulfate
ATP	Adenosine triphosphate
CAZy	Carbohydrate-Active EnZymes
DMSO	Dimethyl sulfoxide
E	Enzyme
E. coli	*Escherichia coli*
EDTA	Ethylenediamine tetraacetic acid
e.g.	exempli gratia, for example
ES	Enzyme-Substrate Complex
FMT	Furanmethanethiol
*Fv*GT	*Fragaria vesca* Glycosyltransferase
GDP	Guanosine-diphosphate
GTs	Glycosyltransferases
HCl	Hydrochloric acid
HPLC	High Performance Liquid Chromatography
IPTG	Isopropyl β-D-1-thiogalactopyranoside
k_{cat}	Turnover number
kDa	Kilodalton
K_M	Michaelis constant
LB	Luria-Bertani
LC-MS	Liquid Chromatography Mass Spectrometry
mQ	milli-Q, ultrapure, deionized water
μM	Micromolar
MS	Mass spectrometry
MW	Molecular weight

m/*z*	Mass-to-charge ratio
NaCl	Sodium Chloride
NCBI	National Center for Biotechnology Information
NDP	Nucleoside-diphosphate
NtGT	*Nicotiana tabacum* Glycosyltransferase
OD	Optical density
P	Product
PAGE	Polyacrylamide Gel Electrophoresis
PBS	Phosphate Buffered Saline
pH	Potentia hydrogenii
PMSF	Phenylmethylsulfonyl fluoride
PO_4	Phosphate
PSPG	Putative Secondary Plant Glycosyltransferase
RLU	Relative Luminescence Unit
rpm	Round per Minute
RT	Room Temperature
S	Substrate
SDS	Sodium dodecyl sulfate
SDS-PAGE	Sodium dodecyl sulfate – Polyacrylamide Gel Electrophoresis
SLs	Strigolactones
TBS	Tris Buffered Saline
TEMED	Tetraacetylethylenediamine
TRIS	Tris (hydroxymethyl) aminomethane
UDP	Uridine 5-diphosphate
UDP-G	Uridine 5′-diphosphoglucose disodium salt
UDP^2 TR-FRET	Transcreener UDP^2 Time Resolved
UDR	UDP Detection Reagent

UGTs	UDP-dependent Glycosyltransferases
UMP	Uridine-monophosphate
UV	Ultraviolet
V_{max}	Maximum reaction rate
*Vv*GT	*Vitis vinifera* Glycosyltransferase

I. Introduction

The formation of plant life on the planet is one of the most significant evolutionary events that have occurred in Earth's history [1]. Plants produce innumerable structurally and functionally diverse metabolites, which play various significant roles in a plants life cycle as well as responding to biotic and abiotic stresses [2]. Plants must continuously adjust their growth, physiology, and development to assure their survival under changing environmental conditions [3]. Therefore, the many complex and natural plant processes induced by internal and external signals are regulated through many different signaling pathways conformed of complex network of interacting molecules and enzymes that enable cells to sense, integrate and respond [4]. This metabolic diversity is resultant from chemical modifications upon the basic skeletal structure of metabolites [2]. The abundance and further study of plants and plant-derived natural products have been an important source of agriculture, food additives, pharmaceuticals, nutraceuticals, pesticides, pigments, fragrances, cosmeceuticals, and medicinal and agricultural raw materials [5].

1.1 Primary and secondary metabolites

Throughout centuries, both primary and secondary plant metabolites have proven to hold a distinct and vital role in human life. Primary metabolites are responsible for crucial growth, physiological development, and reproduction. On the other hand, secondary plant metabolites are not vital for growth or other indispensable processes. However, they are essential in maintaining the plants survival by responding to internal and external signals such as, hormone restoration, effects of drought, defense against infections, offensive chemicals against microorganisms and insects, attracting pollinators, and responding and adapting to environmental stresses [5]. In particular, the production of secondary plant

metabolites is a vital function of plant metabolism [**Figure 1**]. These metabolites are classified under various classes depending on their chemical structures such as phenolics, alkaloids, terpenes, lipid-derived, and carbohydrate-related compounds. The Shikimic acid pathway results in the production of phenolics which impart defense ability to plants [6]. The Nitrogen-containing alkaloids are synthesized from amino acids [7]. Terpenes are synthesized via the Mevalonic acid and Methyl-erythritol-phosphate (MEP; Non-mevalonate) pathway. Small-molecule terpenes often have a strong odor responsible for protecting the plant from predators [8]. Maltol and ethylmaltol, which are derived from carbohydrates and the phenolic vanillin are flavor compounds which are frequently utilized in the food industry as flavor enhancing supplements for increased aroma [9]. The phenolic anthocyanins are plant pigments, and flavonoids such as catechin are involved in plant defense. They are present in almost all plants. Furthermore, β-carotene belongs to the terpenoid class of secondary metabolism and has antioxidative properties. Carotenoids and apocarotenoids are an important source of secondary metabolites, including phytohormones abscisic acid (ABA) and strigolactones (SLs) which play an essential role in adapting plant architecture to nutrition availability and responding to abiotic stress [10, 11]. Apocarotenoids (ABA and SLs) are oxidative degradation products of the carotenoids and originate from the oxidative breakdown of double bonds in the carotenoid polyene, a common metabolic process [11]. Apocarotenoids fulfill many important biological functions both naturally and via enzymatic modifications [12]. Overall, plant secondary metabolites encompass a vast economical value in specialty chemicals such as drugs, flavors, fragrances, insecticides and dyes [13]. The diversity of the plant secondary metabolites arises vastly from various modifications of a basic skeleton by glycosylation, acylation, methylation, hydroxylation, and prenylation having substantial influence on the molecular structure and function [2].

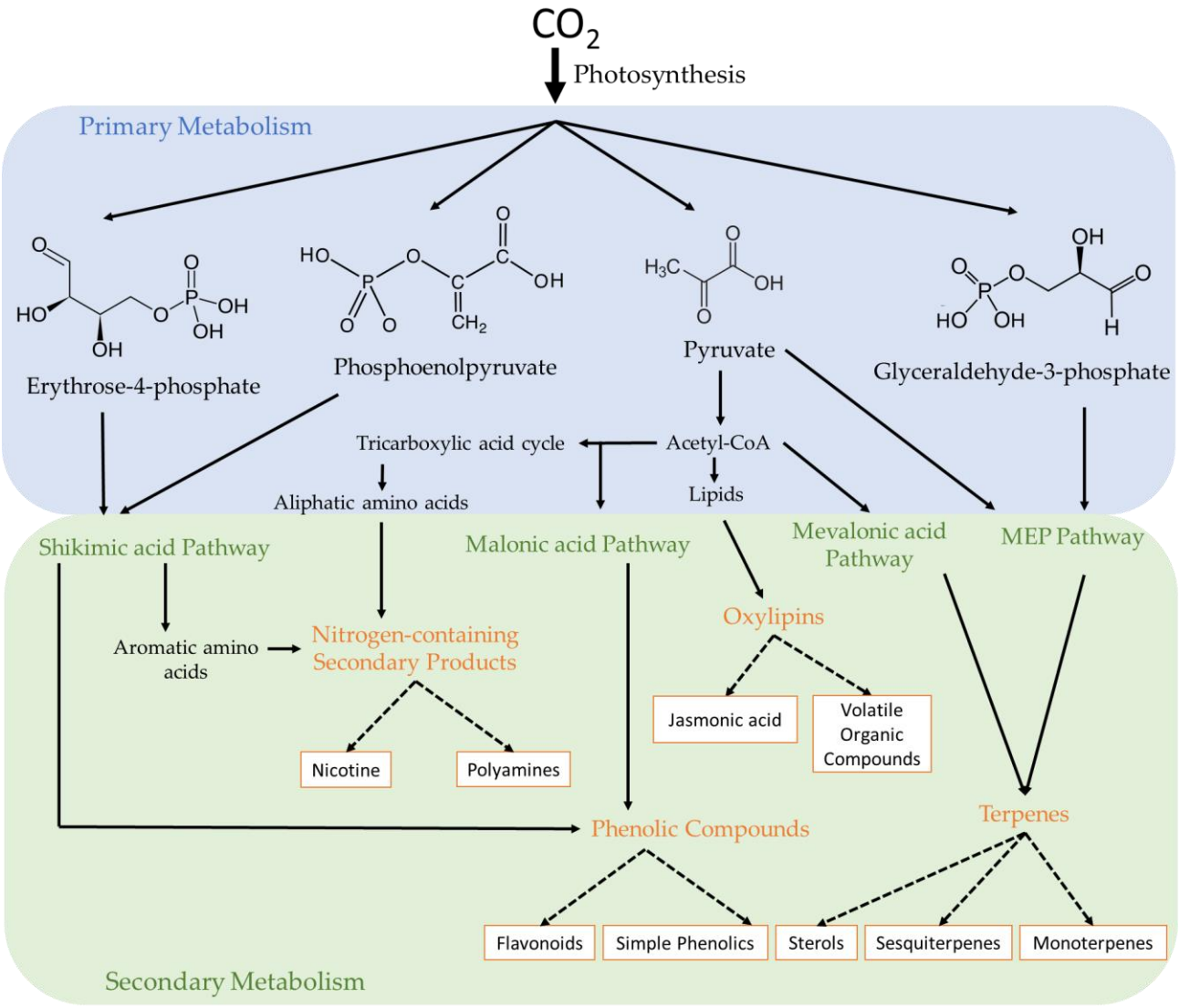

Figure 1. Primary and secondary carbon metabolism. An overview of the biosynthetic pathways involved in the biosynthesis of secondary metabolites. Primary metabolites are compounds that are directly involved in the growth and development of a plant whereas secondary metabolites (orange) are compounds produced in other metabolic pathways that are not essential to the functioning of the plant. Flavonoids, phenolics, sterols, sesquiterpenes, monoterpenes, jasmonic acid, volatile organic compounds, nicotine, and polyamines are secondary metabolites which are essential in signaling and regulation of the primary metabolic pathways, ensuring the well-being of the plant throughout its life cycle. Graphical representation adapted from [14].

1.2 Glycosylation of secondary metabolites

Glycosylation reactions are prevalent in nature and partake in majority of all vital processes [15]. This modification represents the saccharide polymerizations or conjugations of saccharides with other small molecules such as proteins, lipids, nucleic acids, and secondary plant metabolites [15]. The mechanism of glycosylation has been found to reduce hydrophobicity of lipophilic compounds, reduce volatility, enhance energy storage of plants, maintenance of cell structural integrity, information storage and transfer, cell-cell interaction, immune response, virulence, and chemical defense [15, 16]. Most glycosylation reactions employ a class of enzymes - glycosyltransferases (GTs) – which transfer sugar moieties from activated sugar donors to acceptor molecules with high efficiency and regiospecificity [16, 17].

Being an unusually large enzyme family (with more than 106 sub-families) GTs can be classified within different sub-families depending on their structural and functional similarities [18, 19]. Currently, the universally accepted classification of the GT families is mainly established upon sequence similarity collected in the Carbohydrate Active Enzyme database (CAZy, http://www.cazy.org) [20]. More recently, a specific database – PlantCAZyme – was established outlining the immense number of specifically plant GTs [21]. GTs can be classified according to the utilization of specific sugar-donors, mechanism of reaction, the type of glycosidic bond that is formed, crystal structure that the GT has, and by various conserved sequences. They can utilize various activated sugar donors, such as nucleotide-sugars, lipid phosphor-sugar donor and sugar-1-phosphates [15]. Majority of plant GTs utilize UDP-glucose, however UDP-galactose, UDP-rhamnose, UDP-xylose, UDP-arabinose, and UDP-glucuronic acid have also been found as sugar donors [22-25]. Moreover, these enzymes mechanism of action and type of bond that they form can vary from the most common O-glycosylation to N-, S-, and C-glycosylation [26].

Furthermore, the GT families are grouped hierarchically from their 3D structures (fold GT-A, GT-B, GT-C, and GT-D) [27] to their mechanism of reaction (inverting or retaining GTs) [19, 28] **[Figure 2]**.

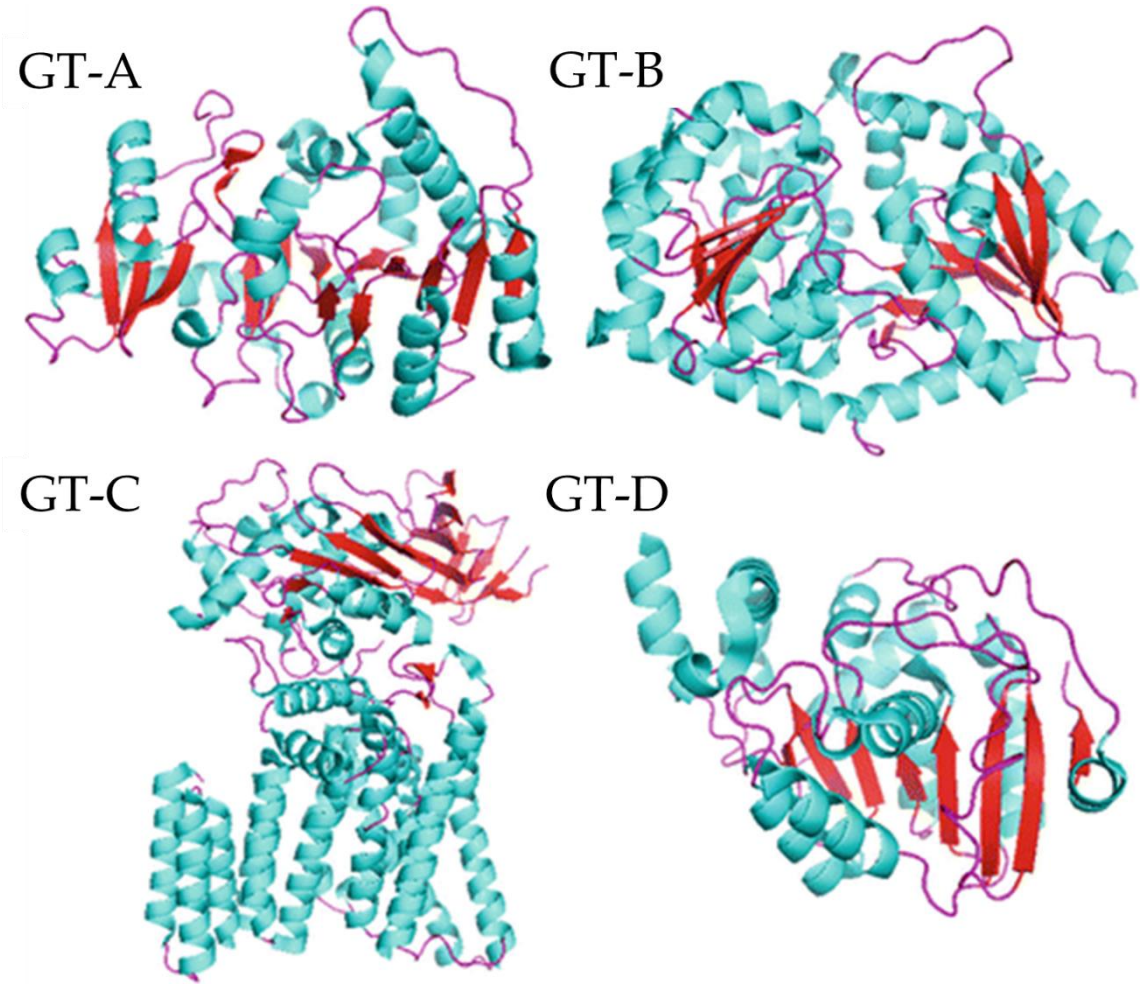

Figure 2. Crystal structure of various GT folds. Graphical representation of the four possible structural GT folds – GT-A GT-B, GT-C, and GT-D. The image was adapted from [29].

GT-A and GT-B folds have been intensively and thoroughly characterized [15]. GTs possessing the GT-A folding structure contain a single Rossmann fold and a conserved metal-binding motif [30, 31]. On the other hand, GT-B folded GTs contain two Rossmann folds which are linked, facing each other, forming an active cleft and

do not encompass a conserved metal-binding motif [32, 33]. The GT-C fold has not yet been substantially characterized and the distinctiveness remains contentious [34-36]. A recently reported GT-D fold was found among bacterial GTs involved in glycosylation of serine-rich repeat streptococcal adhesins which possesses distinct features and a new metal-binding site [37]. Additionally, GT enzyme are classified according to the anomeric configuration of the glycosylated product. "Retaining" GTs are enzymes which retain the stereochemistry at the anomeric center of the donor substrate. In contrast, "inverting" GTs are enzymes which invert the stereochemistry at the anomeric center of the glycosylated product [38].

1.3 Family-1 glycosyltransferases

The glycosylation of proteins, saccharides, lipids, and small molecules within different organisms involves hundreds of diverse GTs. The nucleotide-sugar dependent GTs belong to the Leloir enzymes and the glycosyl transfer often occurs at the nucleophilic oxygen of a hydroxyl substituent of the acceptor [38]. GT family-1, often referred to as UDP GTs (UGTs), are the largest GT family in plants that catalyze the transfer of a glycosyl moiety from UDP sugars to a wide range of acceptor molecules [28]. Crystal structures from various plant UGTs have been analyzed and despite relatively low sequence identities, they all possess the GT-B fold consisting of two Rossmann domains – $\beta/\alpha/\beta$ [38-41]. They are inverting GTs, which employ a direct displacement SN2-like reaction **[Figure 3]**. UGTs encompass a vital role in stabilization, enhancement of water solubility and deactivation/detoxification of natural products, leading to regulation of metabolic homeostasis, detoxification of xenobiotics, and the biosynthesis, storage and transportation properties of secondary metabolites [28].

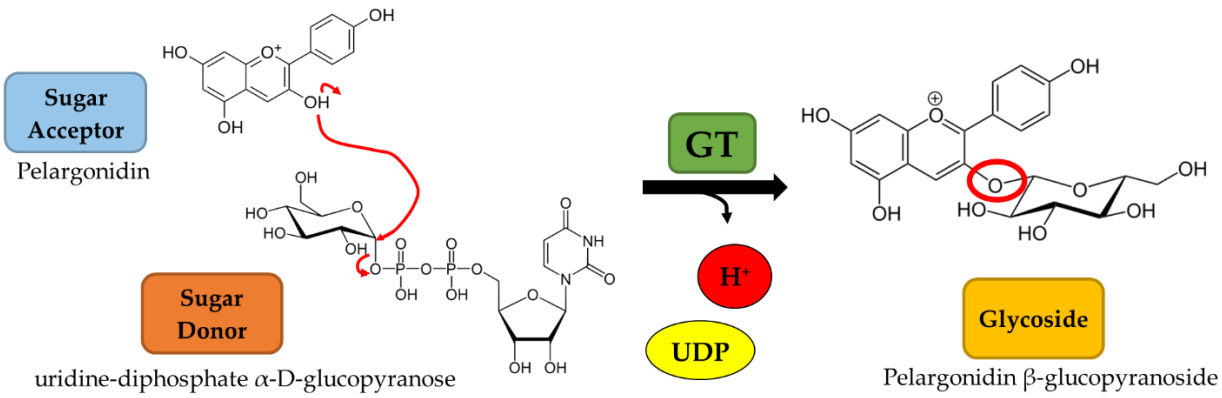

Figure 3. Reaction mechanism of glycoside formation. UGT family-1 GT-B inverting reaction mechanism employing a direct displacement SN2-like reaction.

Present across all domains of life, in plants, UGTs are commonly localized in the cytosol playing a vital role in the biosynthesis of secondary metabolites such as flavonoids, phenylpropanoids, terpenoids, steroids, and regulation of plant hormones [42]. Although each GT within this GT family-1 has quite a high sequence divergence, they all possess a consensus sequence at the C-terminal end, which is involved in binding to the UDP moiety of the sugar nucleotide [43, 44]. This consensus sequence comprising of 44 amino acid residues is termed the plant secondary product glycosyltransferase (PSPG) box [28, 43, 45] **[Figure 4]**. An interaction between the highly conserved HCGWNS motif and UDP-glucose has been reported [46], and it is likely that the last amino acid of the PSPG box controls the selection of the sugar donor [47].

Figure 4. The plant secondary product glycosyltransferase (PSPG) box. Letter size is proportional to the degree of amino acid conservation, image adapted from [48].

1.4 Determination and quantification of glycosyltransferase activity

Understanding the roles of GTs in biosynthetic pathways is key to understanding various biological processes. Their unique and yet simple mechanism allows for further manipulation and utility across numerous applications [49]. Moreover, the pharmaceutical and nutraceutical properties of small molecules have attracted significant attention from chemical and food industries. The biological functionalities of small molecules may be enhanced by increasing their hydrophilicity and stability through glycosylation [50]. Therefore, screening and detection of glycosylation reactions is crucial in employing further applications. However, due to the lack of high-throughput and reliable assays further and additional applications remain elusive. Therefore, a high-throughput method is necessary in order to efficiently and effectively screen through a large number of glycosylation reactions.

Some of the current assay methods for GTs were thoroughly reviewed [51]. For example, radiochemical assays are frequently utilized due to their great sensitivity, which allows quantifying even very low concentrations. Separating the radiolabeled substrate of the reaction from the radiolabeled product in order to quantify the amount of glycoside achieved can be done by various separation methods, however all are time consuming and not completely quantitative. Moreover, utilizing and

disposing of commercially available radiolabeled sugars is expensive and poses health and environmental hazards [52]. Furthermore, immunological methods are also sensitive when it comes to identifying glycosylation products but the requirement of specific antibodies is expensive and often may not be readily available [53]. Enzyme assays and product identification can be combined through different chromatographic methods developed for GT assays. However, usually these methods require substrate fluorescence labeling or particular detection methods [54]. Moreover, mass spectrometry (MS) assays have the advantage of speed and accuracy but are not commonly used as the instrumentation bares extreme high costs [55]. The previous and available methods as well as some recent modifications [56] requiring substrate labeling, high instrument investment, or supplementary enzymes and antibodies, are all based on the detection of the substrate consumption or the formation of the nucleotide product [52]. While methods for direct detection of the glycoside products such as, Liquid Chromatography coupled with Mass Spectrometry (LC-MS) and use of radiolabeled sugar donors have been established, they remain tedious, expensive, and hazardous [51]. Moreover, the lack of GTs and/or other suitable sugar donors [57] restricts the alternative application of secondary GTs as reporter enzymes for activity assays of primary GTs [58]. Although the development of a general 1-Zn(II) NDP sensor assay for rapid evaluation of GT activity was described [58], it unfortunately is unsuitable for family-1 plant GTs.

1.5 High-throughput assays tailored for family-1 plant GTs

A GT generally catalyzes the transfer of a glycosyl moiety from an activated sugar donor to an acceptor molecule. This not only results in the formation of a glycosylated product but also of byproducts such as, a proton from the acceptor molecule, and the free UDP molecule from the sugar donor **[Figure 3]**. Therefore, it is viable to quantify not only the glycosylated product formed, but also the amount of

byproduct. In the case of the pH-sensitive GT assay the proton byproduct is quantified, and according to the reaction scheme its amount is directly proportional to the amount of glycoside **[Figure 5A]** [59]. The pH change that accompanies the GT-catalyzed reactions can be conveniently used in assay development, and aside from GT reaction can further be used in assays for a variety of other enzymes including kinase [60], lipase [61], and phospholipase [62].

A pH-sensitive assay for bacterial β-1,4-galactosyltransferases (GalT1) to rapidly screen change in pH in a glycosylation reaction has already been described [59]. Glucose, galactose, lactose, *N*-acetylgalactosamine, and glucosamine served as acceptor substrates and UDP-glucose, and UDP-galactose were used as donors. The authors were able to stabilize and develop this method and deemed it sensitive, user-friendly and a good advancement in current methodology with regard to initially testing GT functionality. This method was further adapted for *Vitis vinifera* GTs to determine kinetic parameters for multiple substrates [63]. In this study, the optimization was performed to establish a high-throughput pH-sensitive GT assay with lower reaction volumes, automated component addition, and fast data acquisition via a multi-microplate instrument.

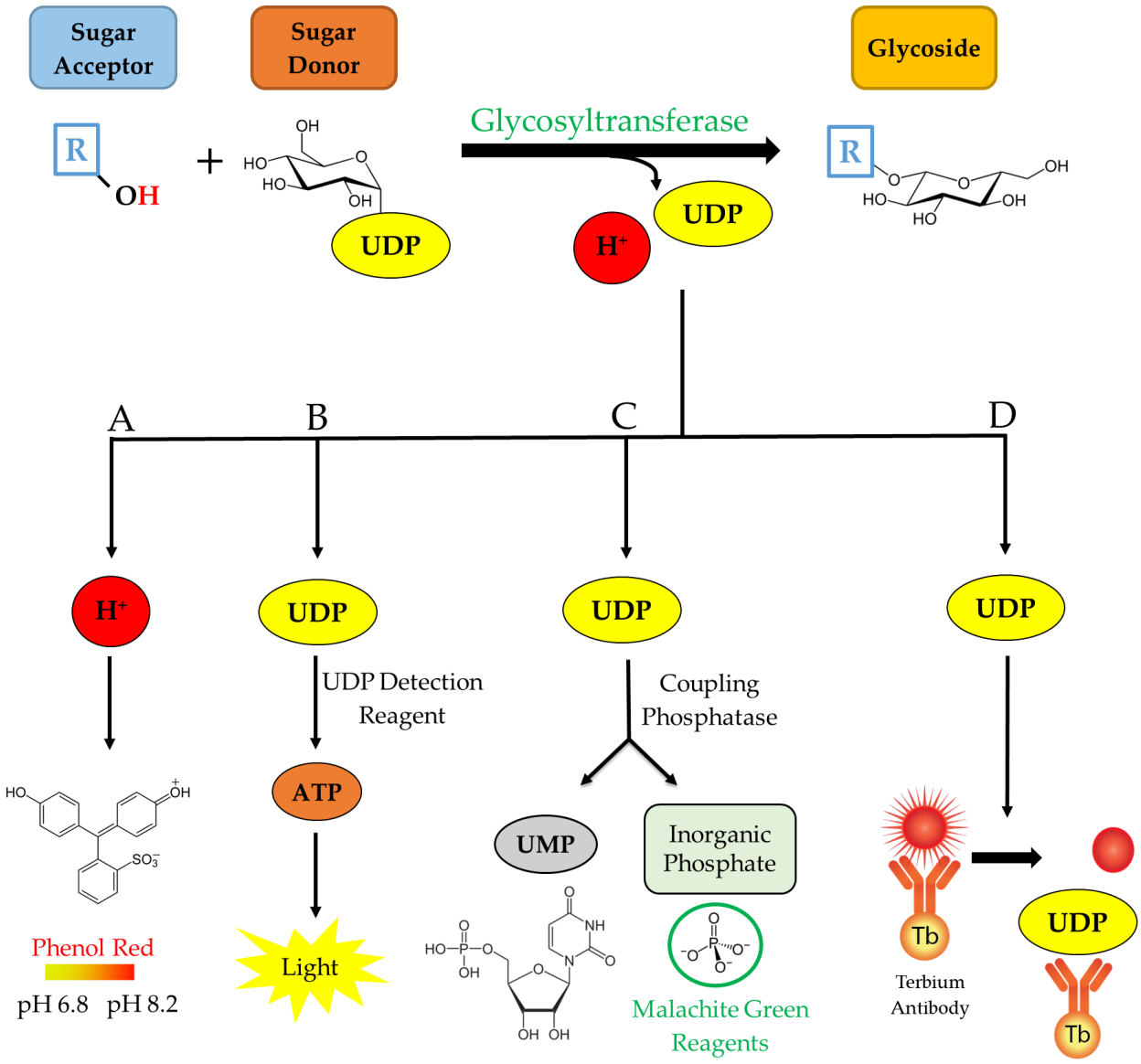

Figure 5. Glycosyltransferase reaction mechanism resulting in the formation of a glycoside in which the by-products are detected by 4 different assays prone to high-throughput screening. (A) Colorimetric pH-sensitive assay (B) UDP-Glo™ assay (C) Phosphate GT assay (D) UDP² TR-FRET immunoassay (graphical representation adapted from [64]. TR-FRET time-resolved fluorescence resonance energy transfer.

Aside from quantifying the proton byproduct from a glycosylation reaction, it is also possible to quantify the amount of UDP released from the sugar donor **[Figure 5B]**. By utilizing and adapting the UDP-Glo™ GT Activity Assay from Promega© the UDP amounts are investigated, and according to the reaction scheme the amount of UDP is directly proportional to the amount of formed glycosylated product **[Figure 5B]**. This bioluminescent assay is a homogeneous, single/reagent addition method that is able to rapidly detect the formation of UDP in GT reactions. A reagent is added to simultaneously convert the UDP product to ATP and generate light in a luciferase reaction. This assay relies on the properties of a proprietary thermostable luciferase that is formulated to generate a stable glow-type luminescent signal and improve performance across a wide range of assay conditions. The signal produced by the luciferase reaction, which is initiated by adding the 'UDP Detection Reagent' is stable for more than 3 hours **[Figure 5B]**. This extended stability allows for the flexibility of batch-mode processing of multiple plates, simultaneously. This assay has been experimented with various GTs and different substrates **[Table 1]**. Various applications of the UDP-Glo™ nucleotide detection assays were studied including glycan biosynthesis, post-translational modifications, and drug metabolism [65].

Moreover, the specificity of transfer of different sugars to different acceptors by diverse GTs such as human recombinant GT (ST6GALT1) was analyzed **[Table 1]**. Their findings proved that this bioluminescent platform detects the activity of any nucleotide-sugar using GT regardless of chemical structure, and kinetic parameters could be determined for different sugars [65]. Interestingly, this method has not been employed and experimented utilizing family-1 plant GTs **[Table 1]**.

Table 1. Application examples of the investigated assays in previous studies. ND, not determined; M, Mechanism; Ret, Retaining; Inv, Inverting; MD, metal-dependence; R, References. Table adapted from [64].

Assay	Application	Enzyme	Species	GT Family	Fold	M	MD	R
pH-Sensitive	-Screening GTs -Saturation mutagenesis library	GTB	*H. sapiens*	6	GT-A	Ret	Mn^{2+}	[66]
		GTA	*H. sapiens*	6	GT-A	Ret	Mn^{2+}	[66]
		GalT1	*H. sapiens*	7	GT-A	Inv	Mn^{2+}	[67]
		LgtB	*N. meningitidis*	25	ND	Inv	Mn^{2+}	[67]
		HP0826	*H. pylori*	25	ND	Inv	ND	[67]
Nucleotide-Glo™ (UDP, GDP, UMP)	-Sugar-nucleotide donor specificity -Screening of GT inhibitors	POMGNT1	*H. sapiens*	13	GT-A	Inv	Mn^{2+}	[68]
		B4GAT1	*H. sapiens*	49	ND	Inv	Mn^{2+}	[68]
		SpGtfA (OGT)	*S. pneumonia*	41	GT-B	Inv	ND	[68, 69]
		DdAgtA	*D. discoideum*	77	ND	Ret	Mn^{2+}	[68]
		POGLUT1	*H. sapiens*	90	ND	Inv	ND	[68]
		β4 Gal-T1	*Bos taurus*	7	GT-A	Inv	Mn^{2+}	[68, 69]
		LARGE1	*H. sapiens*	49 / 8	ND / GT-A	Inv / Ret	Mn^{2+}	[68]
		PglC	*C. jejuni*	4	GT-B	Ret	Mn^{2+}/ Mg^{2+}	[70]
		PglC	*H. pullorum*	4	GT-B	Ret	Mn^{2+}/ Mg^{2+}	[70]
		WecA	*T. maritima*	4	GT-B	Ret	Mn^{2+}/ Mg^{2+}	[70]
		UGT1A1	*H. sapiens*	1	GT-B	Inv	ND	[69]
		GTB	*H. sapiens*	6	GT-A	Ret	Mn^{2+}	[69]
		GALNT1	*H. sapiens*	27	GT-A	Ret	Mn^{2+}	[69]
		ST6GAL1	*H. sapiens*	29	ND	Inv	ND	[71]
		UGT2B17	*H. sapiens*	1	GT-B	Inv	ND	[69]
		FUT2	*H. sapiens*	11	ND	Inv	ND	[69]
		FUT3	*H. sapiens*	10	GT-B	Inv	ND	[69]
		FUT7	*H. sapiens*	10	GT-B	Inv	ND	[69]
		IRX10-L	*A. thaliana*	47	GT-B	Inv	ND	[72]
		AtFUT1	*A. thaliana*	37	GT-B	Inv	ND	[73]
Phosphate GT Assay	-Kinetic analyses	TcdB	*C. difficile*	44	ND	Ret	ND	[74]
		KTELC1	*H. sapiens*	90	ND	Inv	ND	[74]
		ST6GAL1	*H. sapiens*	29	ND	Inv	ND	[74]
UDP^2 TR-FRET	-Discovery of GT inhibitors	GALNT3	*H. sapiens*	27	GT-A	Ret	Mn^{2+}	[75]

Moreover, to quantifying the UDP byproduct after conversion to ATP and measuring the luciferase generated light, it is also possible to quantify the phosphate molecules resulting from phosphatase enzymatic cleavage of the UDP **[Figure 5C]**. By utilizing and adapting the phosphate GT activity assay from R&D Systems© the phosphate amounts are investigated, and according to the reaction scheme the amount of phosphate is directly proportional to the amount of formed glycosylated product. It is a simple, non-radioactive, and high-throughput compatible assay able to determine the enzyme activity of all GTs that use di-phosphonucleotide sugars as donor substrates. A specific phosphatase is utilized to remove an inorganic phosphate quantitatively from UDP. The sensitive colorimetric Malachite Green phosphate detecting reagents subsequently quantitates the released inorganic phosphate. The amount of inorganic phosphate released by the coupling phosphatase is equal to the nucleotide sugar generated consumed or glycoconjugate product; therefore, the rate of inorganic phosphate products reflects the kinetics of a GT reaction **[Figure 5C]**. The phosphatase-coupled GT assay was utilized with various GTs such as, *Clostridium difficile* toxin B, human KTELC1, and human sialyltransferase ST6GAL1 [76] **[Table 1]**. However, it was not yet utilized in analyzing family-1 plant GTs.

It is also possible to quantify the amount of UDP released from the sugar donor via a commercially available immunoassay **[Figure 5D]**. By utilizing and adapting the Transcreener UDP² TR-FRET glycosyltransferase assay from Bellbrook labs© the UDP amounts are quantified. As the free UDP molecules are bound to the antibody, the FRET signal is depleted. It is a competitive immunoassay for UDP with a far-red, time-resolved Förster-resonance-energy-transfer (TR-FRET) readout **[Figure 5D]** and is prone for high-throughput screening with a single addition, mix-and-read format. A similar assay (detecting ADP) was utilized with GmSuSy and PdST GTs [77] and GALNT3 [75] **[Table 1]**. Furthermore, this assay has not been yet employed and adapted to family-1 plant GTs.

1.6 Activation and inhibition of glycosyltransferase activity – allosteric enzymes

Enzymes, such as UGTs, are biological catalysts that influence the rate of biochemical reactions in all living organisms. Furthermore, they can be extracted from these living organisms and applied in *in vitro* environments to achieve various industrial and commercial processes [78]. Several examples include the production of sweetening agents, production or modification of antibiotics, cleaning reagents, and play a pivotal role in analytical devices and processes which contribute to clinical, forensic, and environmental application [78].

In 1913, it was demonstrated by Michaelis and Menten that the ES complex can either dissociate to release the product or dissociate in the reverse direction not resulting in a product formation [79]. The turnover rate, k_{cat}, is a constant which represents that number of substrate molecules that can be converted to product molecules by a single enzyme molecules per unit of time [78]. The initial velocity, v_0, is the initial rapid rate where the curve is in a linear trend and can easily be calculated in order to evaluate the reaction rate over that specific period. This initial velocity can vary upon alteration of substrate or enzyme concentrations, pH of the buffer, temperature conditions, and even purity of the enzyme which reveals and allows to further characterize the specific enzyme [78]. Furthermore, quantifying and calculating kinetics is performed with a series of enzyme assays using the same enzyme concentration with increasing substrate concentration. As the substrate concentration is increased, the rate of reaction increases in a linear-fashion. As the substrate concentration is increased further, the effects of the reaction rate begin to decline until a point where increasing the substrate concentration has no or little effect on the reaction rate. This is due to the fact that all of the active sites of the enzyme are already occupied by the substrate and a saturation point is reached, this is demonstrated by the maximum velocity (V_{max}) [78]. The Michaelis constant (K_M), which is the substrate concentration at half of the maximum velocity (V_{max} / 2)

indicating the affinity of the enzyme for a particular substrate. A lower K_M value indicates that a lower amount of substrate is required to reach half of the maximum velocity – indicating high affinity of the substrate to the enzymes active site. Therefore, less substrate is required to become saturated. A higher K_M value indicates that more units of substrate are required to bind to the active site on the enzyme in order to yield the desired product – indicating low affinity. Therefore, more substrate is required for the active sites to reach saturation [78]. The ratio between the turnover rate, k_{cat}, and the Michaelis constant, K_M, is termed the specificity constant (k_{cat}/K_M) evaluating and defining the enzymes specificity, efficiency, and proficiency [80]. Taking all of the variables into consideration, the rate of reaction and kinetics can be calculated by the Michaelis-Menten equation:

$$V_0 = \left(\frac{V_{max}\,[S]}{[S] + K_M}\right)$$

Molecules that reduce or enhance the activity of an enzyme-catalyzed reaction are known as inhibitors or activators, respectively. These ligands affect the enzymatic activity by either directly or indirectly influencing the properties of the enzymes' active site, known as competitive and noncompetitive inhibitors [81]. A molecule, which possess structural resemblance to the normal substrate, may be able to bind reversibly to the enzyme's active site and act as a competitive inhibitor. A unique characteristic of competitive inhibitors is that they can be "reversed" and displaced from the active site if high concentration of substrate is present, thereby restoring enzyme activity [78]. Therefore, competitive inhibitors may increase the calculated K_M as they increase the concentration of substrate required to saturate the enzyme but at the same time, the V_{max} remains unchanged [78, 82]. A typical graphical representation of a UGT along with a plant secondary metabolite is depicted using the Michaelis-Menten equation which results in a hyperbolic rate profile reckoning the V_{max} and K_M

[83] **[Figure 6A]**. Depending on the environment, the allosteric enzyme present, and purpose of glycosylation the reaction can proceed in an atypical fashion [84]. One of the atypical kinetic schemes is activation which occurs when an activator molecule different from the substrate drives an increase in enzyme activity in favor of the substrate. This type of kinetic model was depicted in drug metabolism as 7,8-benzoflavone was shown to activate the P450-mediated hydroxylation of benzo[*a*]pyrene in rats [85]. Another type includes autoactivation, occurs when the substrate itself activates its own metabolism thus leading to a sigmoidal kinetic profile **[Figure 6B]**. This type of autoactivation was observed in the presence of 2 modifiers (4-methylumbelliferone and 1-naphthol). They changed the UGT2B7-catalyzed zidovudine glucuronidation from a hyperbolic kinetic scheme to a sigmoidal (autoactivation) kinetic relationship [86]. A biphasic metabolism represents an enzyme with multiple binding sites with low and high-affinity binding sites [83] **[Figure 6D]**. This type of profile can be characterized as non-competitive inhibitors which interact with the UGT at a site other than the active site [78]. This interaction does not physically block the substrate-binding site, but it may nevertheless prevent subsequent reactions from proceeding.

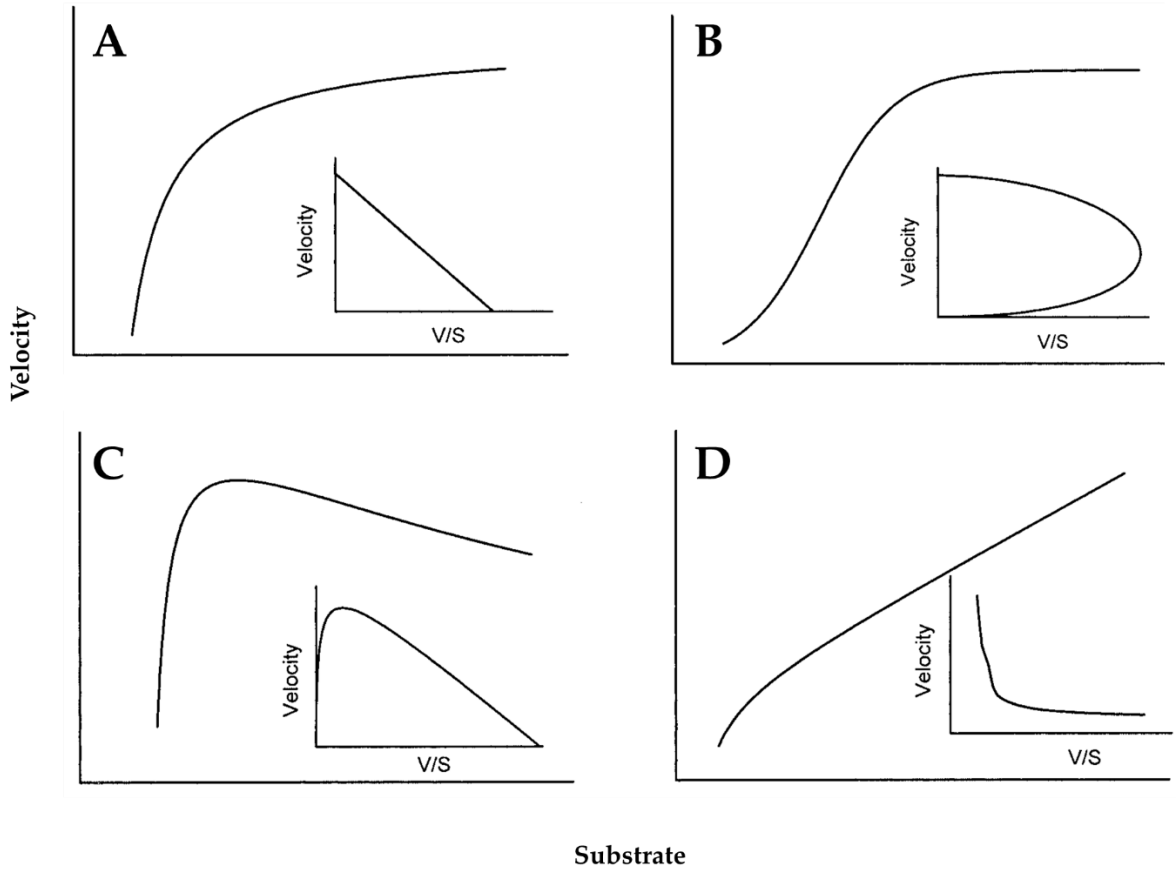

Figure 6. Graphical representation of various kinetic profiles. (A) Michaelis-Menten hyperbolic kinetic profile. (B) Sigmoidal autoactivation profile. (C) Substrate inhibition profile. (D) Biphasic kinetic profile. Adapted from [83].

Another atypical kinetic profile and specifically important for this study is substrate inhibition **[Figure 6C]**. Substrates or molecules that stabilize the protein in its low affinity state act as allosteric inhibitors, and ones that stabilize the protein in its high affinity state act as activators or promoters [78, 81]. GTs are often inhibited by their own substrates resulting in velocity curves that rise to a maximum and then descend as the substrate concentration increases, kinetically evident when V_{max} begins to decrease following the substrate saturation point leading to a convex relationship [83, 87, 88]. This substrate inhibition is often interpreted as an abnormality that results from artificially high substrate concentration in a laboratory setting. However, there

are reasons that substrate inhibition is actually a biologically relevant regulatory mechanism in many significant metabolic pathways [82, 89, 90]. For example, a strawberry UGT – *Fv*UGT1 – glycosylates pelargonidin which is a major anthocyanidin in the strawberry fruit. Anthocyanins are phenolic compounds contributing to the plants' pigment, which attract pollinators, protect plants from pathogens, and environmental stresses [91-94]. Moreover, as a dietary supplement they have antioxidative properties preventing diseases such as cancer and inflammatory disorders [95]. High pelargonidin substrate concentrations exhibited an uncompetitive substrate inhibition of the GT [90]. This substrate inhibition was alleviated by administering calcium/calmodulin [90]. Furthermore, this atypical kinetic profile is seen in many UGTs including plant UGT73C8 and UGT88E1 from *Medicago truncatula* and UGT78K1 [96] from black soy bean with cyanidin substrate [97] and has been displayed in both humans and plant UGTs [96-98]. Moreover, inhibitory effects of UDP (product inhibition) in UGTs have been observed and studied [99]. Yokota *et al.* observed a significant UDP-inhibition and interaction with liver UGTs [99]. These types of inhibitors reduce the V_{max} of the reaction, meanwhile leaving the K_M of the acceptor substrate unaffected [78, 82]. Another study by Luukkanen *et al.* subjected eight human recombinant UGTs and evaluated their kinetic mechanism and substrate inhibition as well as, substrate specificities [100]. Initially, at low substrate concentrations the UGTs followed a typical Michaelis-Menten kinetic profile and as the substrate concentration increased inhibition was observed. The glucuronidation of a drug - entacapone - by one of the UGT isoforms was inhibited by 1-naphthol in a competitive fashion in respect to the drug and in an uncompetitive fashion, with respect to UDP-glucuronic acid. Interestingly, the inhibition by UDP was noncompetitive with respect to the drug and competitive with respect to UDP-glucuronic acid [100]. Other studies have reported that substrate inhibition may arise from binding of a second substrate molecule to the enzyme-substrate complex indicating multiple binding sites for aglycones [86, 101]. Similarly, another study proposed two or more aglycone binding sites in the human UGT1A1

based on the evaluation and interaction of UGT catalyzed buprenorphine and bilirubin glucuronidation [102].

Promoting or inhibiting enzymatic reactions can have vital biological significances and their study can contribute to understanding how plants regulate their metabolic processes in nature. Many applications of UGTs including drug metabolism and understanding the mechanism under question can be elaborated on via the study of atypical kinetic profiles. Previously, atypical kinetic profiles were commonly misinterpreted and incorrectly fitted to the typical Michaelis-Menten kinetic profile due to lack of sensitive analytical techniques. This can in turn lead to false and misinterpreted information on the behavior of UGTs in various environments. In this study, the implementation of UDP-Glo™ assay has allowed in the deciphering substrate inhibition of family-1 plant UGT72AY1 with phenolic-substrate scopoletin. The assay has allowed for the sensitive and rapid screening of UGT72AY1 with many various scopoletin concentrations. Moreover, the use of additional modifiers as potential activators or inhibitors in the glycosylation of scopoletin could be investigated.

1.7 Glycosyltransferase and UDP-glucose hydrolase activities

In every plant species, there are over hundred UGTs which can glycosylate a vast range of small molecules such as, secondary metabolites, hormones, and external toxins [49]. The UGT utilizes various acceptor molecules that can be tested before the initial determination of the donor-sugar nucleotides [68]. Although their functionality can be predicted by genomic and primary amino acid sequence analyses, a single and even minor replacement can alter sugar nucleotide donor and acceptor utilization [103]. Most commonly, they utilize UDP-glucose as a sugar donor and the acceptors vary depending on the plant species **[Figure 3]** [28, 42]. In a traditional GT reaction,

the transfer of the sugar from the donor to the acceptor substrate is followed by the release of the product **[Figure 3].** In an instance when the acceptor substrate is absent, GTs have been reported to exhibit background hydrolysis of the donor substrate, which can be considered the enzymatically catalyzed transfer of the sugar moiety to a water molecule [104-106] **[Figure 7]**. However, other enzymes may possess the activity of hydrolysis as a water molecule competes with the substrate. For example, a Heparosan Synthase PmHS2 enzyme from *Pasteurella multocida* has demonstrated glycosyltransferase and UDP-sugar hydrolase activity [107]. When PmHS2 is incubated in the present of UDP-sugars, the synthesis of heparosan polymers is favored over the hydrolysis of the UDP-sugars [107]. Furthermore, another study demonstrated that *Clostridium difficile* Toxin A in the absence of an acceptor protein can hydrolyze UDP-glucose to UDP and glucose instead of its monoglucosylation of Rho GTPases [108]. Ciesla and Bobak have demonstrated that hydrolase activity of *Clostridium difficile* Toxin B (V_{max}) is greater than of Toxin A by 5-fold. Yet, the K_M of both Toxin A and B for UDP-glucose were similar. Moreover, in the presence of potassium [109] and ammonium [110] the hydrolase activity of the toxins was more favored, meanwhile sodium had no effect on the activity [109]. Interestingly, manganese and magnesium acted as activators driving the toxins enzymatic activity towards hydrolysis [109]. Another study utilizing human, bovine, bacterial, and protozoan GTs were able to detect hydrolase activity with UDP-Glo™ [68]. If the water molecule acts as the acceptor substrate in an SN2-like reaction mechanism the UDP and hydrogen ion will be the resulting byproducts, however no glycoside will be formed. Therefore, the glycoside will not be detected via LC-MS methods. On the other hand, methods detecting the by-products such as, UDP-Glo™, will be able to detect levels of the free-UDP resultant from the hydrolase activity. In the present study, the hydrolase activity of UGT72AY1 is evaluated utilizing the tailored UDP-Glo™ assay.

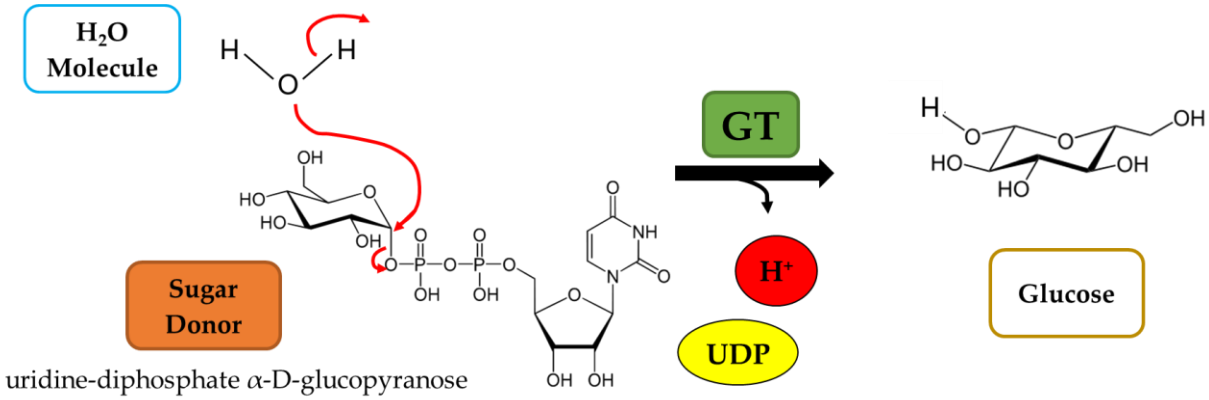

Figure 7. Reaction mechanism utilizing a water molecule as an acceptor substrate. UGT family-1 GT-B inverting reaction mechanism employing a direct displacement SN2-like reaction with a water molecule resulting in UDP and H+ byproducts and no glycosidic product.

1.8 Aims of the doctoral research

The application spectrum of GTs and their glycoside products is immense in many aspects of cosmetics, food industry, and drug design [111-113]. In order to investigate further innovative applications and find new emerging GTs with unprecedented catalytic activities a robust, high-throughput, and reliable method is sought for. In this thesis, the colorimetric pH-based assay, two enzyme-coupled assays (UDP-Glo™ and phosphate GT activity assay), and one immunological assay (Transcreener UDP² TR-FRET) were selected, employed and tailored to suit family-1 plant GT from *Vitis vinifera, Vv*dGT13 (UGT72B27). The substrate screening and kinetics were executed with all four methods utilizing one GT and various plant secondary metabolites. Furthermore, following the employment of the assays their advantages and disadvantages were analyzed. The aim was to select a high-throughput method that could be utilized for rapid screening and quantifying kinetics of family-1 plant GTs with various substrates.

Plant secondary metabolites, which can allosterically or competitively change an enzyme's active site to either enhance or inhibit glycosylation can be of a great advantage in both nature and commercial purposes. Substrate and allosteric inhibition of family-1 plant GTs from *Nicotiana benthamiana* (*Nb*GTfc4 / UGT72AY1), *Malus x domestica* (KalcoAS1 / UGT72B46), and *Pyrus communis* (WilliamsAS4 / UGT72B50 and ConferenceAS4 / UGT72B51) were studied with the newly established and tailored UDP-Glo™ method as well as, LC-MS. Moreover, the innate hydrolase activity of family-1 GTs was investigated. The enzymes were manipulated with various activators and inhibitors (plant secondary substrates) to further understand the biological significance and their influence on the Michaelis-Menten model.

II. Materials & Methods

2.1 Materials & chemicals

Chemicals were purchased with highest purity from Roth (Karlsruhe, Germany), Sigma-Aldrich (Steinheim, Germany), or Fluka (Steinheim, Germany) unless otherwise stated. The CLARIOstar plate reader (BMG Labtech, Ortenberg, Germany) was used for enzyme activity measurements.

Table 2. List of chemicals and materials utilized during the doctoral thesis

Chemical Name	Chemical Formula	Molecular Weight (g/mol)	Company
Acetic Acid	C2H4O2	60.05	Carl Roth
30% Acrylamide, Rotipohorese® Gel 30	C3H5NO	71.08	Carl Roth
Agarose	(C12H18O9)x	306.27	Sigma-Aldrich
Ammonium persulfate (APS)	(NH4)2S2O8	228.2	Carl Roth
Ampicillin Sodium Salt	C16H18N2NaO4S	397.39	Carl Roth
Brilliant blue G	C47H48N3NaO7S2	854.02	Sigma-Aldrich
5-Bromo-4-chloro-3-indoly phosphate (BCIP) (Na-salt)	C8H4BrClNO4P 2Na	397.46	Carl Roth
Chloramphenicol	C11H12Cl2N2O5	323.15	Carl Roth
dNTP (mixed A+T+D+C)			Promega
N,N-Dimethylformamide	C3H7NO	73.09	Carl Roth
Ethanol	C2H5OH	46.07	Merck
Ethylenediamine tetraacetic acid (EDTA)	C10H14N2Na2O8·2H2O	372.24	Merck
L-Glutathione reduced	C10H17N2O6S	307.33	Carl Roth
Glycine	C2H5NO2	75.07	Carl Roth

Glycosyltransferase Activity Assay	--	--	R&D Systems
Isopropanol	C3H8O	60.1	Carl Roth
Isopropyl β-D-1-thiogalactopyranoside (IPTG)	C9H18O5S	238.3	Carl Roth
Magnesium chloride	MgCl2	95.21	Carl Roth
Magnesium sulfate	MgSO4	120.31	Carl Roth
Methanol	CH3OH	64.70	Carl Roth
Phosphoric acid	H3PO4	97.99	Sigma-Aldrich
Potassium chloride	KCl	74.56	Carl Roth
Potassium dihydrogen phosphate	KH2PO4	136.09	Carl Roth
Sodium chloride	NaCl	58.44	Carl Roth
Sodium dihydrogen phosphate dihydrate	NaH2PO4·2H2O	156.01	Carl Roth
Sodium dodecyl sulfate (SDS)	C12H25NaO4S	288.36	Carl Roth
Tetramethylethylendiamin (TEMED)	C6H16N2	116.21	Carl Roth
UDP² TR-FRET Assay	--	--	BellBrook Labs
Tris	C4H11NO3	121.15	Carl Roth
Tryptone			Carl Roth
Tween 20	C58H114O26		Carl Roth
UDP-Glo™ Assay			Promega
Uridine 5′-diphosphoglucose disodium salt (UDP-Glucose)	C15H22N2Na2O17P2	610.27	Sigma-Aldrich
X-Gal	C14H15BrClNO6	610.27	Carl Roth
Yeast extract		408.60	Carl Roth

Table 3. List of substrates utilized during the doctoral thesis

Substrate Name	Molecular Weight (g/mol)
Abscisic acid (ABA)	264.32
Apocarotenal	416.64
β-carotene	536.87
Carvacrol	150.22
Coniferyl alcohol	180.20
Coniferyl aldehyde	178.18
p-coumarylalcohol	150.17
p-coumarylaldehyde	148.16
m-cresol	108.14
o-cresol	108.14
α-damascone	192.30
β-damascone	192.30
DMP	154.16
Furaneol	128.13
Farnesol	222.37
Furanmethanethiol (FMT)	114.17
Guaiacol	124.14
Hydroquinone	110.11
α-ionol	194.31
β-ionol	194.31
α-ionone	192.30
β-ionone	192.30
MDMP	168.19
MMP	138.16
Phenol	94.11
Phloroglucinol	126.11
trans-resveratrol	228.25
Retinol	286.45
Sinapyl aldehyde	208.21
Sinapyl alcohol	210.23
Scopoletin	192.17
Thymol	150.22
Umbelliferone	162.14

2.2 Heterologous protein expression with phosphate-containing buffers

Protein expression was performed in the *E.coli* BL21 (DE3) pLysS cells harboring pGEX-4T-1 vector providing resistance against ampicillin and chloramphenicol and the *UGT72B27* sequence. Similarly, the heterologous protein expressions of UGT72AY1, UGT72B50, UGT72B51, and UGT72B46 were performed. A pre-culture was prepared by adding 2 µl of the cryostock culture to 10 ml lysogeny broth (LB) supplemented with 100 µl/mg ampicillin and 34 µl/mg chloramphenicol **[Table 4].** The pre-culture was grown at 37 °C for 16 hours in 50 mL Erlenmeyer flasks. The overnight culture was further propagated for 2 - 3 hours in 400 mL of LB supplemented with ampicillin and chloramphenicol until the optical density (OD) at 600 nm reached 0.5 – 0.6.

Table 4. Composition of LB medium for cultivation of microorganisms

Component	Composition
Tryptone	10 g / L
NaCl	10 g / L
Yeast Extract	5 g / L
pH	7.0

The expression of the protein of interest was induced by the addition of isopropyl-β-D-thiogalactopyranoside (IPTG) at a final concentration of 0.2 mM. The culture was grown for 20 hours at 18 °C for 16 hours shaking at 200 rpm. After harvesting the cells at 40,000 *g* (4 °C, 20 minutes), *E. coli* cell pellet was subjected to a freeze thaw cycle and resuspended in 2 ml of 2 mM Na-phosphate buffer (pH 8.0) and 10 µM of proteinase inhibitor, phenylmethylsulfonyl fluoride (PMSF). The cells were further disrupted via sonification (Sonopuls HD 2070 homogenizer) in phosphate-

buffered saline (PBS) buffer for 6 cycles (30 seconds each cycle, 30 seconds pause, 10% power) **[Table 5]**. After cell disruption, the cells were centrifuged at 200,000 *g* (4 °C, 20 minutes) and the clear supernatant containing the protein was obtained. Commercial glutathione S-transferase binding (GST)-resin (Novagen, Darmstadt, Germany) was utilized and the recombinant GST-bound proteins were purified according to manufacturer's instructions **[Table 5]**. The protein concentration was further determined via Roti-Nanoquant (Roth, Karlsruhe, Germany) according to manufacturer's protocol and the presence of the recombinant proteins was verified by SDS-PAGE and Coomassie Staining **[Table 6, Figure 9, and Figure 10]**

Table 5. Composition of phosphate-containing and phosphate-free containing buffers for heterologous protein expression

Buffer	Component	Composition
10X PBS Buffer Phosphate-containing	Na_2HPO_4	6.1 g / L
	KH_2PO_4	2 g / L
	NaCl	80.5 g / L
	KCl	2 g / L
	pH	7.3
10X TBS Buffer Phosphate free	Tris	121.9 g / L
	pH	7.5
10X GST Elution Buffer	Reduced Glutathione	3.08 g / 100 mL
	Tris / HCl (pH 8.0)	50 mL / 100 mL

Table 6. Buffers and solutions utilized for SDS-PAGE and Coomassie staining

Buffer	Component	Composition
10 X Running Buffer	TRIS	30 g / L
	Glycine	144 g / L
	SDS	10 g / L
Colloidal Coomassie	$AL_2(SO_4)_3$ x 16 H_2O	50 g / L
	EtOH	100 mL / L
	Coomassie G250	0.2 g / L

2.3 Heterologous protein expression with phosphate-free buffers

In order to subject the purified protein with the phosphate GT activity assay, all buffers and components along the purification process must be phosphate-free. The protocol and all the concentration of all buffers remained the same as described above with the sole difference that the 'phosphate' content was replaced with 'tris'. As an example, the PBS buffer was exchanged for the Tris-buffered saline (TBS) buffer **[Table 5]**. The purification of the protein was successful as determined by SDS-PAGE gels and Coomassie Staining **[Table 6, Figure 8, and Figure 9]**.

2.4 Glycosyltransferase (GT) activity assays

Glycosylation assays of several selected substrates acting as sugar acceptors and uridine-diphosphate-glucose (UDP-glucose) acting as sugar donor were performed using UGT72B27 from *Vitis vinifera*. The enzymatic reactions were performed with 50 mM Tris HCl (pH 7.5), 100 μM UDP-glucose, varying concentration of substrate (dissolved in DMSO), and 5 μg of purified protein with a total reaction volume of 50 μl. All of the enzymatic reactions were executed in

Eppendorf tubes utilizing incubators at 30 °C, 10 minutes, and shaking at 400 rpm. The kinetics and activity of the GT was analyzed via various activity assays described below.

Table 7. Optimal enzymatic reaction conditions for various GTs

Enzyme	Species	Amount (μg)	Incubation time (min)	Temperature (◦C)	pH
UGT72B27	*Vitis vinifera*	5	10	30	7.5
UGT72AY1	*Nicotiana benthamiana*	0.5	10	40	7.5
UGT72B50	*Pyrus communis*	5	30	30	7.5
UGT72B51	*Pyrus communis*	5	30	30	7.5
UGT72B46	*Malus x domestica*	5	30	30	7.5

2.5 Determination of kinetic parameters using a pH-sensitive colorimetric assay

A calibration curve was established as previously described [63]. In brief, the calibration curve was arranged in a 2 mM sodium phosphate buffer (pH 8, 120 μL) containing 0.01 mM phenol red, 0.1 mM $MnCl_2$, 10 mM substrate, and 5 μg purified UGT72B27, with the addition of varying amounts of 10 mM hydrochloric acid to a range of final concentration of 0.1, 0.2, 0.3, 0.4, 0.5, and 0.6 mM. The respective OD_{557} was recorded. A quantitative linear relationship between proton concentration and absorbance was established.

For the determination of kinetic parameters, 0.01 mM phenol red, 0.1 mM $MnCl_2$, varying substrate concentration from 0-2000 μM, and 5 μg purified UGT72B27

were mixed with phosphate buffer (2 mM, pH 8). The assay was commenced by the addition of the UDP-glucose to a final concentration of 2 mM and a final reaction volume of 120 µl. The respective absorbance at 557 nm was recorded for each sample at 10 second intervals for a total of 3 minutes until a constant signal was obtained. The enzyme activities were calculated from the calibration curve. All measurements were executed in triplicates and the values were averaged. Finally, K_M and V_{max} were calculated by nonlinear regression of the Michaelis-Menten equation using the Microsoft Excel Solver.

In establishing a high-throughput process for the pH-sensitive colorimetric assay, the reaction conditions remained the same as previously described. The enzymatic reaction was prepared in 96-well plate in a total volume of 120 µl. The reaction was commenced with the addition of UDP-glucose utilizing the injector function of the multi-plate reader. The components were thoroughly 'shaken' and incubation took place inside the plate reader at the optimal temperature. Upon the particular reaction time, the OD was directly measured. All measurements were executed in triplicates with negative and positive controls **[Table 8]** [64].

2.6 Determination of kinetic parameters using the UDP-Glo™ glycosyltransferase assay

The commercial kit UDP-Glo™ glycosyltransferase assay was purchased from Promega (Mannheim, Germany). Parts of the assay were established according to manufacturer's protocol meanwhile, other parts were tailored to fit the specificity of the working GT. The UDP-Detection Reagent (UDR) was prepared and the reaction was executed in 384-well plates. To estimate the amount of UDP produced in the enzymatic reaction, a UDP standard curve was established according to manufacturer's conditions. Briefly, a 0-1000 µM UDP standard was prepared in a 384-well plate. A 1000 µM UDP solution was added in the first well and was serially

diluted across 24 wells with the last well serving as a no-UDP control. Respectively, the UDR was added to the corresponding wells, the plate was incubated at room temperature for 60 minutes, and finally the relative luminescence (RLU) signal was measured with the CLARIOStar microplate reader. A calibration curve was extrapolated from the average of these measurements. Moreover, along with the UDP standard curve an enzyme titration was performed where 10 μg/μL of UGT72B27 was serially diluted and subjected to an incubation of one hour at 30 °C with acceptor (thymol) and donor substrate (UDP-glucose) consequently heat stopped to terminate the reaction.

For the determination of kinetic parameters, a 50-μl GT reaction was prepared as follows: 50 mM Tris/HCl (pH 7.5), 100 μM UDP-glucose, 5 μg purified UGT72B27, with varying concentrations of substrate ranging from 0–2000 μM. The reaction was commenced by the addition of the sugar-donor, UDP-glucose. Termination of the enzymatic reaction was executed by incubating at 75 °C for 10 minutes, the precipitated enzyme was removed via centrifugation and subsequently 5 μl of UDR was added to 5 μl of the enzymatic reaction in 384-well plate (1:1 ratio). The plate was allowed to equilibrate at room temperature for 60 minutes in the dark. Following the incubation period, the relative luminescence (RLU) signal was measured via the plate reader. The enzyme activities were calculated from the calibration curve and the respective RLU signal. All measurements were executed in triplicates with appropriate controls (positive, negative) and the values were averaged **[Table 8]**.

Table 8. The negative controls and blanks that were utilized when performing all four HTP assay kinetics

Control	Component
Negative 1 (no active GT)	Tris/HCl buffer
	UDP-glucose
	Empty vector (no GT)
	Substrate
Negative 2 (no donor substrate)	Tris/HCl buffer
	GT
	Substrate
Negative 3 (no acceptor substrate)	Tris/HCl buffer
	UDP-glucose
	GT
Blank 1	Only H_2O
Blank 2	Only DMSO

2.7 Determination of kinetic parameters using the phosphate glycosyltransferase activity assay

The commercial kit phosphate glycosyltransferase activity kit was purchased from R&D Systems (Abingdon, UK). The principle of the assay along with the materials provided were utilized according to manufacturer's conditions. The method was tailored to fit the needs and specificity of the working GT. To estimate the amount of UDP produced in the enzymatic reaction, a phosphate standard curve was established according to manufacturer's conditions. Briefly, 100 μM of the phosphate standard was prepared in 1X Assay Buffer (500 μL of Phosphatase buffer 1, 500 μL of

100 mM $MnCl_2$, 4.0 mL of deionized water). The standard was serially diluted across 12 wells in a 96-well plate. To each well, 30 µL of Malachite Green Reagent A and B were added according to manufacturer's protocol. Subsequently, the plate was incubated for 20 minutes at room temperature and the optical density (OD) at 620 nm was measured using the CLARIOstar microplate reader. Each dilution was performed in triplicates and the average was utilized to produce a calibration curve with Optical Density at 620 nm versus concentration of UDP. Moreover, along with the UDP standard curve an enzyme titration was performed where 10 µg/µL of UGT72B27 was serially diluted and subjected to an incubation of one hour at 30 °C with acceptor (thymol) and donor substrate (UDP-glucose) consequently heat stopped to terminate the reaction.

For the determination of kinetic parameters, a 50-µl GT reaction was prepared as follows: 200 mM Tris/HCl (pH 7.5), 100 µM UDP-glucose, 5 µg purified UGT72B27, with varying concentrations of substrate ranging from 0–2000 µM. The reaction was commenced by the addition of the sugar-donor, UDP-glucose. Termination of the enzyme reaction was executed via heating the reaction to 75 °C for 10 minutes. Subsequently, the reaction was centrifuged for 20 minutes to remove the precipitated enzyme and 25 µL was aliquoted into a 96-well plate. Correspondingly, 20 µL of 1X Assay Buffer and 5 µL of 20 µg/µL Coupling phosphatase was added. Together, all components in the microplate were incubated at 37 °C for 60 minutes. Following the 2-step incubation, 30 µL of Malachite Green Reagent A, 100 µL of distilled water, and 30 µL of Malachite Green Reagent B were added to the corresponding well containing the GT reaction in a step-wise manner. Following a 20-minutes room temperature incubation, the OD at 620 nm was measured using CLARIOstar. The amount of phosphate detected was directly proportional to the amount of UDP produced. The calibration curve was utilized to determine the enzymatic activity. All measurements were executed in triplicates with appropriate controls and the values were averaged **[Table 8]**.

2.8 Determination of kinetic parameters using the transcreener UDP² TR-FRET assay

The commercial kit transcreener UDP² TR-FRET glycosyltransferase assay was purchased from BellBrook Labs (Wisconsin, USA). The principle of the assay along with the materials provided were utilized according to manufacturer's conditions. Before commencing the measurements, the optimization of the maximum TR-FRET Window of the plate reader and the determination of the optimal UDP HiLyte647 Tracer concentration were conducted according to manufacturer's conditions. To estimate the amount of UDP produced in the enzymatic reaction, a UDP standard curve was established according to manufacturer's conditions. Briefly, a 12-point standard curve was prepared using concentrations of UDP-glucose and UDP from 1 µM to 1000 µM. Fifteen µL of each standard was aliquoted into the corresponding well of a 384-well plate and 5 µL of the UDP-Detection mixture (8 nM UDP² Antibody-Tb, 1X Stop & Detect Buffer C, 4 x (EC_{85}) UDP HiLyte647 Tracer) was added. The plate was incubated for 60 minutes at room temperature and the TR-FRET signal was measured via the plate reader. Each dilution was performed in triplicates and the average was utilized to produce a calibration curve with UDP (µM) versus TR-FRET 665:615 ratio.

For the determination of kinetic parameters, a 50-µl GT reaction was prepared as follows: 200 mM Tris/HCl (pH 7.5), 100 µM UDP-glucose, 5 µg purified UGT72B27, with varying concentrations of substrate ranging from 0–2000 µM. The reaction was commenced by the addition of the sugar-donor, UDP-glucose. Termination of the enzyme was executed via heating the reaction to 75 °C for 10 minutes. Subsequently, the reaction was centrifuged for 20 min to remove precipitated enzyme and 15 µL of the enzymatic reaction was aliquoted into a 384-well plate. Five µL of the 1X UDP Detection Mixture was added to each corresponding well and the plate was incubated for 60 minutes at room temperature. The TR-FRET signal was detected via plate reader

and the UDP amounts were extrapolated from the standard curve. The TR-FRET signal is inversely proportional to the amount of UDP present in the reaction. All measurements were executed in triplicates with appropriate positive and negative controls **[Table 8]**.

2.9 Evaluation of glycosyltransferases hydrolase activity

The recombinant proteins were assayed for UDP-glucose hydrolase activity in the presence of UDP-glucose. The by-products were identified by UDP-Glo™ assay. The UDP-Glo™ assay was utilized as described above in **Section 2.6**. The GT reaction was arranged according to **Table 9** and the reaction conditions were followed according to **Table 7** depending on the GT and its optimal conditions under study.

Table 9. Reaction set-up for the study of potential hydrolase activity of GTs.

Component	Final Concentration
Tris/HCl buffer	50 mM
GT Enzyme	according to Table 7
Acceptor substrate	none
Donor substrate UDP-glucose	100 μM
MilliQ H_2O	up to 100 μL

The UDP-glucose hydrolase activity was further investigated by the addition of various substrates that could have an activating or inhibitory effect on the hydrolase activity of the GT. These substrates were not known to be glycosylated by the enzyme under study and therefore, were selected as candidates for activation or inhibition of hydrolase activity. The substrates that were tested include retinol and β-carotene. The

UDP-Glo™ assay was utilized as described above in **Section 2.6** and the reaction was subjected to Liquid Chromatography Mass Spectrometry (LC-MS) analysis in order to ensure that the activating or inhibiting substrate is not glycosylated. **Table 10** outlines the reaction conditions and components that were prepared to study the activation and inhibition of GT hydrolase activity.

Table 10. Inhibition/activation of UGT hydrolase activity

Component	Final Concentration
Tris/HCl buffer	50 mM
GT Enzyme	according to Table 7
Substrate (retinol, β-carotene)	0 - 1200 μM
UDP-glucose	100 μM
MilliQ H_2O	up to 100 μL

2.10 Glycosyltransferase activity by LC-MS

The recombinant proteins were assayed for glycosylation activity with different substrates and the products were identified by LC-MS **[Table 11]**. The enzyme reaction was prepared according to **Section 2.4** and **Table 7** depending on the GT under study. For LC-MS analysis, the reaction was incubated in the dark for 17 hours and terminated via heating at 75 °C for 10 minutes. Subsequently, the reaction was centrifuged at high speed for 20 minutes. Thirty μL of the supernatant was utilized for LC-MS analysis. The samples were analyzed on an Agilent 6340 HPLC, which consisted of a capillary pump and a variable wavelength detector. The column was a LUNA C18 100A 150 x 2 mm (Phenomenex). LC was performed with the following binary gradient system: solvent A water with 0.1% formic acid; and solvent

B, methanol with 0.1% formic acid. The gradient program used was as follows: 0-3 minutes 100% A to 50% A / 50% B; 3-6 minutes 50% A / 50% B to 100% B; 6-14 minutes hold 100% B; 14 – 14.1 minutes 100% B to 100% A; 14.1 – 25 minutes hold 100% A. The flow rate was 0.2 mL/min. Attached to the LC was a Bruker esquire 3000 plus mass spectrometer with an electrospray ionization (ESI) interface that was used to record the mass spectra. The ionization voltage of the capillary was 4000 V and the end plate was set to -500V. MS spectra were recorded in alternating polarity mode and nitrogen was used as nebulizer gas at 30 p.s.i. and as dry gas at 330 C and 9 L/min [114]. LC-MS data were analyzed with Data Analysis 5.1 software (Bruker Daltronics).

Table 11. Diagnostic ions and wavelengths used for the detection of the glucoside products formed by UGTs from different substrates by LC-MS. *m*/*z* includes the mass of formic acid (CH_2O_2) 46 g/mol from the column.

Substrate	Diagnostic ions	*m*/*z* of the glucoside	UV Wavelength
ABA (Abscisic acid)	[M+HCOO]-	471	280
Apocarotenal	[M+HCOO]-	623	280
β-Carotene	[M+HCOO]-	743	280
Coniferylaldehyde	[M+HCOO]-	385	280
Coniferylalcohol	[M+HCOO]-	387	280
p-Coumarylaldehyde	[M+HCOO]-	355	280
p-Coumarylalcohol	[M+HCOO]-	357	280
α-Damascone	[M+HCOO]-	399	280
β-Damascone	[M+HCOO]-	399	280
FMT (Furan-2-ylmethanethiol)	[M+HCOO]-	321	280
Furaneol	[M+HCOO]-	335	280
Hydroquinone	[M+HCOO]-	317	280
α-Ionol	[M+HCOO]-	401	280
β-Ionol	[M+HCOO]-	401	280
α-Ionone	[M+HCOO]-	399	280
β-Ionone	[M+HCOO]-	399	280
Retinol	[M+HCOO]-	493	280
Scopoletin	[M+HCOO]-	399	280
Sinapylaldehyde	[M+HCOO]-	415	280
Sinapylalcohol	[M+HCOO]-	417	280
Umbelliferone	[M+HCOO]-	369	280

2.11 Enhancement and inhibition of glycosyltransferase activity

In this experiment, it was tested if the addition of a modifier (enhancing or inhibiting substrate) would affect the glycosylation of a substrate. UGT72AY1 glycosylates scopoletin with high efficiency. Potential modifiers/ligands including farnesol, apocarotenal, abscisic acid, β-carotene, and FMT were added in concentrations ranging 0, 50, 100, 200 μM. The assay was prepared according to **Table 12** and subjected to LC-MS quantification as described in **Section 2.10**. The reaction conditions included 0.1 μg of enzyme, incubation at 40 °C for 17 hours, and the reaction was terminated via heating the components to 75 °C for 10 minutes.

Table 12. Enhancement and/or inhibition of glycosyltransferase activity

Component	**Final Concentration**
Tris/HCl buffer	50 mM
GT Enzyme	according to Table 7
Substrate	50 μM, 100 μM, 200 μM
modifier/ligand	0 μM, 50 μM, 100 μM, 200 μM
UDP-glucose	100 μM
MilliQ H_2O	up to 100 μL

III. Results

In this doctoral thesis, high throughput methods for glycosyltransferase assessment and detection have been investigated and improved. This part of the results has been published in a peer-reviewed journal [64]. The newly established methods have uncovered additional activities of some UGTs known to be UDP-glucose hydrolase activity. This activity was further investigated and some novel and interesting findings were revealed. Furthermore, activation and inhibition of some plant UGTs was tested. All results were thoroughly documented and verified with a well-established LC-MS detection method and cross-referenced to previous publications.

3.1 Heterologous protein expression

For thorough biochemical characterization of recombinant proteins, the UGTs from *Vitis vinifera* (UGT72B27), *Nicotiana benthamiana* (UGT72AY1), *Pyrus communis* (UGT72B50, UGT72B51), and *Malus x domestica* (UGT72B46) cloned in pGEX-4T-1 expression vector containing an N-terminal glutathione S-transferase (GST-fusion) tag were generated in *E.coli* BL21 (DE3) pLysS cells, affinity purified and verified by SDS-PAGE and stained with Coomassie [**Figure 8, Figure 9, and Figure 10**].

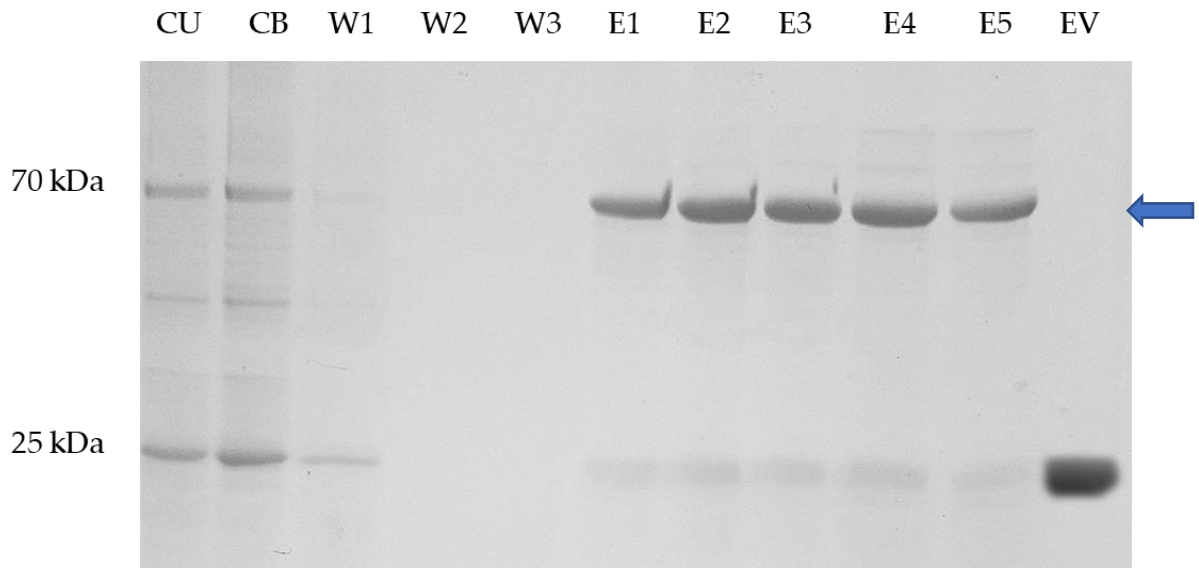

Figure 8. Image of the resulting Coomassie stained SDS-PAGE following the phosphate-free protein purification of the recombinant UGT72B27. CU = Crude protein unbound to GST resin. CB = Crude protein following the binding. W1 = first buffer wash. W2 = second buffer wash. W3 = third buffer wash. E1 – E5 = first to fifth elution of the purified recombinant protein. EV = empty PGEX-4T1 vector containing only the GST vector without the recombinant protein. The blue arrow indicates the target protein.

The resultant SDS-PAGE gels verified the presence and purity of the recombinant proteins at approximately 70 – 80 kDa (recombinant protein ~55 kDa with the GST tag ~25 kDa). The empty vector (EV) serving as a negative control presented a distinct band at approximately 25 kDa representing the GST protein (indicating the absence of the recombinant protein). Crude (CU, CB) and wash fractions (W1, W2, W3) show the presence of the protein of interest along with the other proteins present from *E. coli*. Elutions one to five (E1, E2, E3, E4, E5) indicate the purified eluted protein following the GST-resin binding. Several gels were performed following protein purifications via phosphate-based buffers **(Section 2.2)** and phosphate-free buffers **(Section 2.3)** and are presented in **Figure 9 and Figure 10**.

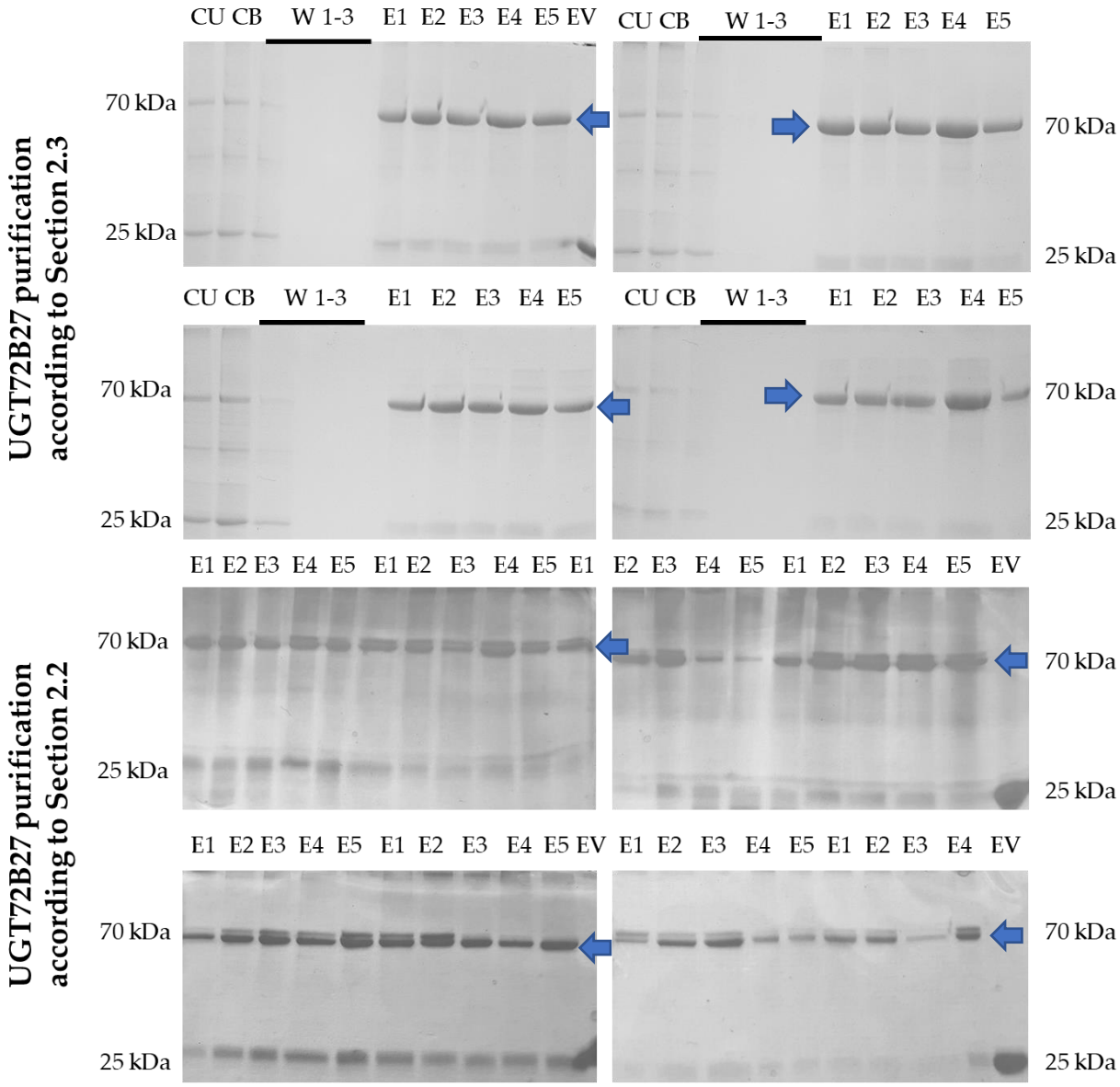

Figure 9. SDS-PAGE Coomassie stained gels from *Vitis vinifera* UGT72B27 – purified according to Sections 2.2 and 2.3. CU – Crude unbound to GST. CB – Crude bound to GST. W 1-3 – Wash Elutions 1, 2, and 3. E1 – E5 – Recombinant protein elutions 1 to 5. EV – Empty vector without recombinant protein. Elutions represented are from different protein purifications conducted throughout the study. Some Elutions, CU, CB, and W 1-3 are not shown. Arrows indicate target proteins.

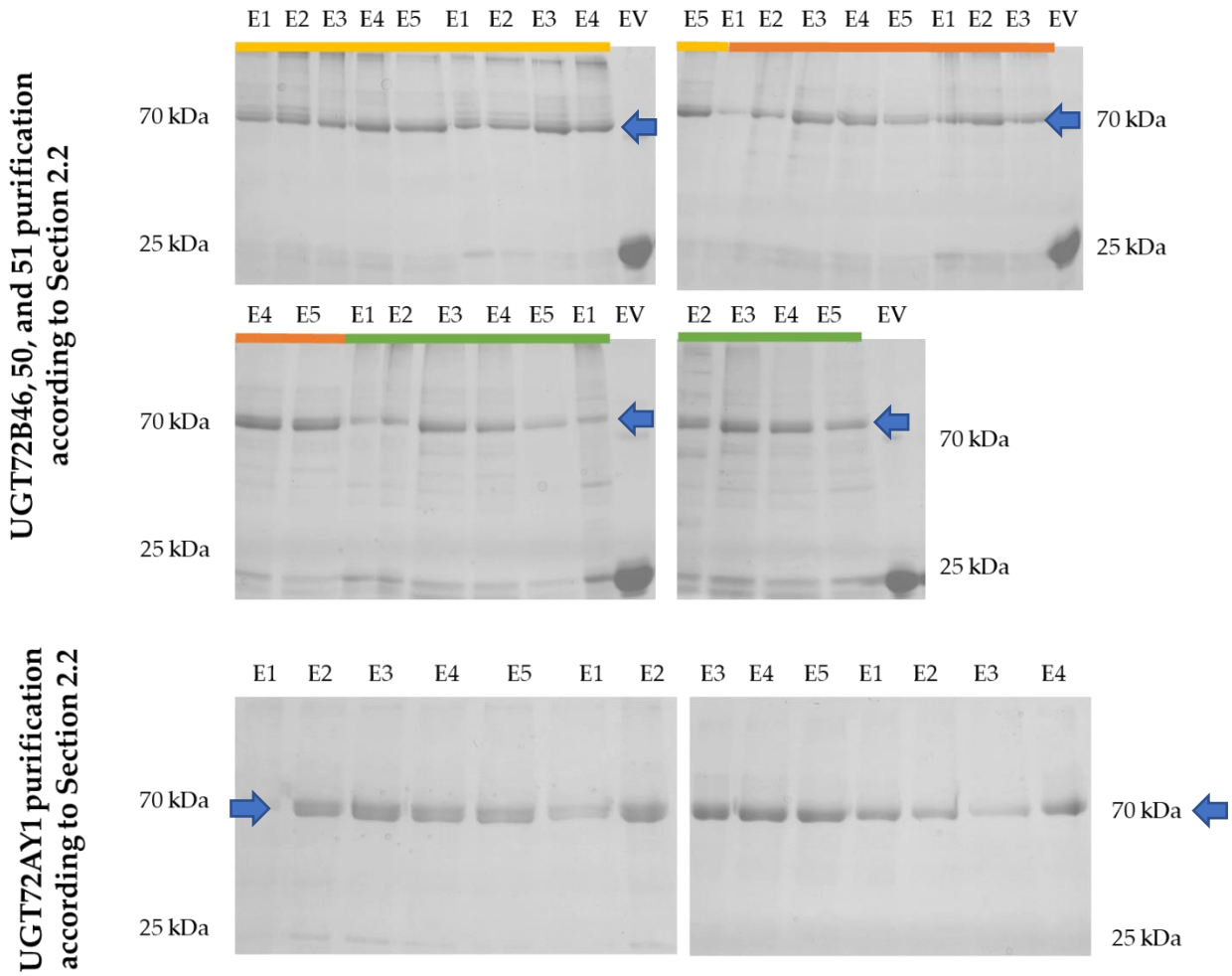

Figure 10. SDS-PAGE Coomassie stained gels from *Pyrus communis* (UGT72B50 and 51) (yellow and orange), *Malus x domestica* (UGT72B46) (green), and *Nicotiana benthamiana* (UGT72AY1) purified according to Sections 2.2. E1 – E5 – Recombinant protein elutions 1 to 5. EV – Empty vector without recombinant protein. Elutions represented are from different protein purifications conducted throughout the study. Some Elutions, CU, CB, and W 1-3 are not shown. Arrows indicate target proteins

3.2 The pH-sensitive colorimetric glycosyltransferase activity assay

The assay was adapted from [52] and utilized in the determination of kinetic data of UGT72B27 [63] in high-throughput (HTP). The experimental setup included a 96-well plate where all the reaction components were added except for the sugar donor (UDP-glucose) and the pH indicator phenol red. Low molecular weight phenols and furaneol were used as acceptor substrates [**Figure 11**]. The program on the microplate reader was set-up where it is utilizing the injector functions adding the appropriate amount of UDP-glucose and phenol red in a sequential manner, thereby validating its HTP potential. The shaker function and incubation function of the multi-plate reader was employed for the automation of the mixing of the reaction components, and incubating the reaction at the appropriate temperature. Following the reaction time, the measurements at the wavelength of 557 nm were obtained. The observation of data was unsuccessful as no viable data could be collected. The data of the technical and biological replicates varied considerably; reproducible results were unattainable. The pH-sensitive assays appear to be very susceptible to interferences and therefore it was concluded that this colorimetric assay cannot be executed in a high-throughput format. In this study, for the comparison of the kinetic properties with subsequent assays the numerical data from [63] was utilized [**Table 13**].

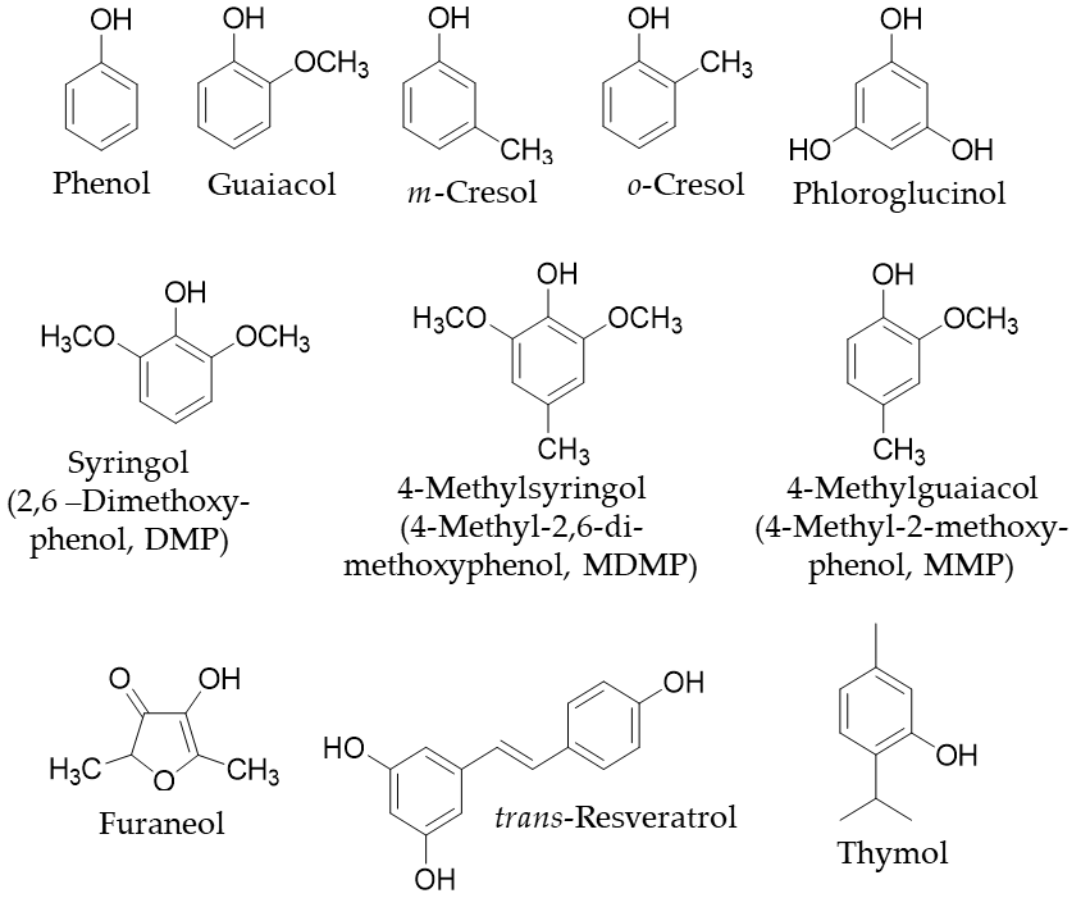

Figure 11. Chemical structures of plant secondary metabolites. These were utilized in the detection of kinetic properties of UGT72B27 for the comparison analysis of the HTP methods.

3.3 UDP-Glo™ glycosyltransferase activity assay

The protocol was followed according to manufacturer's instructions. Prior to utilizing this assay, all the manufacturer recommended metrics and measurement thresholds were identified and tested to ensure it is able to function with the plant GT and hydrophobic substrates under question. For example, the gain and focal length on the plate reader's illuminometer program was adjusted to fit the assay. As well as, the substrates contained appropriate DMSO concentrations to ensure proper and unhindered luminescence signals in order to remain within the UDR's threshold. Finally, the standard curve with increasing amount of UDP-glucose was conducted **[Figure 12]**.

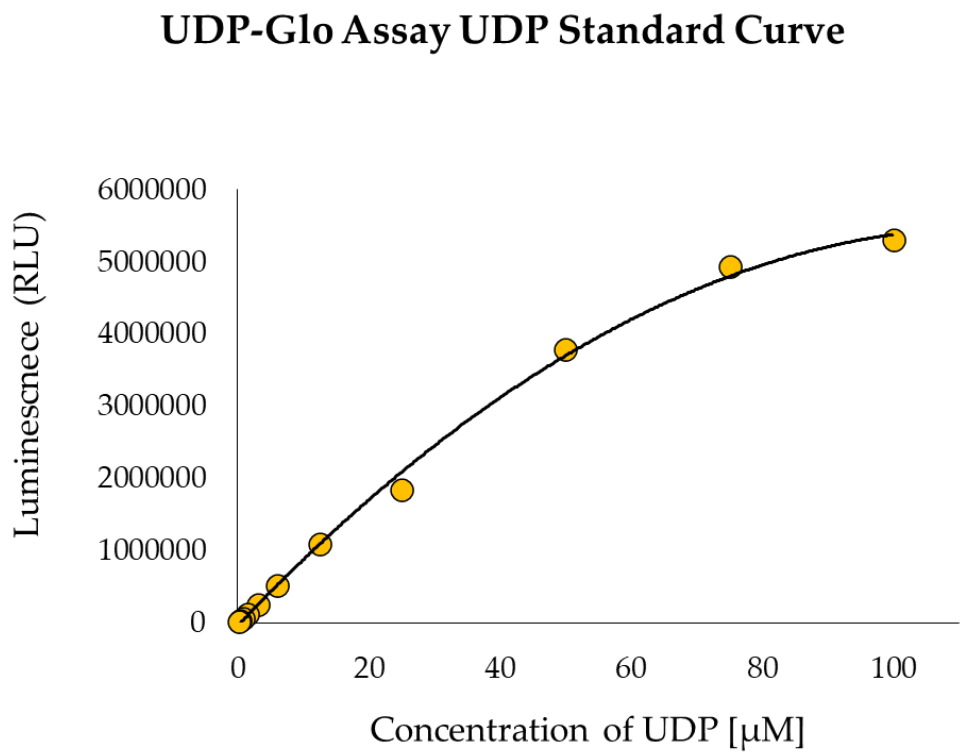

Figure 12. Standard curve for UDP concentration was established with the UDP Glo™ assay. The luminescence is directly proportional to the concentration of UDP produced. n=2.

Moreover, the protocol was tailored to plant GTs by incorporating an additional heat-stop inactivation step at 75 °C after the enzyme reaction. It turned out that the UDR stopping agent provided by the manufacturer is a metal chelating detergent, which terminates the enzymatic reaction of a metal-depending GT. Since UDP-forming activity of UGT72B27 after addition of UDR was still detected, an additional heat-inactivation step was used prior to the addition of UDR to ensure the termination of the catalysis of the plant enzyme [**Figure 13**]. The comparison of the two graphs shows that less UDP is formed after heat-inactivation of the enzyme and the curve better fits the Michaelis-Menten kinetics model. It seems that UGT family-1 enzymes are not highly dependent on metal ions. Although divalent cations (e.g., Mg^{2+}) are required for full activity of GT-B enzymes, including plant enzymes of the UGT family-1, there is no evidence of a metal ion bound in the GT-B structures [115]. Furthermore, the assay was utilized to establish the optimal conditions for the enzyme. As a result, with the UDP-Glo™ GT activity assay it was determined that the optimal conditions for the working enzyme, UGT72B27, are pH of 7.5, for 10 minutes, and at 30 °C, which is in accordance to the results obtained with the pH-sensitive assay for UGT72B27 [63].

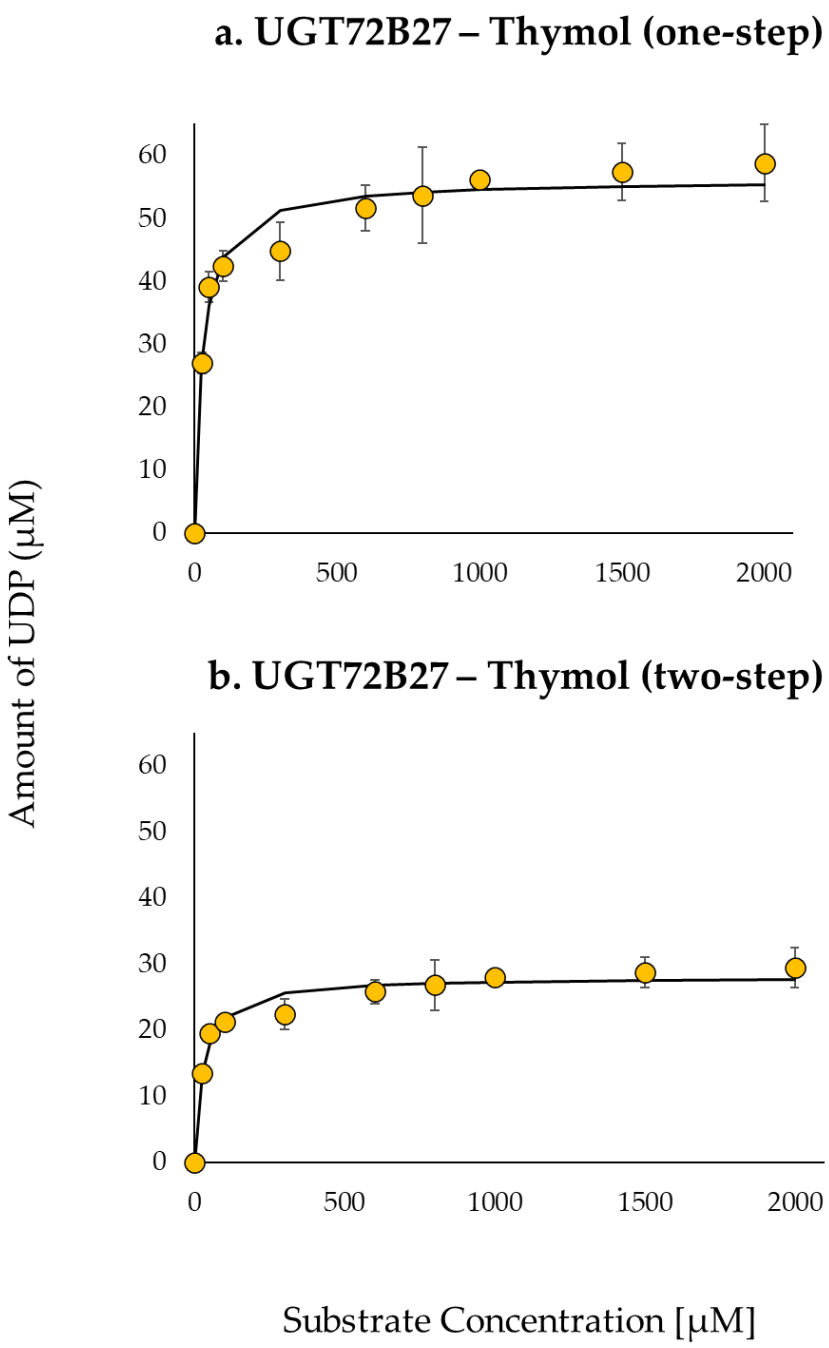

Figure 13. Graphical representation of the optimization of the UDP-Glo™ assay, (a) UGT72B27 with thymol employed according to manufacturer's conditions in a one-step manner where kinetic data was calculated. (b) UGT72B27 with thymol executed in two-steps with an additional heat stop GT inactivation prior to UDR addition, ultimately tailored to fit plant family-1 GTs.

Furthermore, the assay was tested and its functionality was verified by utilizing UGT72B27 with various naturally occurring substrates including guaiacol (2-methoxyphenol), resveratrol, thymol, syringol (2,6–dimethoxyphenol, DMP), 4-methylguaiacol (4-methyl-2-methoxyphenol, MMP), m-cresol, o-cresol, phloroglucinol, phenol, 4-methylsyringol (4-methyl-2,6-dimethoxyphenol, MDMP), and furaneol [**Figure 11**]. The reaction was allowed to proceed at the optimal conditions in 384-well plates and upon heat inactivation and addition of UDR the free UDP was converted to ATP generating light [**Figure 5**]. The intensity of the light was detected and was converted to the amount of UDP in μM using the previously obtained standard curve **[Figure 12]**. The kinetic properties were calculated through the Michaelis-Menten equation. When comparing the results of the pH-sensitive assay determined by single measurements [63] with the results obtained with the UDP-Glo™ activity assay in 384-well plate, it can be seen that the two assays with the same GT and substrates yield different kinetic parameters **[Table 13].** The pH-sensitive assay showed higher K_M and k_{cat} values than the UDP-Glo™ assay. In general, the pH-sensitive assay yielded higher k_{cat}/K_M values in comparison to the UDP-Glo™ assay **[Table 13]** [64].

Table 13. Kinetic values of purified UGT72B27 enzyme obtained via three different methods. (a) pH-sensitive assay, data obtained from colleagues [63], obtained by single measurements. (b) UDP-Glo™ assay measured in 384-well plate [64], and (c) phosphate glycosyltransferase activity assay, measured in 96-well plate [64]. Substrate concentrations were varied from 10-3000 μM, Guaiacol: 2-Methoxyphenol, DMP: 2,6-Dimethoxyphenol, MMP: 2-Methoxy-4-methylphenol, MDMP: 4-Methyl-2,6-dimethoxyphenol. K_M (μM), k_{cat} (sec^{-1}), k_{cat}/K_M (mM^{-1} sec^{-1}). n=3. (*) since the publication, this value was corrected.

Substrate	a. pH-sensitive assay			b. UDP-Glo™ assay			c. Phosphate GT assay		
	K_M	k_{cat}	k_{cat}/K_M	K_M	k_{cat}	k_{cat}/K_M	K_M	k_{cat}	k_{cat}/K_M
Guaiacol	*32 ± 1	2.3 ± 0.02	72.53 ± 3	23 ± 1	0.08 ± 0.02	3.7 ± 1	28 ± 3	0.13 ± 0.003	4.7 ± 0.6
***trans*-Resveratrol**	36 ± 5	0.6 ± 0.05	17.0 ± 3.8	21 ± 5	0.004 ± 0.0001	0.2 ± 0.05	15 ± 1	0.02 ± 0.002	1.3 ± 0.2
Thymol	53 ± 0.25	0.7 ± 0.07	13.5 ± 1.4	28 ± 7	0.04 ± 0.003	1.4 ± 0.1	20 ± 1	0.07 ± 0.001	3.3 ± 0.2
DMP	211 ± 52	1.9 ± 0.05	8.8 ± 2.4	23 ± 3	0.09 ± 0.003	3.7 ± 0.6	41 ± 4	0.1 ± 0.004	2.3 ± 0.3
MMP	115 ± 22	0.9 ± 0.01	8.0 ± 1.6	41 ± 9	0.06 ± 0.001	1.4 ± 0.3			
***m*-Cresol**	48 ± 19	0.4 ± 0.02	7.9 ± 3.5	14 ± 3	0.04 ± 0.002	2.6 ± 0.6	15 ± 2	0.05 ± 0.0005	3.4 ± 0.5
Phloroglucinol	77 ± 10	0.5 ± 0.05	7.1 ± 1.6	35 ± 4	0.05 ± 0.006	1.3 ± 0.3	47 ± 4	0.09 ± 0.006	1.9 ± 0.3
***o*-Cresol**	148 ± 14	0.5 ± 0.04	3.6 ± 0.6	40 ± 5	0.05 ± 0.002	1.4 ± 0.2	32 ± 2	0.06 ± 0.005	1.8 ± 0.3
MDMP	278 ± 22	0.5 ± 0.04	1.9 ± 0.3	173 ± 28	0.05 ± 0.005	0.3 ± 0.07	143 ± 13	0.06 ± 0.002	0.5 ± 0.1
Phenol	326 ± 83	0.6 ± 0.04	1.8 ± 0.6	153 ± 24	0.04 ± 0.002	0.3 ± 0.06	62 ± 0.5	0.07 ± 0.007	1.1 ± 0.1
Furaneol	478 ± 45	0.5 ± 0.04	1.0 ± 0.2	453 ± 35	0.02 ± 0.002	0.04 ± 0.007			

3.4. Phosphate glycosyltransferase activity assay

The protocol was followed according to manufacturer's instructions. According to the manufacturer's directions, the coupling phosphatase enzyme (CP) is to be added at the same time as the GT enzyme in a one-step reaction. However, not all GTs function at these conditions and cannot be stopped using the metal chelating agent provided, especially plant GTs which probably do not possess a metal center [115] **[Figure 14]**. The curves obtained by applying the original protocol did not allow calculation of kinetic data. Therefore, the manufacturer's protocol was tailored to UGT72B27 from *V. vinifera* and was executed in a two-step procedure. The GT reaction was allowed to proceed in 96-well plate. Afterwards, the GT was inactivated by heating and then CP enzyme was added that the inorganic phosphate could be cleaved off the free UDP. The amount of the released phosphate was determined by Malachite Green reagents and the optical density was measured. The optimized protocol enabled the calculation of kinetic data presented in **Table 13**.

Prior to utilizing this assay, all the metrics and measurement thresholds were identified and tested to ensure it is able to function with plant GT's and hydrophobic substrates. For example, protein purification protocols were adjusted to ensure all contents remain phosphate-free whilst conserving the proteins activity. Moreover, the CP concentration diluted in the 1X Assay Buffer was tested to ensure proper amounts and its feasibility and activity with the new assay conditions.

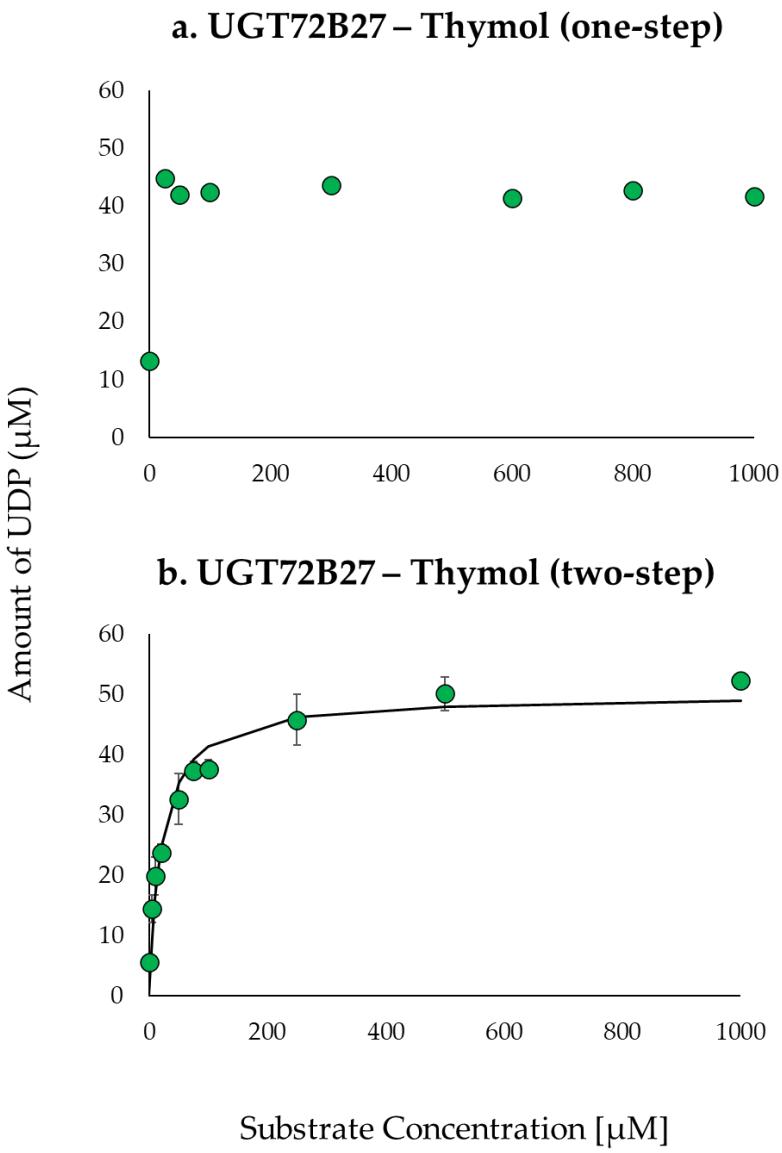

Figure 14. Graphical representation of the optimization of the phosphate assay, (a) UGT72B27 with thymol employed according to manufacturer's conditions in a one-step manner where kinetic data could not be calculated. (b) UGT72B27 with thymol executed in two-steps with an additional heat stop GT inactivation prior to CP addition, ultimately tailored to fit plant family-1 GTs.

Finally, the standard curve for phosphate was established **[Figure 15]**. Furthermore, the assay was utilized to establish the optimal conditions for the enzyme, ensuring that the results obtained will be comparable to the already known optimal conditions. As a result, with the phosphate glycosyltransferase activity kit it was determined that the optimal conditions for the working enzyme, UGT72B27, are pH of 7.5, for 10 minutes, and at 30 °C, which are identical to the conditions obtained by the UDP-Glo™ assay.

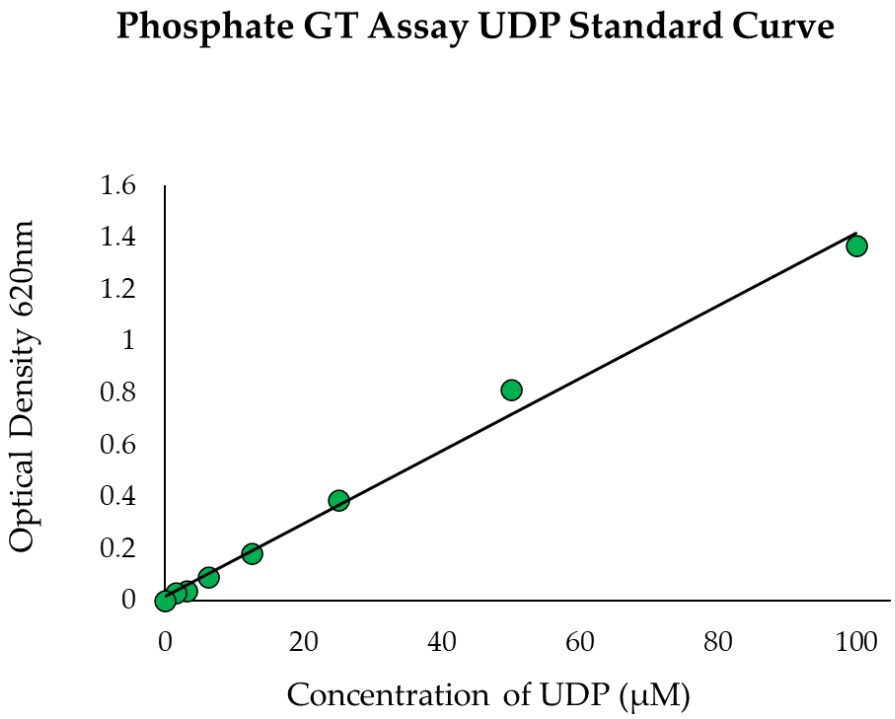

Figure 15. Standard Curves for UDP concentration were established with the Phosphate GT Assay. The optical density is directly proportional to the concentration of UDP produced. n=2.

Furthermore, the assay was tested and its functionality was verified by utilizing UGT72B27 with various naturally occurring phenolic substrates and furaneol **[Figure 11]**. The two-step reaction with the phosphatase enzyme was carried out and the OD_{620} was measured and converted to the phosphate concentration (pmol/well). With the obtained data, the kinetic properties were calculated through the Michaelis-Menten equation **[Table 13]**. Similar to the UDP-Glo™ assay, the phosphate GT assay showed lower K_M and K_{cat} values than the pH-sensitive assay. Interestingly, the kinetic values obtained via the phosphate activity assay are very similar and not statistically different to those obtained through the UDP-Glo™ activity assay. The two assays, even though performed independently of each other, yielded similar kinetic results **[Table 13, Figure 16]**. Meanwhile, the pH-sensitive assay yielded completely dissimilar kinetic values **[Table 13]**. This further indicated that the pH-sensitive assay is unreliable in conducting kinetic analyses and was excluded from further studies.

For further comparison of the two successful methods – UDP-Glo™ and phosphate GT activity assay – a general independent substrate screen utilizing other plant secondary metabolites was performed [**Figure 17**]. When conducted with two assays, majority of the substrates have showed similar to nearly-similar detected UDP concentration amounts.

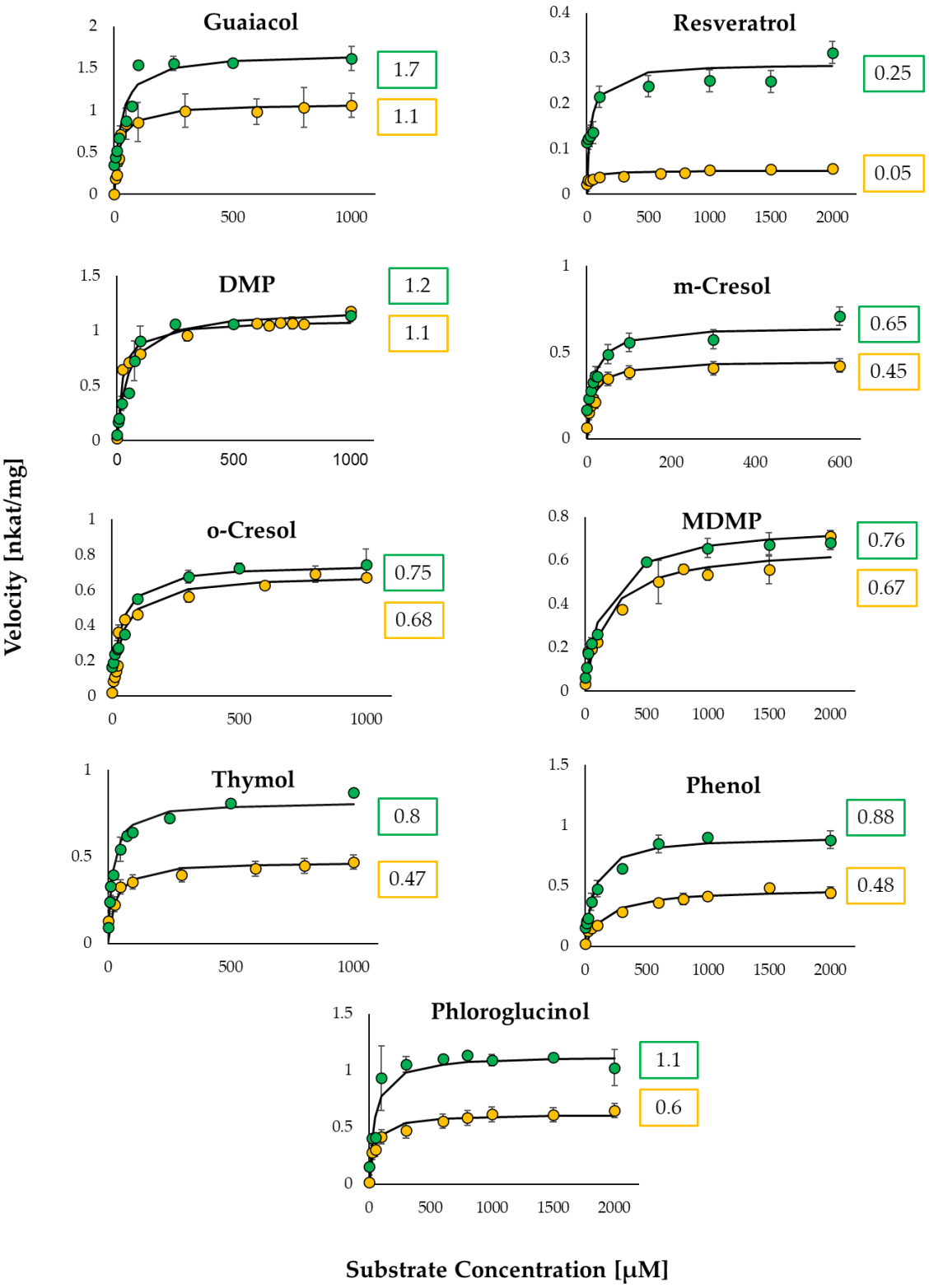

Figure 16. Michaelis-Menten curves for the substrates glycosylated by UGT72B27 quantified with UDP-Glo™ assay (yellow) and phosphate GT activity assay (green). The maximum velocity (V_{max}) (nkat/mg) are presented per curve and color-coded according to the assay. n=3.

This indicates that the two assays are able to generate similar and comparable results. The UDP-Glo™ and phosphate GT activity assay have shown consistent and similar substrate specificity of UGT72B27 with 28 out of 32 new substrates (87.5%). Although, four substrates (naphthol, β-citronellol, ellagic acid) out of 32 (12.5%) showed dissimilar UDP amounts and thus, GT activity when tested with the two assays. Therefore, it seems that there is no universal assay, which is suitable for all different substrates. Alternative HTP assays as well as, LC-MS should be applied to avoid overlooking potential GT acceptors.

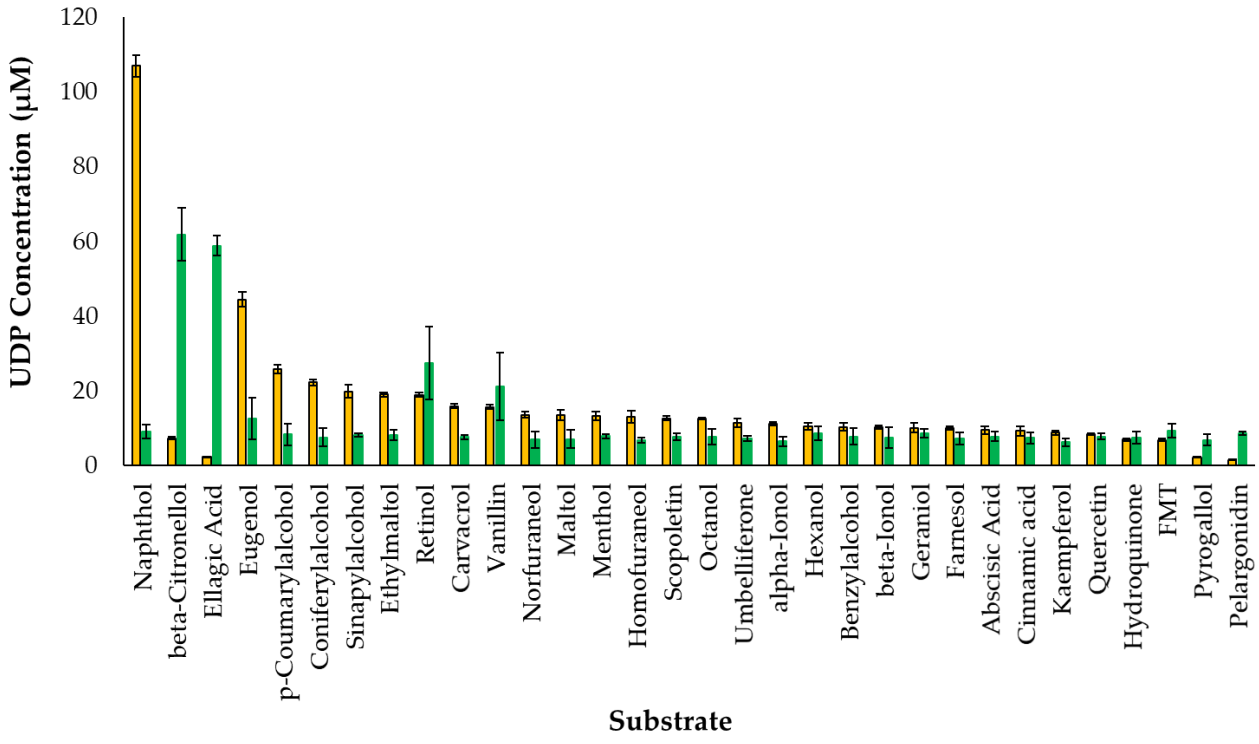

Figure 17. General comparison of substrate screen of UGT72B27 analyzed via UDP-Glo™ assay (yellow) and phosphate GT activity assay (green). n=3.

3.5 Transcreener UDP^2 TR-FRET assay

The protocol was followed according to manufacturer's instructions. Being a competitive immunoassay for UDP with a far-red, time-resolved Foerster-resonance-energy-transfer (TR-FRET) readout, the assays' idea is a quick mix and read format. Theoretically, the assay should be applied and utilized with a broad range of substrates and UGTs. Upon initiating the assay with the respective UGT and substrates, all the metrics and measurement thresholds were identified and tested to ensure it is able to function with plant GTs and hydrophobic substrates. For example, the Z' value is a factor used to assess the quality of a screening assay. A Z' value of 1 is ideal, 0.5-1 is an excellent assay, and below 0.5 is marginal indicating the assay is not suitable for screening purposes [116]. The Z' value obtained for the assay was above 0.7 and the standard curve was established. As indicated by the manufacturer, the antibody is stable and multiple thaw-and-freeze cycles are acceptable. However, from day-to-day the standard curve values changed and were unreproducible which indicated that the antibody is unstable. The antibody was precipitating on multiple occasions and even when fresh kit reagents were ordered, the attempts were all unsuccessful. Following the difficult and lengthy establishment of the parameters, the substrate screens and kinetics were vastly different between biological and even technical replicates. The 'stop and detect buffer C' was utilized to stop the GT reaction in a one-step format; however, it was discovered that this only worked for GTs with a metal center. Therefore, the assay was altered by adding an additional step to heat stop the reaction and successfully terminate the GT. Despite this, the assay could not yield stable and consistent results **[Figure 18].** It is evident that the same combination of enzyme, acceptor and donor substrate along with the tailored step for plant family-1 GTs, the assay could not yield a quantifiable readout as compared to the UDP-Glo™ assay **[Figure 13]** and phosphate GT activity assay **[Figure 14]**.

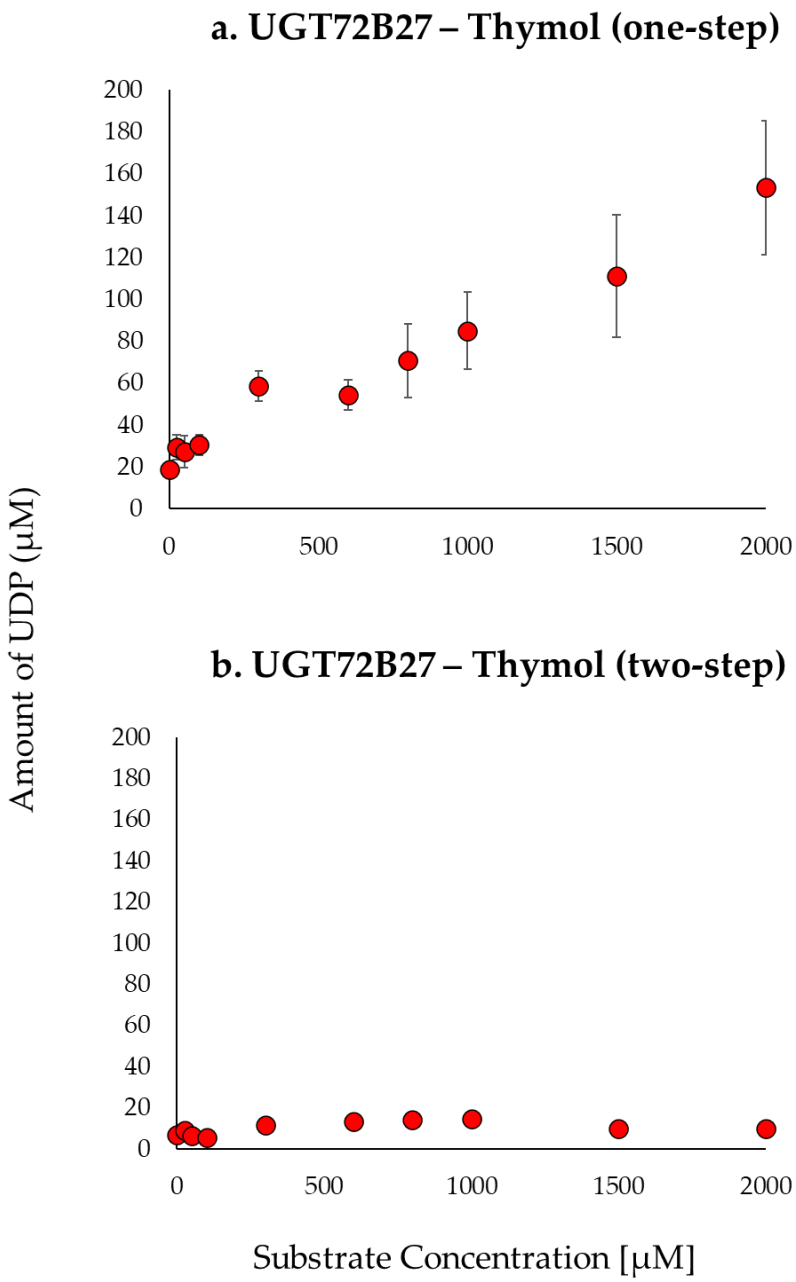

Figure 18. Graphical representation of the optimization of the UDP[2] TR-FRET immunoassay, (a) UGT72B27 with thymol employed according to manufacturer's conditions in a one-step manner where kinetic data could not be calculated. (b) UGT72B27 with thymol executed in two-steps with an additional heat stop GT inactivation prior to antibody addition.

3.6 Glycosyltransferases with an inherent hydrolase activity

Following the establishment and tailoring of UDP-Glo™ assay to suit family-1 plant GTs, the method has been employed by several colleagues in screening and kinetic analyses of various GTs from a vast range of species along with many secondary metabolites. Upon screenings and kinetic analyses, findings demonstrating a GTs' innate hydrolase activity, which in the absence of an acceptor molecule led to the rapid degradation of UDP-glucose in some GT reactions. Without the presence of an acceptor substrate, the water is acting as a substrate producing glucose and free UDP – allowing UDP-Glo™ assay to detect UDP and produce quantifiable luminescence signals (RLU) **[Figure 7]**. The luminescence signal was increasing as the incubation time was increasing. To further investigate the nature of this hydrolase activity and whether it can be activated or inhibited, several assays were conducted as mentioned in **Section 2.9.**

Three homologous GTs from *Pyrus communis* (UGT72B50 and UGT72B51) and *Malus x domestica* (UGT72B46) have studied. The three GTs were subjected to optimal reaction conditions as outlined in **Table 7.** The GTs were tested for activity with their natural substrate, hydroquinone, and the products were analyzed via LC-MS revealing positive activity **[Figure 19]**.

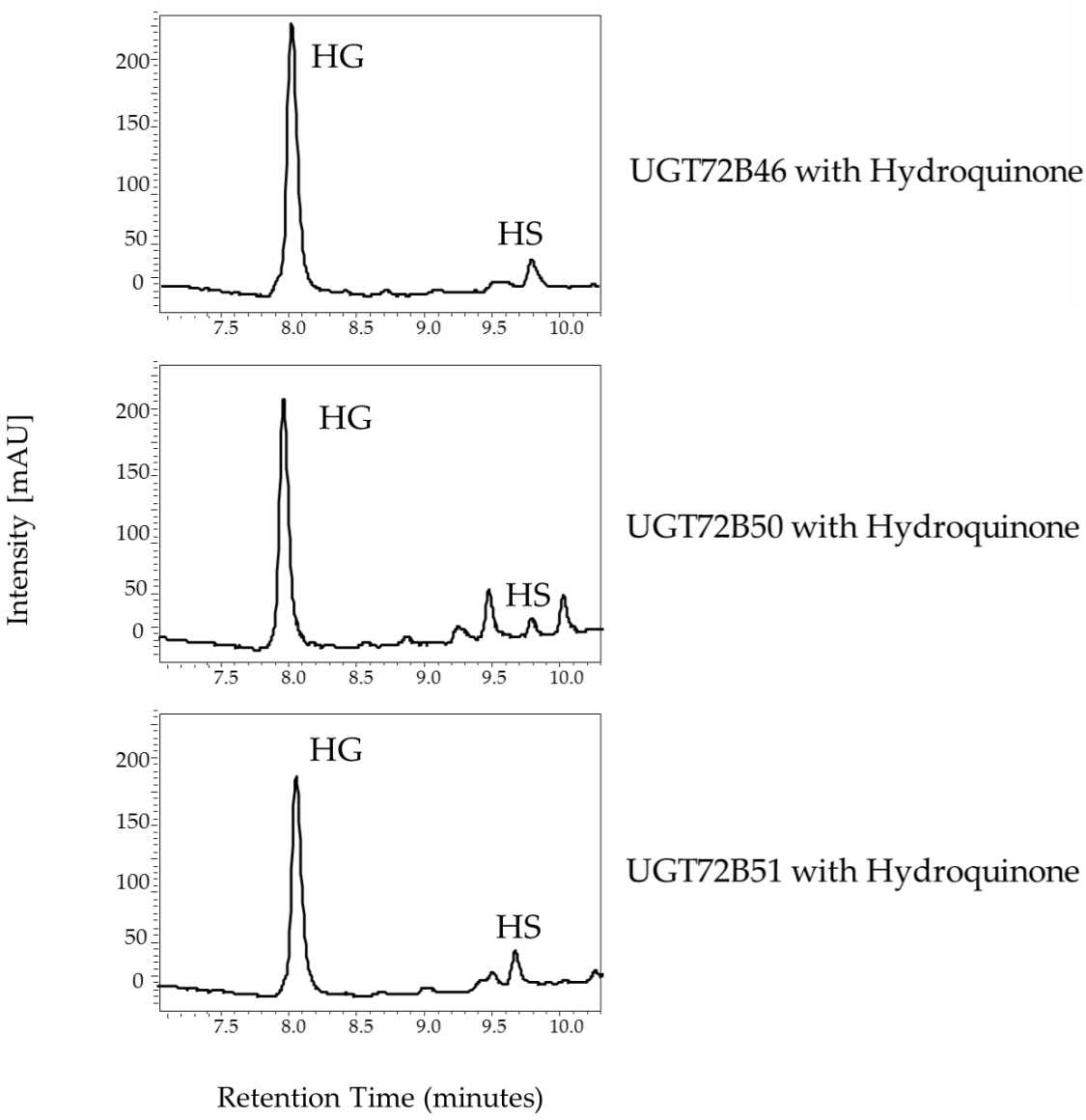

Figure 19. LC-MS analysis of the glucoside product formed by *Malus x domestica* (UGT72B46) and *Pyrus communis* (UGT72B50 and 51) from hydroquinone. UV trace at 280 nm. HG, hydroquinone glucoside. HS, hydroquinone substrate. X-axis represent retention time and Y-axis represent intensity.

The hydrolysis reaction was allowed to proceed without an acceptor substrate and only with the donor substrate (UDP-glucose) as outlined in **Section 2.9**. A control was included which contained all of the same parameters but without an active enzyme (grey). The findings reveal a linear increase in relative enzyme activity over time **[Figure 20]**. This indicates that with the presence of the enzyme and absence of the acceptor substrate, hydrolysis has taken place and the free-UDP was detected by the UDP-Glo™ assay.

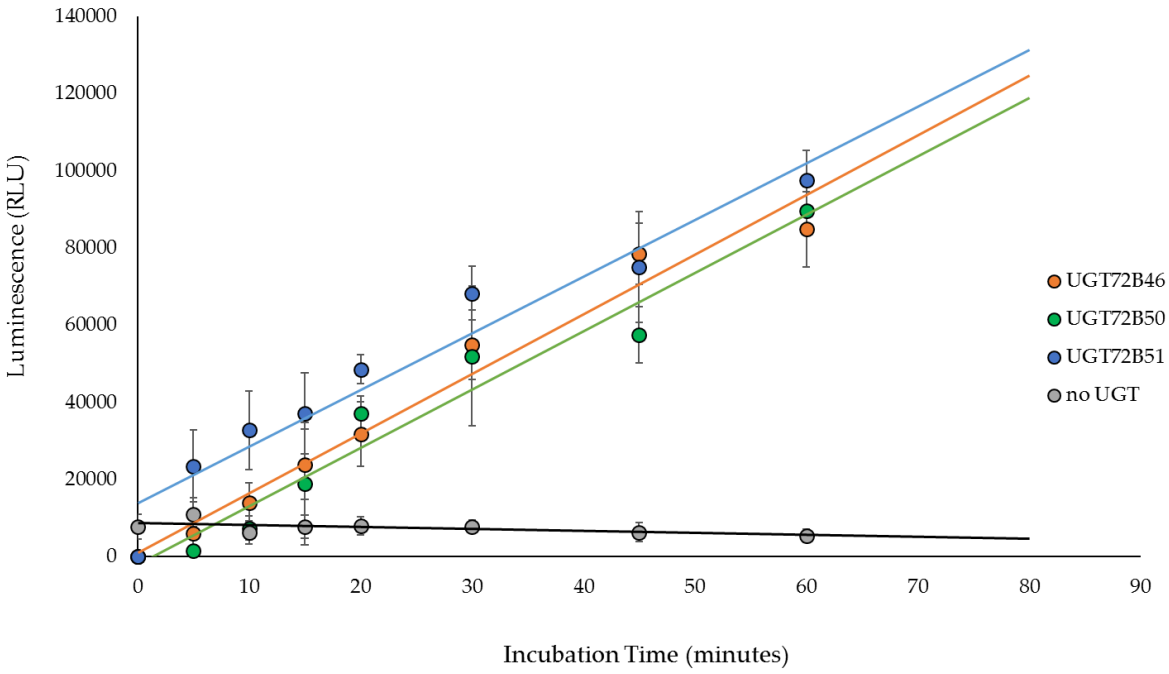

Figure 20. Positive hydrolase activity of UGT72B46, UGT72B50, and UGT72B51 with relative enzyme activity over time**.** n=3.

In addition to UGT72B46, UGT72B50, and UGT72B51, it has already been shown by colleagues that UGT72AY1 from *Nicotiana benthamiana* shows UDP-glucose hydrolase activity, which could be inhibited by β-ionone and β-ionol. Since retinol and β-carotene also have a β-ionone ring structure and are therefore structural

homologues, their effect on the UDP-glucose hydrolase activity of UGT72AY1 was investigated. LC-MS analysis showed that retinol is not glucosylated by UGT72AY1 and β-carotene cannot be glucosylated because it has no hydroxyl group.

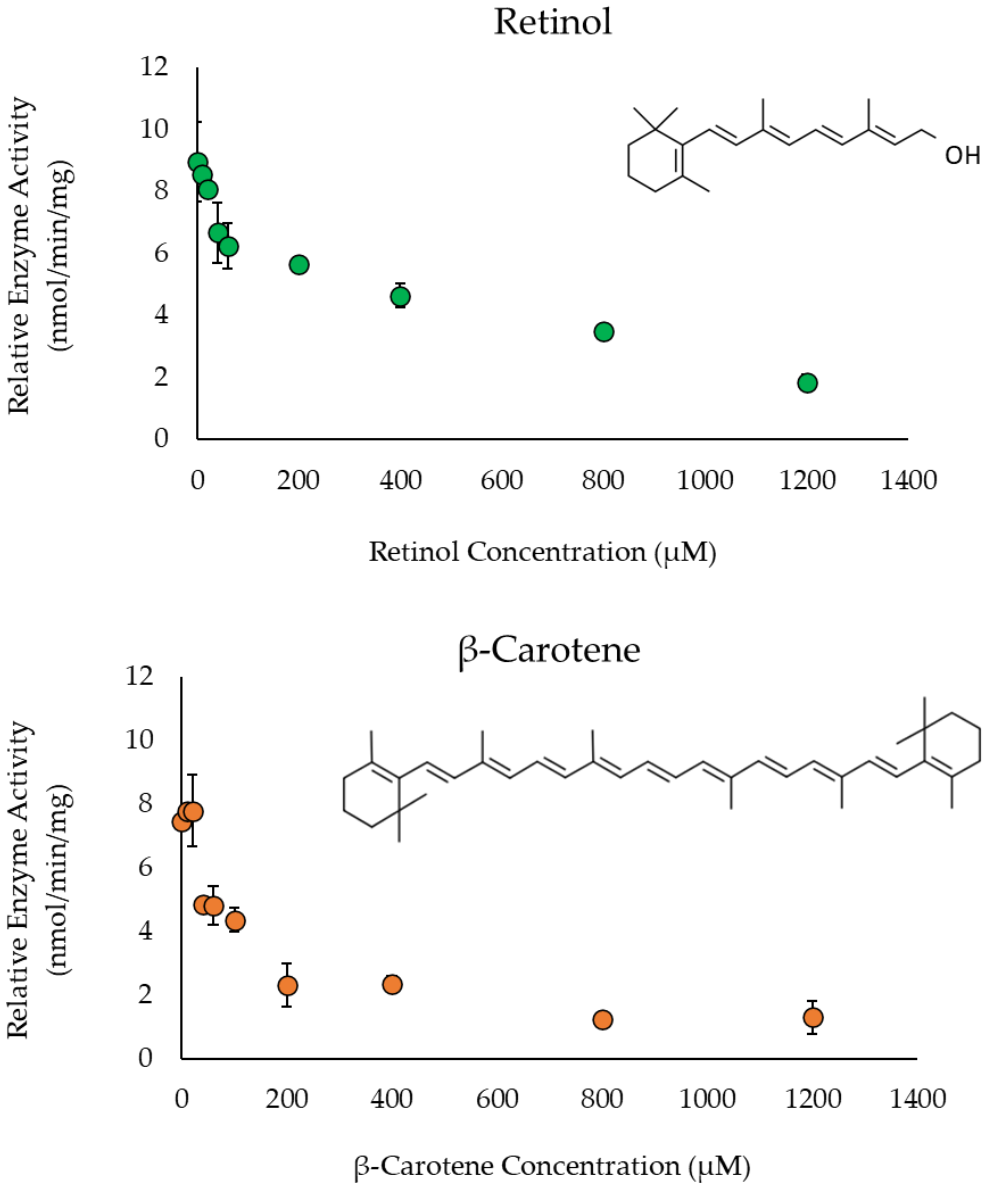

Figure 21. Inhibition of UGT72AY1 hydrolase activity with increasing concentrations of retinol (green) and β-carotene (orange). n=3.

Moreover, when the two substrates are added in increasing concentrations to solutions containing UGT72AY1 and UDP-glucose, and subjected to UDP-Glo™ analysis, the production of UDP shows a distinct downward trend [**Figure 21**]. This downward curve indicates that as the concentration of the substrate increases the relative UDP-hydrolase activity decreases. This signifies that with an increased amount of substrate the hydrolase activity of the GT is diminished – resulting in a competitive allosteric inhibition. The substrates, retinol and β-carotene, are competing with the water molecules and are blocking the active sites of UGT72AY1 preventing hydrolysis. Further research can be undertaken in order to calculate the kinetic data of the hydrolase activity incorporating different UGTs and a vast spectrum of secondary metabolites.

3.7 Enhancement and inhibition of glycosyltransferase activity

Functional analyses utilizing the tailored and established HTP method, UDP-Glo™ – along with LC-MS allowed for the further investigation of enhancement and/or inhibition of glycosyltransferase activity. UGT72AY1 has a wide range of acceptor substrates including, scopoletin [117].

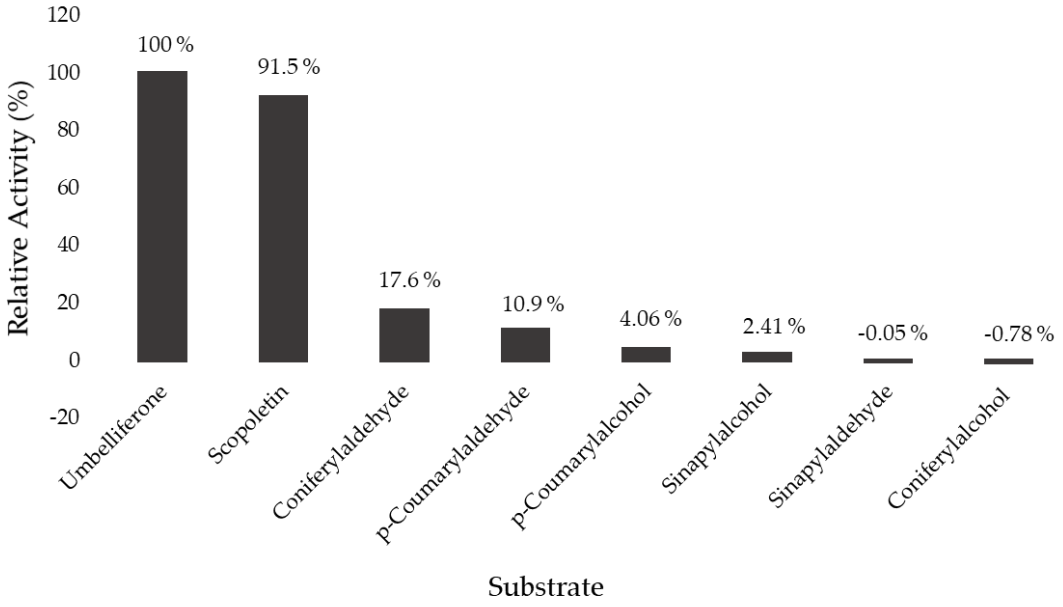

Figure 22. Substrate screen of UGT72AY1 with various substrates analyzed with UDP-Glo™.

To further investigate the functionality of the enzyme, it was subjected to a glycosylation reaction under optimal conditions [**Table 7**] along with additional substrates of similar chemical structure and backbone to scopoletin including, umbelliferone **[Figure 23]**, coniferyl aldehyde, *p*-coumaryl aldehyde, *p*-coumaryl alcohol, sinapyl alcohol, sinapyl aldehyde, and coniferyl alcohol **[Figure 24].**

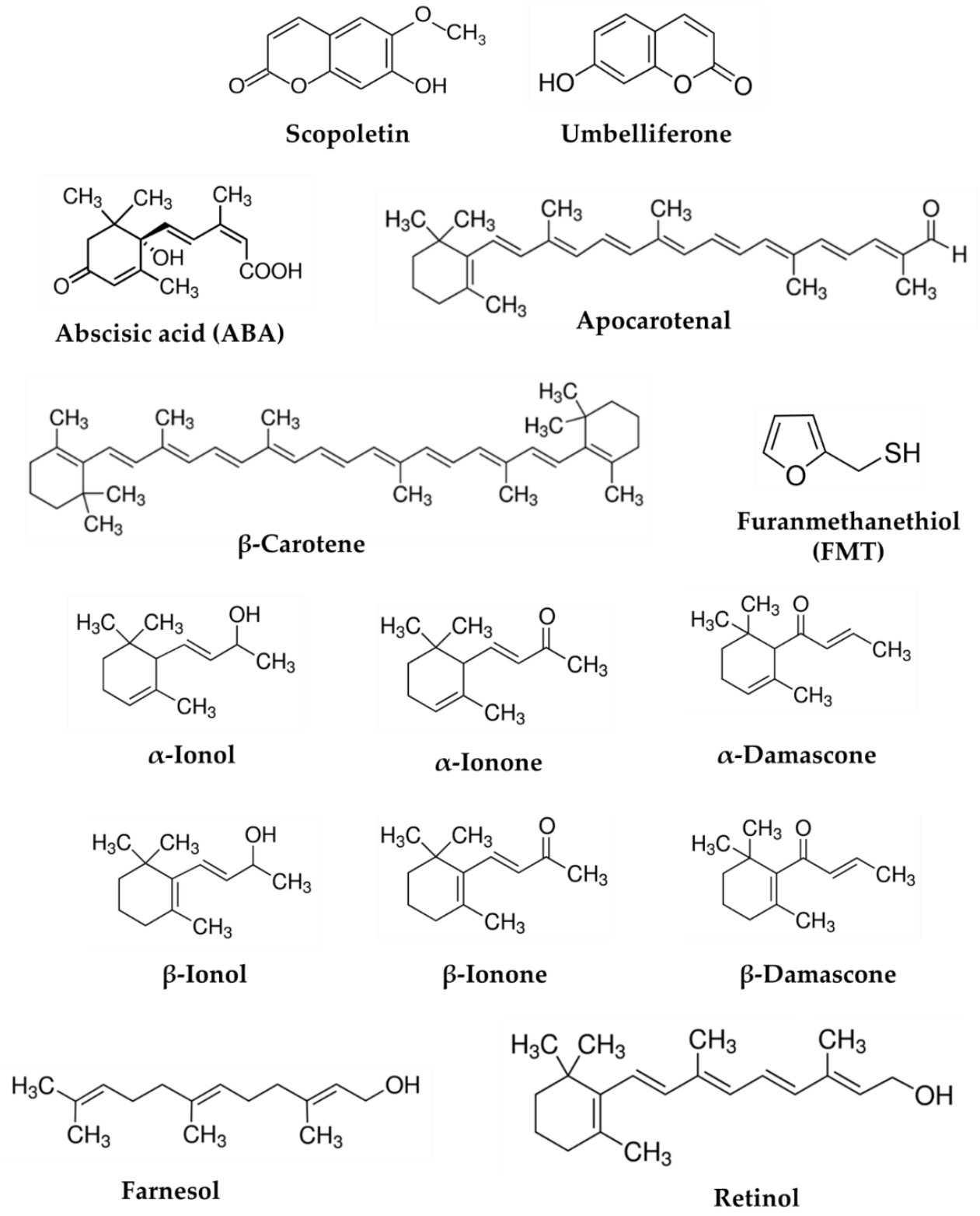

Figure 23. Chemical structures of the substrates utilized for the enhancement and inhibition of UGT72AY1 scopoletin and umbelliferone glycosylation.

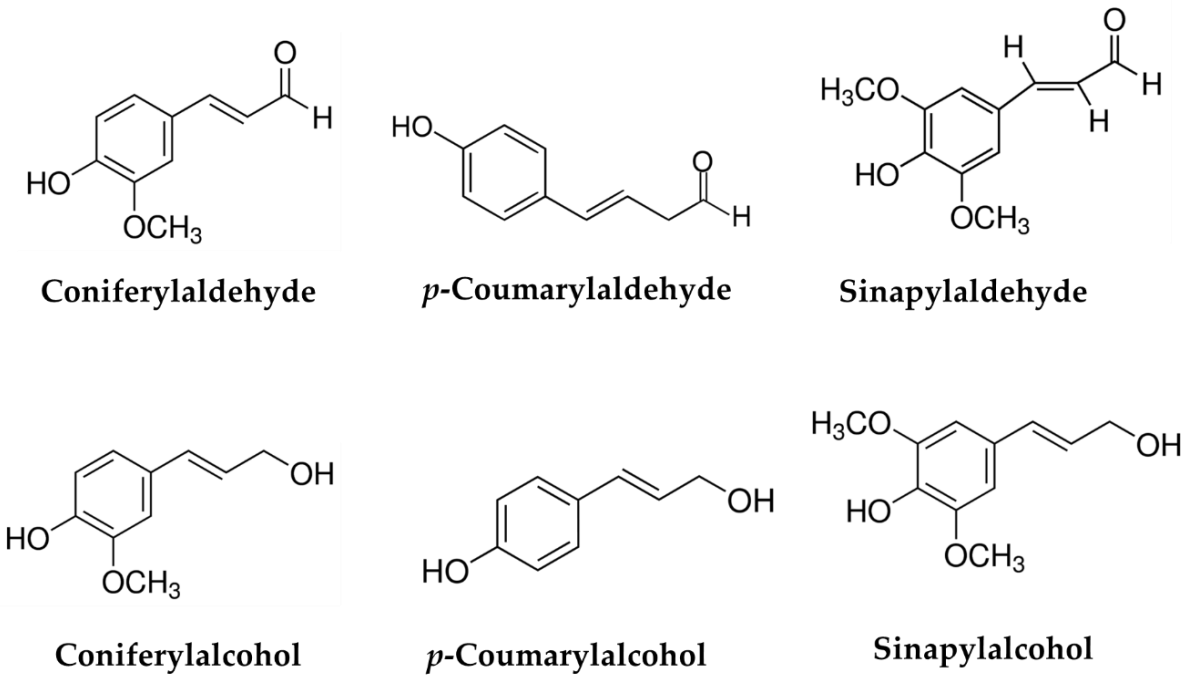

Figure 24. Chemical structures of additional plant secondary metabolites that were tested throughout this study.

The results have revealed that UGT72AY1 is able to readily glucosylate umbelliferone in comparison to the rest of the six substrates **[Figure 22].** Scopoletin substrate serves as a positive control indicating that the enzyme is indeed active and functioning accordingly. Umbelliferone showed a relative activity of 100%, which is comparable to the well glucosylated substrate, scopoletin (91.5%). Coniferyl aldehyde showed a relative activity of only 17.6% and *p*-coumaryl alcohol showed an activity at 10.9%. The remaining substrates – *p*-coumaryl alcohol, sinapyl alcohol, sinapyl aldehyde, and coniferyl alcohol yielded a relative activity at 4.06%, 2.41%, -0.05%, and -0.79% respectively **[Figure 22]**. The glucosylated products were subjected to LC-MS analysis to exclude potential errors and undetectability. As expected, UGT72AY1 was able to convert scopoletin and umbelliferone substantially **[Figure 25A, Figure 27A].** The LC-MS result for coniferyl aldehyde was consistent with the UDP-Glo™ results,

resulting in a low conversion rate **[Figure 29 and Figure 30]**. The remaining six substrates **[Figure 24]** showed an even lower conversion rate via LC-MS analysis (results not shown), consistent with the UDP-Glo™ results **[Figure 22].** The UDP-Glo™ results are consistent with the LC-MS results, further proving that the established and tailored UDP-Glo™ method can be utilized for an initial substrate screen.

Since natural products carrying a β-ionol ring structure were able to inhibit the UDP-glucose hydrolase activity of UGT72AY1 **[Figure 21],** we studied the effect of related compounds on the glucosyltransferase activity of this enzyme. The findings from **Figure 22** have encouraged the further study of enhancement and/or inhibition of scopoletin and umbelliferone glycosylation by the addition of various plant secondary metabolites (modifiers). Scopoletin glycosylation was evaluated after the addition of α-ionol, β-ionol, farnesol, α-ionone, β-ionone, abscisic acid (ABA), α-damascone, β-damascone, FMT, β-carotene, retinol, and apocarotenal **[Figure 23].** LC-MS analyses have revealed that some modifiers are able to drive the glycosylation of scopoletin meanwhile, others can have an inhibitory or no effect at all **[Figure 25, Figure 26]**.

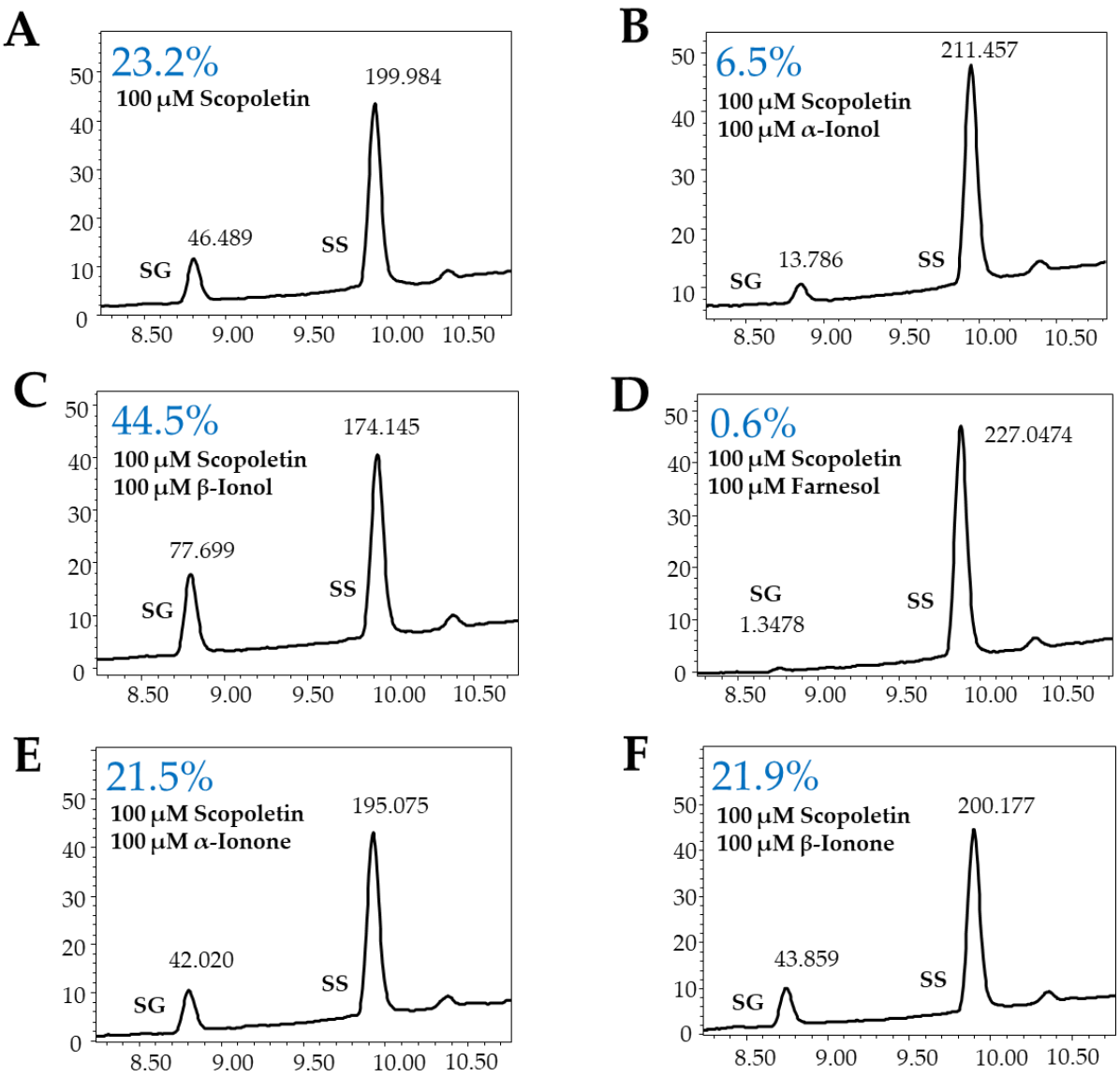

Figure 25. Enhancement and inhibition of UGT72AY1 scopoletin glycosylation evaluated with LC-MS with various plant secondary metabolites. Area (calculated in the UV trace at 280 nm) of peaks are displayed along with the calculated peak ratio in percent (blue). SG, scopoletin glucoside. SS, scopoletin substrate. X-axis represent retention time and Y-axis represent intensity.

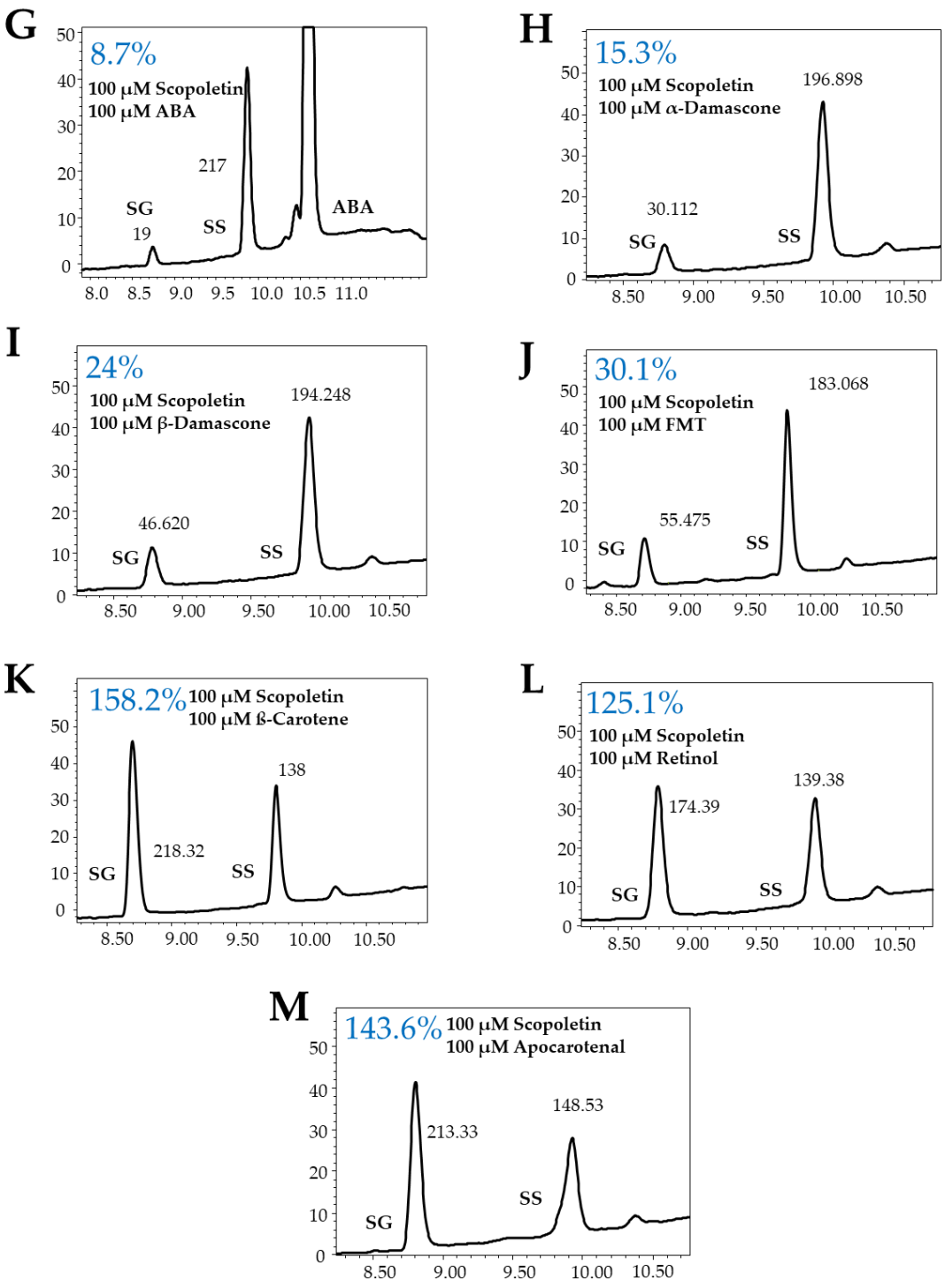

Figure 26. Enhancement and inhibition of UGT72AY1 scopoletin glycosylation evaluated with LC-MS with various plant secondary metabolites. Area (calculated in the UV trace at 280 nm) of peaks are displayed along with the calculated peak ratio in percent (blue). SG, scopoletin glucoside. SS, scopoletin substrate. X-axis represent retention time and Y-axis represent intensity.

The ratio of glucoside produced to remaining scopoletin substrate was 23.2% in assays without any modifier **[Figure 25 A]**. With the addition of 100 μM of β-ionol the production of scopoletin glucoside is increased to 44.5% **[Figure 25 A and C].** A similar trend was expected to be seen with the addition of α-ionol, however it does not show an increase in scopoletin glucoside production **[Figure 25 A and B]**. The presence of α-ionone, β-ionone, α-damascone, β-damascone, and FMT did not have an effect on the scopoletin glucoside to remaining substrate ratio, indicating that the presence of those substrates does not drive or inhibit scopoletin glucoside production under the conditions applied **[Figure 25 E and F, Figure 26 H, I, and J]**. On the contrary, the presence of ABA and farnesol has revealed a decrease in the scopoletin glucoside and remaining substrate ratio from 23.2% **[Figure 25 A]** to 8.7% **[Figure 26 G]** and 0.6% **[Figure 25 D]**, respectively. This indicates that ABA and farnesol have an inhibitory effect on scopoletin glucosylation by means of allosteric inhibition. The presence of β-carotene, retinol, and apocarotenal have shown a positive effect on scopoletin glucoside production by increasing the scopoletin glucoside to remaining scopoletin ratio from 23.2% **[Figure 25 A]** to 158.2%, 125.1%, and 143.6% respectively **[Figure 26 K, L, and M].** This is a substantial increase and enhancement of scopoletin glucoside production.

Umbelliferone, being a structurally similar compound to the substrate scopoletin of UGT72AY1, was subjected to the same enhancement and inhibition assays and then quantified by LC-MS. Umbelliferone glycosylation was evaluated after the addition of α-ionol, β-ionol, farnesol, α-ionone, β-ionone, ABA, α-damascone, β-damascone, FMT, β-carotene, retinol, and apocarotenal **[Figure 23].** LC-MS analyses have revealed that all modifiers are able to drive the glycosylation of umbelliferone **[Figure 28, Figure 29]**. The ratio of glucoside produced to remaining umbelliferone substrate is 30.5% if no modifiers are present **[Figure 27 A]**.

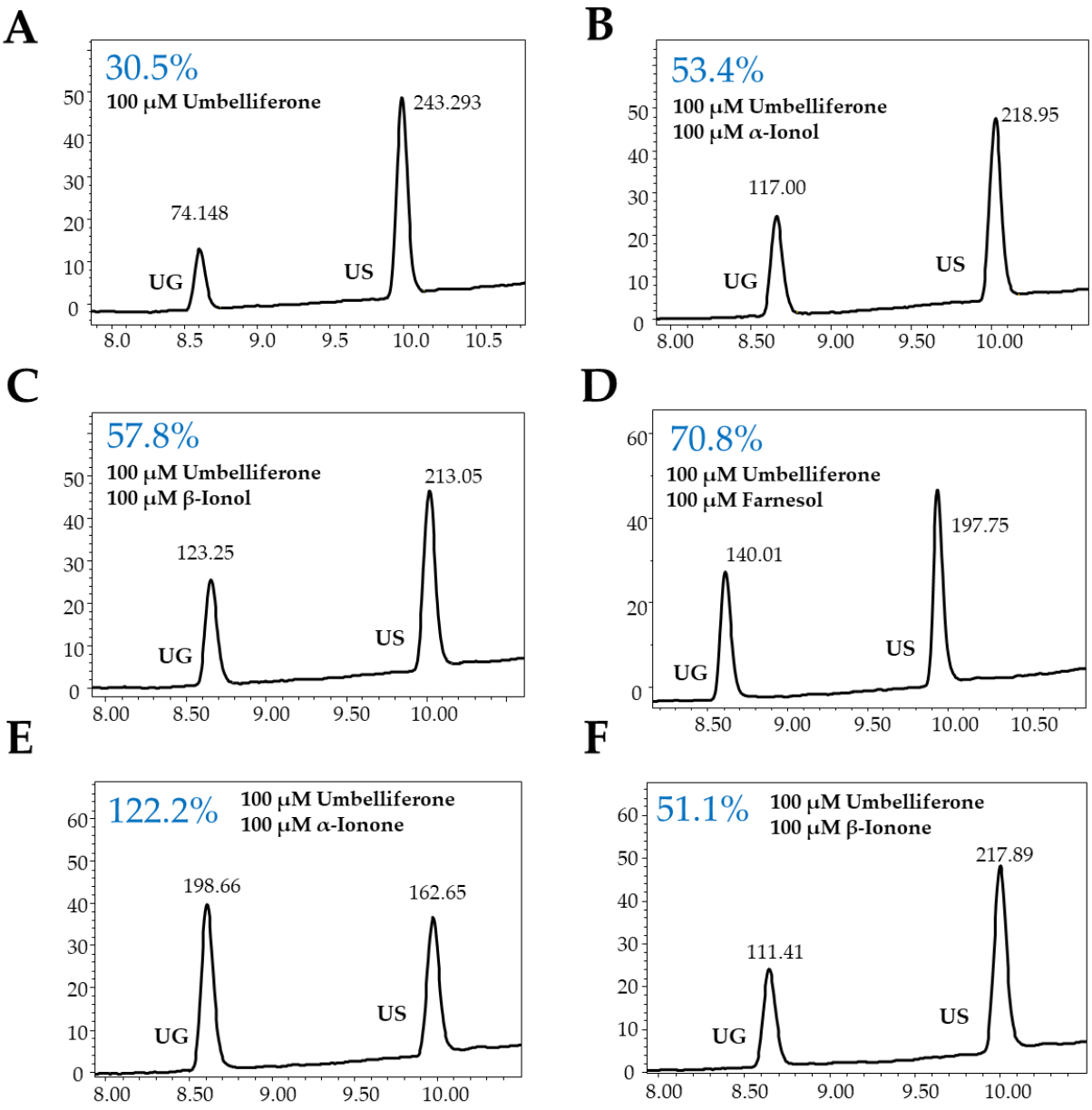

Figure 27. Enhancement and inhibition of UGT72AY1 umbelliferone glycosylation evaluated with LC-MS with various plant secondary metabolites. Area of peaks (calculated in the UV trace at 280 nm) are displayed along with the calculated peak ratio in percent (blue). UG, umbelliferone glucoside. US, umbelliferone substrate. X-axis represent retention time and Y-axis represent intensity.

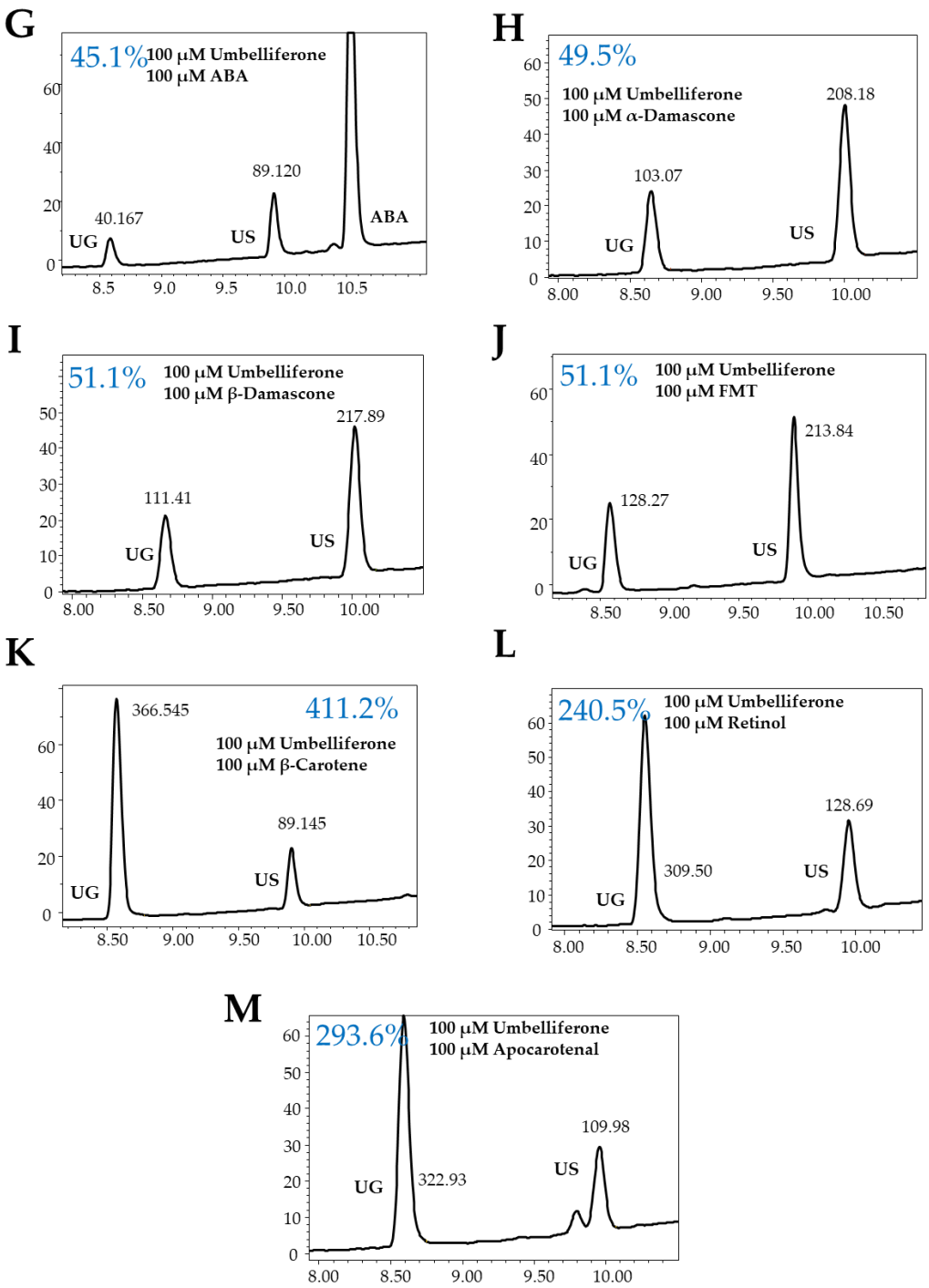

Figure 28. Enhancement and inhibition of UGT72AY1. Umbelliferone glycosylation evaluated with LC-MS with various plant secondary metabolites. Area of peaks (calculated in the UV trace at 280 nm) are displayed along with the calculated peak ratio in percent (blue). UG, umbelliferone glucoside. US, umbelliferone substrate. X-axis represent retention time and Y-axis represent intensity.

The presence of α-ionol, β-ionol, farnesol, α-ionone, β-ionone, ABA, α-damascone, β-damascone, FMT, β-carotene, retinol, and apocarotenal increased the umbelliferone glucoside to remaining substrate from 30.5% to 53.4%, 57.8%, 70.8%, 122.2%, 51.1%, 45.1%, 49.5%, 51.1%, 51.1%, 411.2%, 240.5%, and 293.6% respectively **[Figure 27 and Figure 28]**. Some substrates such as β-carotene, retinol, and apocarotenal had a much larger effect on the enhancement of umbelliferone glucoside production in comparison to the other substrates. Glucosylation of coniferyl aldehyde, coniferyl alcohol, *p*-coumaryl aldehyde, *p*-coumaryl alcohol, sinapyl aldehyde, and sinapyl alcohol are not favored by UGT72AY1 **[Figure 22].** Even in the presence of the above-mentioned enhancement modifiers, the concentration of coniferyl aldehyde glucoside was not increased **[Figure 29 and Figure 30].**

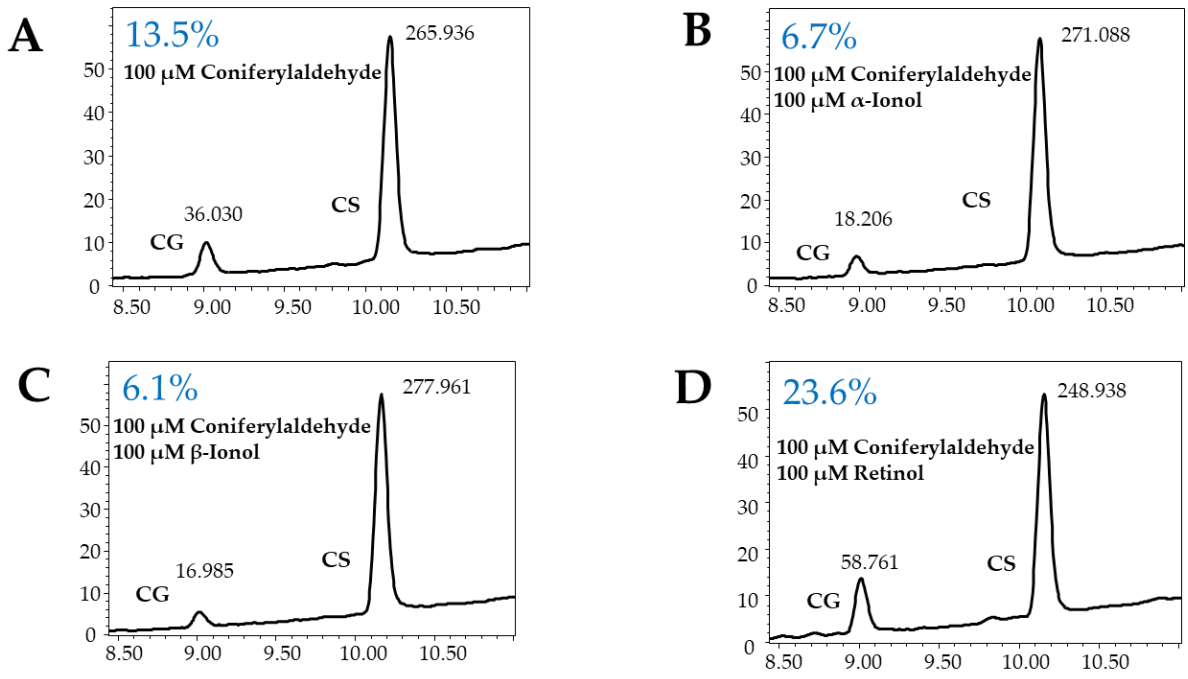

Figure 29. Enhancement and inhibition of UGT72AY1. Coniferyl aldehyde glycosylation enhancement and inhibition with various plant secondary metabolites analyzed via LC- MS. Area of peaks (calculated in the UV trace at 280 nm) are displayed along with the calculated peak ratio in percent (blue). CG, Coniferyl aldehyde glucoside. CS, Coniferyl aldehyde substrate. X-axis represent retention time and Y-axis represent intensity.

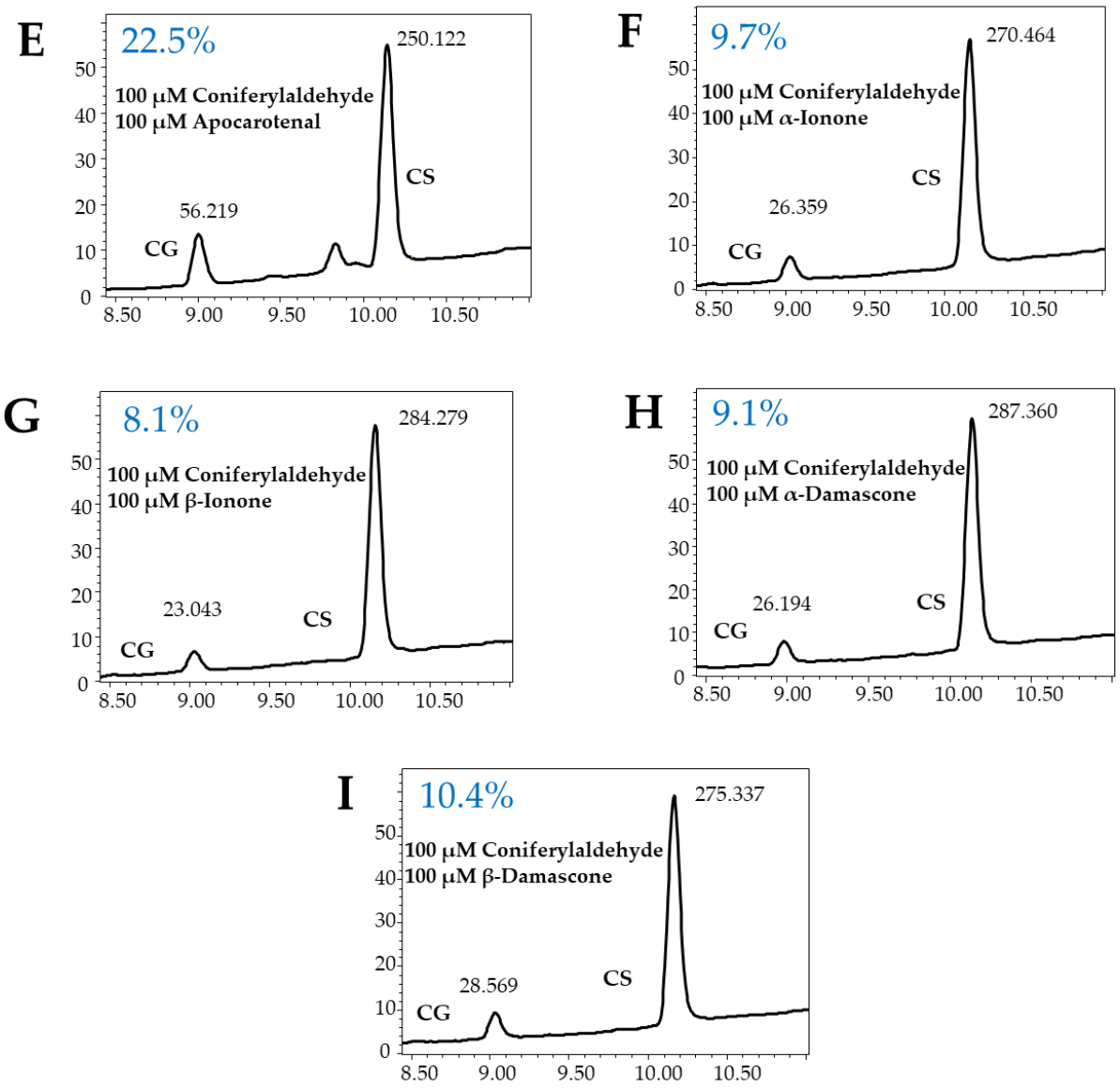

Figure 30. Enhancement and inhibition of UGT72AY1. Coniferyl aldehyde glycosylation enhancement and inhibition with various plant secondary metabolites analyzed via LC-MS. Area of peaks (calculated in the UV trace at 280 nm) are displayed along with the calculated peak ratio in percent (blue). CG, Coniferyl aldehyde glucoside. CS, Coniferyl aldehyde substrate. X-axis represent retention time and Y-axis represent intensity.

The study and investigation of enhancement or inhibition and being able to direct glucoside formation in either direction is thought to have many applications across several industries where glycosylation plays a key role. These findings have set the stage to further investigate the enhancement and inhibitory effects of scopoletin glucoside formation under various concentrations of scopoletin substrate and the enhancing or inhibiting modifier **[Figure 31]**. Based on **Figure 25** and **Figure 26**, FMT was chosen as a modifier, which does not have an effect on scopoletin glucoside production. Farnesol and ABA were chosen as modifiers which have an inhibitory effect on scopoletin glucoside formation as the glucoside to remaining substrate percentage was decreased from 23.2% to 0.6% and 8.7%, respectively **[Figure 25 A, D, and Figure 26 G]**. Apocarotenal and β-carotene were chosen as modifiers which have an enhancement effect on scopoletin glucoside formation as the glucoside to remaining substrate ratio was increased from 23.2% to 158.2% and 143.6%, respectively **[Figure 26 K, M].** The experiment was set up according to **Table 12** and subjected to LC-MS analysis. Without addition of a modifier, the peak area of the scopoletin glucoside signal was 2.8 ± 0.05; 8.7 ± 0.63, and 31.5 ± 4.3 mAU for enzyme assays containing 200, 100 and 50 μM scopoletin, respectively. With the addition of the enhancer substrates (50 μM – 200 μM), β-carotene and apocarotenal, to 50 μM of scopoletin substrate (blue) the peak area was increased to 800 and 300 mAU, respectively indicating enhancement of scopoletin glucoside production **[Figure 31 A and B]**. The increase was less pronounced at higher concentrations of the scopoletin substrate (100 and 200 μM).

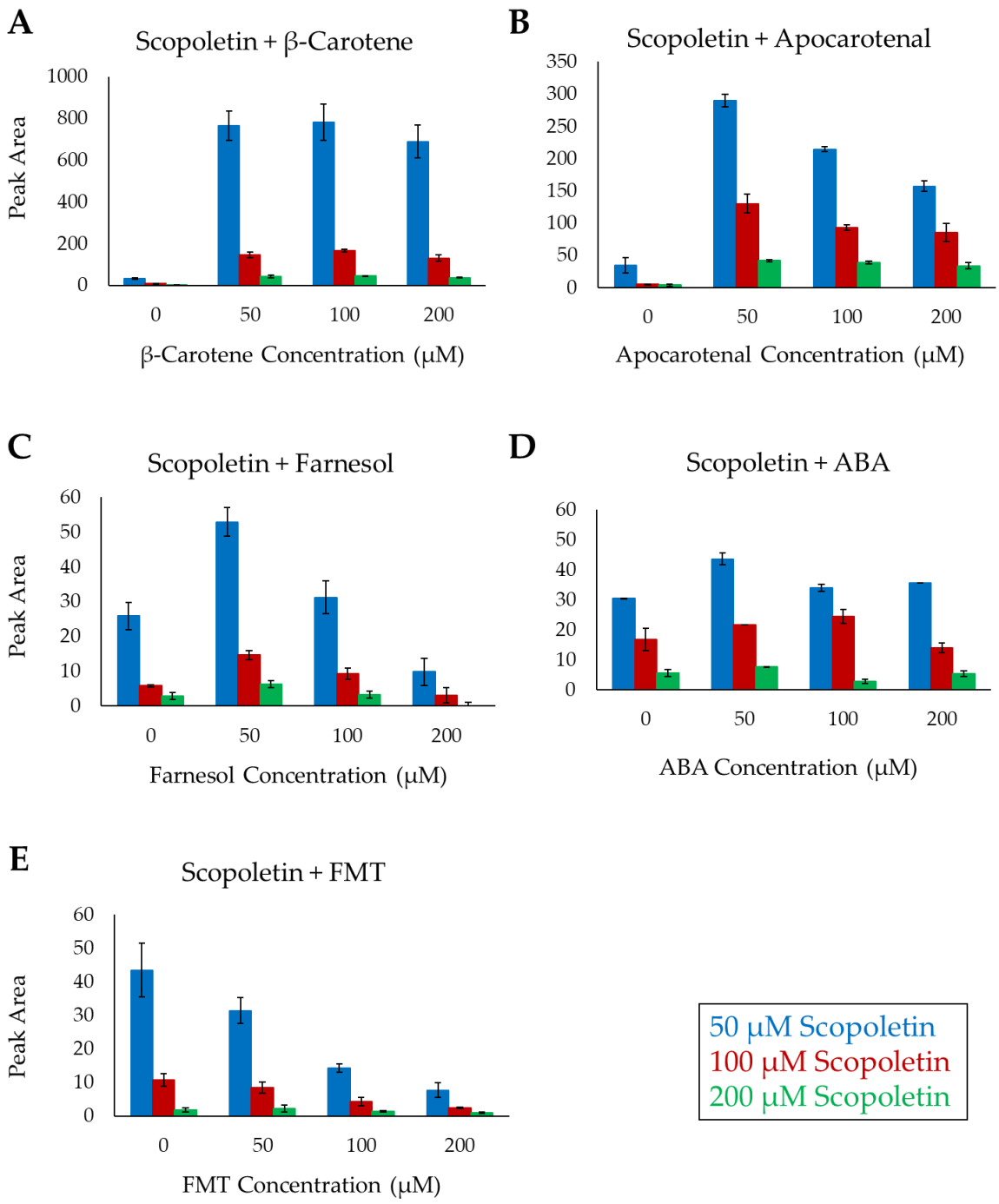

Figure 31. Enhancement and inhibition of UGT72AY1 scopoletin glycosylation with various secondary plant metabolites. (A) β-carotene, (B) apocarotenal, (C) farnesol, (D) ABA, (E) FMT. Defined amounts (50, 100 and 200 µM) of scopoletin substrate were added, and modifiers A-E were added in a range of 0 – 200 µM, and peak area (mAU) was calculated. n=3.

The addition of ABA at different concentrations did not display a substantial enhancing or inhibitory effect of scopoletin glucoside production **[Figure 31 D]**. The presence of farnesol at a high concentration of 200 μM showed a substantial inhibitory effect on scopoletin glucoside production independent of the scopoletin concentration used while a low concentration of farnesol (50 μM) seemed to enhance the formation of scopoletin glucoside **[Figure 31 C]**. Finally, FMT although from previous LC-MS analysis **[Figure 26 J]** was found to have no effect on scopoletin glucoside production, has revealed that with an increasing concentration (50 μM – 200 μM) it inhibits scopoletin glucoside production **[Figure 31 E]**.

Higher concentrations of scopoletin (100 μM and 200 μM) without any enhancers or inhibitory substrates have shown a lower peak area in contrast to when a lower amount of 50 μM of scopoletin substrate is present **[Figure 31]**. This is due to substrate inhibition, when the high concentration of the substrate is inhibiting itself in producing the glucoside by over-occupying the active site [87, 100] **[Figure 32]**. Moreover, the enhancement or inhibitory effects of the above-mentioned substrates cannot be evaluated when the scopoletin substrate concentration is too high. Therefore, optimal conditions and optimal concentrations should always be evaluated and utilized when conducting comparative and functional analyses.

IV. Discussion

The mechanism of UGTs in biosynthetic pathways with the conjugation of sugar units is simple yet unique, altering essential properties of secondary metabolites [42]. Over the years, GTs have attracted significant attention in a broad spectrum of applications in pharmaceuticals, cosmeceuticals, nutraceuticals, and agriculture. However, the lack of a stable HTP method of detection of plant GTs and/or requisite substrates restricts the further application of these enzymes. Therefore, given the vast application spectrum and importance of UGTs, a high-throughput assay amenable to family-1 plant GTs is crucial. With this, novel enzymes and substrates can be discovered and allosteric enhancers and/or inhibitors can be applied to study the reaction mechanism of specific enzymes. In this study, a HTP stable method was designed and tailored to suit family-1 plant GTs. The advantages and drawbacks are thoroughly outlined and their feasibility is described. Furthermore, the establishment of a HTP method allowed for the further manipulation of GTs by directing their hydrolase and glycosylation activities towards enhancement or inhibition. These findings set the stage for further analyses and characterization of new potential GTs and plant secondary metabolites as well as, novel applications.

4.1 pH-sensitive glycosyltransferase activity assay

The pH-sensitive assay is a simple, inexpensive, and fast method that detects protons released due to the sugar transfer ultimately changing the pH level of the entire reaction **[Figure 3]**. This change in pH is quantitatively determined by the addition of the pH indicator phenol red, which results in a color change ranging from yellow to red with pH values from 6.8 to 8.2, respectively **[Figure 5]**. The assay was employed from [59] and used for plant GTs by [63]. The previously mentioned studies

conducted this assay in a non-HTP manner by utilizing separate Eppendorf tubes and 10 mm quartz cuvettes. In this doctoral study, it was endeavored to adapt this method to HTP format by utilizing 96-well plates, decreasing the total volume of the reaction, and automating the addition of each reaction reagent in its respective well. The kinetic results obtained by [63] were stable and reliable and executed in 10 mm quartz cuvettes utilizing a spectrophotometer. The newly pH-sensitive assay adapted to HTP method in this study yielded unreliable and unstable results with the exact same GT and substrates. The kinetic values were vastly different between all technical and biological replicates, and it was not possible to reproduce the same results with the HTP method as in the study of [63]. This may be because the pH-sensitive assay is highly susceptible to disturbances. For example, the automated injector function as well as the plate mixing function may not homogenize the reaction components to the same extend as when prepared in separate Eppendorf tubes. Although, this assay has already been successfully applied in HTP format for the screening of GT saturation mutagenesis libraries [67]. In this case, the assay was used for the screening of mutant GTs with the same oligosaccharides using suitable controls on each plate. As the system was optimized for screening in a solution with a weak buffer capacity, the authors noted that it is difficult to accurately quantify the initial enzyme reaction rates due to the drop in absorbance as the GT is added to the reaction mixture. In addition, the absorption coefficient of the pH indicator interferes with the measurement as the reaction progresses [118]. Different adjustments have to be made including the use of higher buffer concentration, larger amount of the indicator dye and increase in substrate concentration before the assay can be used for specific activity measurements [67]. However, increased substrate concentrations may limit the measurement of enzyme activity. In addition, chromophoric/fluorophoric substrates lead to erroneous results similar to substrates with acidic hydrogens (e.g. acids and phenolics) whereby the capacity of the weak buffer can be exceeded. The above-mentioned examples may contribute to the witnessed instability of the pH-sensitive assay when phenols were tested as substrates of GT in HTP format. Theoretically, this

assay in HTP format would encompass several advantages including low costs, not requiring specialized equipment, and time efficient **[Table 14].** However, the drawbacks include its instability, unreliability across various substrates and unsuitability for HTP processing with various substrates. As the cost per assay is relatively low **[Table 14]**, it can be utilized for an initial and quick screen of substrates but is not feasible for further quantitative experiments.

Table 14. Advantages and disadvantages of the three high-throughput detection methods - The pH-sensitive assay, UDP-Glo™ assay, and phosphate glycosyltransferase activity assay. Adapted from [52, 64, 65, 77]

	pH-Sensitive Assay	UDP-Glo™ Assay	Phosphate GT Assay
Advantages	▪ Simple, cheap and fast ▪ Requires no specialized equipment ▪ Can be used with crude protein ▪ Useful for screening of one acceptor with multiple GTs	▪ Simple, fast, and sensitive ▪ Easy handling ▪ Usable for High-throughput ▪ Stable readout signal ▪ Requires no labelled substrate	▪ Simple, fast, and sensitive ▪ Easy handling and detection ▪ Usable for High-throughput ▪ Stable absorbance signal ▪ Requires no labelled substrate
Disadvantages	▪ Unstable ▪ Not applicable for HTP analyses of kinetic data – only for initial screening	▪ UDP-glucose hydrolase activity produces false positive results ▪ DMSO concentration must be under 10% ▪ Adjustment necessary for metal-independent GTs	▪ One-step reaction is not application to metal-independent GTs ▪ UDP-glucose hydrolase activity produces false positive results ▪ All components of the reaction must be phosphate-free (cross-contamination can pose a risk) ▪ DMSO concentration must be under 10%
	0.01€ / assay	0.25 € / assay	0.35 € / assay

4.2 UDP-Glo™ glycosyltransferase activity assay

The UDP-Glo™ assay is a stable, fast, and easily executed method, which detects the free UDP molecule released following the glycosyl transfer **[Figure 5]**. Subsequently, the free UDP is converted to ATP via a luciferase reaction and luminescence is detected and read via the luminometer. The luminescence is directly proportional to the amount of free UDP, hence the amount of glycosylated product produced. The kinetics of the family-1 plant UGT72B27 from *Vitis vinifera* along with the phenolic substrates **[Figure 11]** were carried out and tested with the UDP-Glo™ method. The assay was executed in a 384-well plate, which made the result readout fast, simple, and easy. According to the manufacturer's instructions, the UDR is to be added directly to the GT reaction upon completion in a 1:1 ratio. This would yield the termination of the GT reaction and ultimately convert the UDP to ATP. However, following some test experiments it was noted that the plant GT (UGT72B27) reactions are not completely terminated by the UDR solution. Upon the implementation of the additional step of heat-inactivation to terminate the reaction, the observed UDP amounts were approximately half the amount that were observed when UDR was added directly **[Figure 13]**. Although the UDR recipe is not transparent due to company confidentiality, it was revealed to us that it has a metal chelating detergent. This indicated that the lack of the metal center of the plant GTs prevents the ability to utilize the stopping agents of the kit to terminate the reaction. Therefore, when the reaction is not terminated and the UDR is directly added the GT is not fully stopped and it continues to function resulting in a higher amount of glycoside and UDP. Building upon this, this method was tailored with an additional heat inactivation step to suit family-1 plant GTs. Another study tested different plant GTs from *Nicotiana benthamiana* with different substrates and the results obtained with the tailored UDP-Glo™ method established in this study were consistent and viable [117]. Generally, the method was also successfully applied for the rapid screening of sugar-nucleotide

donor specificities of glycosyltransferases by determining of their UDP-sugar hydrolase activities [68]. Therefore, in addition to the transferase activity of GTs, the innate UDP-sugar hydrolase activity of GTs can also be determined using the UDP-Glo™ assay. Aside from the general transferase reactions that can be detected, we have uncovered a significant hydrolase activity for UGT72AY1 from *Nicotiana benthamiana* utilizing the tailored UDP-Glo™ assay **[Section 4.5]**.

This assay has several advantages including easy handling, no radiolabeled substrate required, and is sensitive in detecting even low UDP amounts **[Table 14]**. The drawbacks include concentration of DMSO, which must be less than 10% otherwise, it inhibits the luciferase enzyme and hinders the luminescence signal. This could indicate that highly hydrophobic substrates would not be able to be subjected to this experimentation, as it would require high concentration of DMSO in order to dissolve and dilute it. Side activities by other activities such as UDP-glucose hydrolase could interfere with the results yielding false positives. Therefore, in this case LC-MS should be implemented in order to overlook potential false positives or negatives. The cost per assay is reasonable at 0.25€ per assay **[Table 14]**, and can be employed in multiple, fast, and reliable screenings of substrates. The UDP-Glo™ has proven to be a stable and reliable HTP method, which can be confidently adapted when screening and performing kinetic analyses of family-1 plant GTs.

4.3 Phosphate glycosyltransferase activity assay

The phosphate GT assay is a colorimetric assay that is fast, stable, and prone to HTP screening which detects the free inorganic phosphate, which cleaved off by a coupling phosphatase (CP) from the free UDP following the glycosyl transfer **[Figure 5].** According to the manufacturer's directions, the reaction should be executed in a one-step manner where the CP is simultaneously added along with the GT enzyme.

The stopping agent provided by the kit is a metal chelating agent, which interacts with the GT's metal center and quenches its activity. The GTs previously utilized with this commercial assay were from GT families other than from family 1 as in this study **[Table 1]**. Subjecting the family-1 GT UGT72B27 from *Vitis vinifera* with phenolic substrates **[Figure 11]** under the one-step protocol as suggested by the manufacturer, resulted in unquantifiable data as the GT reaction was not stopped with the provided buffer reagent **[Figure 14]**. Therefore, a tailored two-step phosphate colorimetric assay including a heat inactivation step was used to carry out the kinetics of UGT72B27 along with phenolic substrates **[Table 13]**. The phosphate assay and the UDP-Glo™ assay yielded nearly identical or similar Michaelis-Menten values **[Table 13]** in contrast to the pH-sensitive assay. The phosphate assay also has many advantages as it has easy handling, produces stable signals, and the entire assay is not time-consuming **[Table 14]**. However, the one-step reaction is not applicable to plant GTs and thus results in an extra step that must be carried out in contrast to how the kit is advertised by the manufacturer. Nevertheless, including the additional step required to terminate the enzyme the employment of the assay is HTP. Another important aspect is that all components of the reactions, including the purification of the protein, must not contain any trace of phosphate as the Malachite reagents are very sensitive and can interfere with the absorbance signal. Therefore, the handling should be executed with much care and in a so-called sterile environment. Another drawback as with the UDP-Glo™ assay is that the concentration of solvents and detergents should not exceed 10%. Any concentrations higher than 10% will interfere with the Malachite reagents and diminish the absorbance signal. The price per assay is estimated at 0.35 €, which is higher than the other assays described but is nonetheless reasonable. Overall, the phosphate assay is stable and can be easily utilized with family-1 plant GTs in a two-step manner.

4.4 Transcreener UDP² TR-FRET glycosyltransferase activity assay

The Transcreener UDP² TR-FRET assay is a competitive immunoassay, which is based on the detection of the free UDP following a glycosyl transfer **[Figure 5].** This assay has been employed in the discovery of GT inhibitors [75]. The buffer included with this commercial kit is added in a one-step format and should stop the GT reaction. However, after several attempts and further testing it was revealed that this 'stop and detect buffer C' did not work on the GT undertaken in this study. According to the manufacturer, the ingredients of the 'stop and detect buffer C' are confidential but we were able to reveal that it contains a metal chelating detergent hence, able to stop GTs with a metal center. Therefore, the assay was altered by adding an additional step to heat stop the reaction and successfully terminate the GT. Although this assay has not been utilized with plant GTs until now, the assay was validated by other studies such as screening with 8,000 compounds using a polypeptide N-acetylgalactosaminyltransferase containing a metal center as the target [75] **[Table 1]**. The attempts in this study in utilizing this assay with a plant GT were unfortunately unsuccessful **[Figure 18]**. Further attempts with the additional heat-inactivation to stop the enzyme and utilize the antibody conjugated with a fluorophore, the results were still unstable and yielded day-to-day inconsistencies. Moreover, this assay was employed with other class of enzymes such as protein kinases and several considerations and drawbacks are present. For example, the interference by fluorescent compounds [119] or the inner-filter effect [120] need to be considered when employing such methods while utilizing red-shifted fluorophores for detection can reduce interferences caused by low-molecular weight compounds [119]. Furthermore, a drawback for this type of system is that a calibration of the antibody concentration based on the ATP/ADP is required to omit the variability of ATP [121]. Theoretically, the assay should be easy and the execution is advertised to be a quick mix and read format. However, the assay did not provide stable and consistent results

when a family-1 UGT72B27 from *Vitis vinifera* was utilized with phenolic substrates and thus, was eliminated from all further experiments.

4.5 Comparative analysis of high-throughput GT activity assays

Following the tailoring and optimization of the four above-mentioned HTP assays, a family-1 GT was subjected to kinetic analyses with various plant secondary substrates. It has been previously found that UGT72B27 prefers phenols as acceptor substrates including the smoke-derived phenolic xenobiotics guaiacol, MMP, DMP, MDMP, m-cresol, and o-cresol, *trans*-resveratrol, as well as furaneol **[Figure 11]** [63]. UDP-Glo™ and phosphate GT activity assay was utilized to quantify the kinetics of all of these phenolic substrates **[Table 13].** Although, the structures of MMP, DMP, and MDMP are quite similar **[Figure 11]** the phosphate assay did not provide reproducible data for MMP. However, LC-MS results confirmed the production of MMP glucoside [63] and UDP-Glo™ assay showed substantial kinetic data **[Table 13]**. Similarly, furaneol was unquantifiable with the phosphate assay. Correspondingly, *trans*-resveratrol presented different kinetic values for both assays (UDP-Glo™ K_M of 21 μM and phosphate assay K_M of 15 μM) in comparison to the pH-sensitive assay (K_M of 36 μM), although it is known that its glycosylation is favored for this substrate. This may be due to its hydrophobic properties (multiple aromatic structures) requiring to be dissolved in DMSO concentrations which exceed both assays' thresholds, making it poorly quantifiable at higher substrate concentrations. Correspondingly, low k_{cat} and k_{cat}/K_M values **[Table 13]**. A study by Maier-Salamon *et al.*, quantified and compared resveratrol consumption by UGTs and formation of resveratrol glucuronides in different species (dog, rat, mouse, and human) utilizing HPLC method [122]. Therefore, it can be concluded that there is no universal assay that would fit all substrates due to their structural diversity. Alternative HTP assays should be applied to avoid overlooking potential GT acceptors. Moreover, it can also

be concluded that HTP quantification is possible and favorable when utilizing plant GTs, but due to the promiscuity of GTs more than one established method is beneficial **[Table 14]**. In this case, both the UDP-Glo™ assay and phosphate GT activity assay can be utilized to screen and quantify kinetics of various GTs with different substrates. Even with the additional enzyme inactivation step that needs to be implemented for both assays, the two new methods propose an efficient, cost-effective, and robust HTP method for analysis of plant GTs.

4.6 Enhancement and inhibition of glycosyltransferase and UDP-glucose hydrolase activity of family-1 plant GTs

GTs mechanism of action – the transfer of a sugar molecule onto an acceptor changes its chemical properties altering the respective bioactivity, volatility, and membrane signaling [42]. Plant family-1 GTs play a significant role in the growth and development of plants as well as, regulating hormones and signaling molecules, which are responsible for the response to environmental changes and stress factors [12, 49]. *In vitro* studies have presented that a single GT can glycosylate multiple substrates of diverse chemical features and at the same time, different GTs can glycosylate the same substrate [42, 123-125]. The fact that plant GTs of small molecules are able to glycosylate acceptors in a regioselective manner and even transfer glycosyl residues to different sites on a molecule, usually means they possess different chemical properties, bioactivities, and play various roles in the plant. This sets the stage for the vast application spectrum of these enzymes whilst many still remain elusive. For example, the regioselective glucosylation of quercetin yields different quercetin monoglucosides each encompassing different levels of chemical reactivity and hydrophobicity [124, 126]. Quercetin is a flavonoid which plays a role in pollen function and is widely utilized as a dietary supplement in food, beverages, and nutraceuticals [42]. Moreover, strong UDP-inhibition was observed in liver

microsomal phenol UGTs ultimately suggesting that UDP interacts directly with the transferase protein and not through various membranes or other co-factors [99]. Among many other plant secondary metabolites and all of their potential applications, the enhancement or inhibition of GTs and being able to direct the glycosylation may reveal many potential new applications in agriculture, medicine, and consumer-end products.

Throughout this study, an inherent UDP glucose hydrolase activity was observed among several family-1 UGTs. During a standard *in vitro* glycosyltransferase reaction, the acceptor substrate performs a nucleophilic attack on the donor substrate releasing a proton and UDP as by-products, producing a glycoside **[Figure 3].** The glycoside can be observed with LC-MS analysis and the by-products can be observed with UDP-Glo™ or phosphate GT activity assay. At the same time, it is plausible for water molecules to be accepted and engage in a nucleophilic attack on the donor substrate, thereby releasing a proton and UDP as by-products whilst yielding a glucose molecule (instead of a glucoside) **[Figure 7]** [104-106]. This glucose molecule will not be quantified with LC-MS but the by-products can indeed be determined with UDP-Glo™ or phosphate GT activity assay. A study by Sheikh *et al.* has utilized UDP-Glo™ assay and detected the formation of the free nucleotide-phosphate leaving group from the activated donor with bacterial and human UGTs [68]. In this study, each *in vitro* GT reaction was performed alongside three important negative controls including without an active GT, without an acceptor substrate, and without a donor substrate as depicted in **Table 8**. Upon performing these *in vitro* studies, when the values from UDP-Glo™ for the negative control without an acceptor substrate were yielding higher RLU values than the experiment samples, further testing was necessary (indicating hydrolase activity). Meanwhile, LC-MS results indicated an absence of a glycosylated product. UGT72B46, UGT72B50, and UGT72B51 glycosylate their natural substrate hydroquinone – depicting their active nature **[Figure 19]**. These enzymes were tested for innate hydrolase activity by removing hydroquinone as an

acceptor substrate and subjecting the GTs with the donor substrate, buffer, and water to incubate at optimal temperature over time **[Figure 20]** as in [68]. The findings revealed that as the incubation time was proceeded, the amount of UDP detected by UDP-Glo™ has increased for all three GTs. When no donor substrate (UDPG) was present, the amount of UDP detected over time remained unchanged. Similar hydrolase activity was detected in [68] where GtfA from *S. pneumoniae* demonstrated hydrolase activity also in the presence of divalent cations. This indicates that the water molecule was indeed acting as an acceptor molecule and performing a nucleophilic attack on the donor substrate, releasing the free-UDP **[Figure 7 and Figure 20]**. The UDP-glucose hydrolase activity of UGT72B46, UGT72B50, and UGT72B51 is not favored over the glycosyltransferase activity because when both hydroquinone and water (acceptor substrates) are present, the hydroquinone glycosylation is preferred **[Figure 19]**. Similarity in a study by Chavaroche *et al*., PmHS2 favored the synthesis of heparosan polymers over hydrolysis of UDP-sugars [107].

Furthermore, UGT72AY1 from *N. benthamiana* has demonstrated a significant UDP-glucose hydrolase activity, which was initially observed by a colleague. To further this observation, the inhibition of this UGT's hydrolase activity by structurally related natural products was investigated. Retinol and β-carotene were subjected to an *in vitro* GT reaction with UGT72AY1 and UDP-glucose as a donor substrate. These two substrates are not glycosylated by UGT72AY1 but when added in increasing amounts the relative enzyme activity was considerably decreased **[Figure 21]**. Without the substrates present, the relative enzyme activity is approximately 9 nmol/min/mg. As the substrates are added in increasing concentration, the relative activity is diminished in a negative hyperbolic fashion **[Figure 21]**. Since the two substrates, retinol and β-carotene, are not glycosylated by this GT – it is possible to conclude that they are allosterically inhibiting the hydrolase activity of UGT72AY1. A study performed similar hydrolase activities of *C. difficile* Toxins A and B where they executed a time course of toxin-mediated UDP-glucose hydrolase activity [109]. In

order to further understand the magnitude of hydrolase activities, they also performed kinetic analysis [109]. Some UGTs have been reported to contain multiple aglycone binding sites [86, 102], and it can be hypothesized that UGT72AY1, UGT72B46, UGT72B50, and UGT72B51 do have multiple binding sites hence the reason for both hydrolase and glycosyltransferase activities. In order to determine this for certain, mutagenesis and bioinformatic research of the enzyme should be conducted. Moreover, in order to quantify the hydrolase activity of UGT72AY1 further kinetic analyses and quantification of this activity should be executed.

The above-mentioned findings of the inhibition of the UDP-glucose hydrolase activity of GTs have set the stage to further investigate if certain secondary metabolites are able to allosterically inhibit or enhance the glucosyltransferase activity of UGT72AY1. The initial substrate screen quantified by UDP-Glo™ has revealed that scopoletin and umbelliferone are readily glycosylated by this GT, 91.5% and 100% respectively **[Figure 22].** This is due to their structural chemical resemblance and similarity, which is probably able to fit well into the active site of UGT72AY1 **[Figure 23].** The *in vitro* GT activities were conducted with 100 μM of scopoletin and 100 μM of umbelliferone each comprising with 100 μM of potential activator or inhibitor – ABA, apocarotenal, β-carotene, FMT, α-ionol, β-ionol, α-ionone, β-ionone, α-damascone, β-damascone, farnesol, and retinol **[Figure 23]**. The GT reaction with equal concentrations of scopoletin or umbelliferone with an activating or inhibiting modifier was subjected under optimal conditions and analyzed via LC-MS **[Figure 25, 26, 27, 28].** Accordingly, scopoletin without any modifier produced a glycoside to substrate ratio of 23.2% **[Figure 25 A]**. Interestingly, farnesol and ABA showed a decrease in scopoletin glucoside production which could be due to the binding of this substrate to an allosteric site on the enzyme causing a conformational change where scopoletin can no longer access the active site **[Figure 25 D and Figure 26 G]**. As it was previously reported that a UGT could possess more than one aglycone binding site [102]. β-Carotene, retinol, and apocarotenal are not glycosylated by UGT72AY1 but

when added as a modifier along scopoletin, are able to drive scopoletin glucosylation and increase product formation to 158.2%, 125.1% and 143.6% respectively **[Figure 26 K, L, M]**. Similarly, the same trend was observed with umbelliferone glucoside formation where β-carotene, retinol, and apocarotenal drove umbelliferone glucoside formation from 30.5% to 411.2%, 240.5%, and 293.6% respectively **[Figure 27 A, Figure 28 K, L, M].** β-Carotene, retinol, and apocarotenal are apocarotenoids which function as allosteric activators of glycosyltransferases yet, have shown to inhibit the GTs innate UDP-glucose hydrolase activity **[Figure 21]**. This can have tremendous effects on a broad range of applications where GTs versatility is of great commercial importance from agriculture to medicine. Directing or targeting the enhancement or inhibition of certain glycosylated products will not only increase the value of the product of interest, but will unravel many potential new applications.

To further investigate the effects of some substrates on their ability to enhance or inhibit scopoletin glucosyltransferase, β-carotene, apocarotenal, farnesol, ABA, and FMT were added as modifiers **[Figure 31].** Upon the execution of kinetics with UGT72AY1 and scopoletin, substrate inhibition was observed **[Figure 32]**. It is evident as the reaction proceeded in an atypical fashion **[Figure 6].** Similar substrate inhibition was observed by Peng *et al.* with *Fv*UGT1 and increasing concentrations of pelargonidin where after 250 μM of substrate the V_{max} began to decrease [90]. Furthermore, a UGT78K1 from soybean displayed substrate inhibition by cyanidin substrate at 100 μM [97]. VtGT6 from grape displayed substrate inhibition when the concentration of flavanol exceeded 150 μM [127]. With the case of scopoletin, more than 20 μM of substrate the V_{max} decreased representing substrate inhibition **[Figure 32]**. To date, it is still unclear whether substrate inhibition occurs in nature but it has been successfully depicted *in vitro* [128, 129]. It is postulated that substrate inhibition could contribute to the regulation of synthesis in biochemical processes *in vivo*. As an example, substrate inhibition of UGT78K1 observed by cyanidin may influence the cytotoxic effects of high cytosolic cyanidin 3-O-glucoside concentrations [97]. Another

interesting example where substrate inhibition could positively affect intracellular functions was observed by Chang *et al.* [130]. They concluded that the catalysis and substrate inhibition of dehydroepiandrosterone and androsterone by SULT2A1 may regulate homeostasis and metabolism of these compounds to maintain appropriate steroid levels [130]. In general, substrate inhibition in glucuronidation reactions is believed to be dependent and affected by the UGT isoform and substrate structure. This is evidently so with UGT1A1 and UGT1A3 which are the two isoforms highly prone to substrate inhibition kinetics [98]. Also, subjecting two structurally similar isoflavones – prunetin and genistein – to glucuronidation by UGT1A1 follows Michaelis-Menten kinetics and substrate inhibition kinetics, respectively [131]. A study by Maier-Salamon *et al.* found that human and dog UGT isoforms displayed substrate inhibition when the resveratrol substrate concentration exceeded 700 μM. at the same time, UGTs from rat and mouse did not depict substrate inhibition but rather a typical substrate saturation [122]. We have also found that UGT72AY1 is highly prone to substrate inhibition with scopoletin but not with other similar substrates. It would be worth to perform bioinformatic and mutation analyses to be able to determine the structural significance and potential binding sites of the substrate inhibition.

By increasing FMT concentration from 0 to 200 μM in increments of 50 for the 50 μM scopoletin concentration, the peak area was subsequently decreased. Whereas for the samples with 100 μM and 200 μM of scopoletin FMT showed no effect – which is in accordance to **Figure 26 J** (100 μM of scopoletin with 100 μM of FMT). This may again be due to the fact that scopoletin substrate has an inhibition effect on itself, and this can be confirmed by comparing the peak areas of 50 μM, 100 μM, and 200 μM of scopoletin with 0 μM of FMT which were approximately 40, 10, and 1 mAU respectively **[Figure 31 E].** With 50 μM of scopoletin the peak area is the highest indicating that most of the substrate is utilized to produce scopoletin glucoside. With higher scopoletin concentrations, the substrate inhibition is more favored and the FMT

has no effect on alleviating this inhibition and/or enhancing scopoletin glucoside production [87].

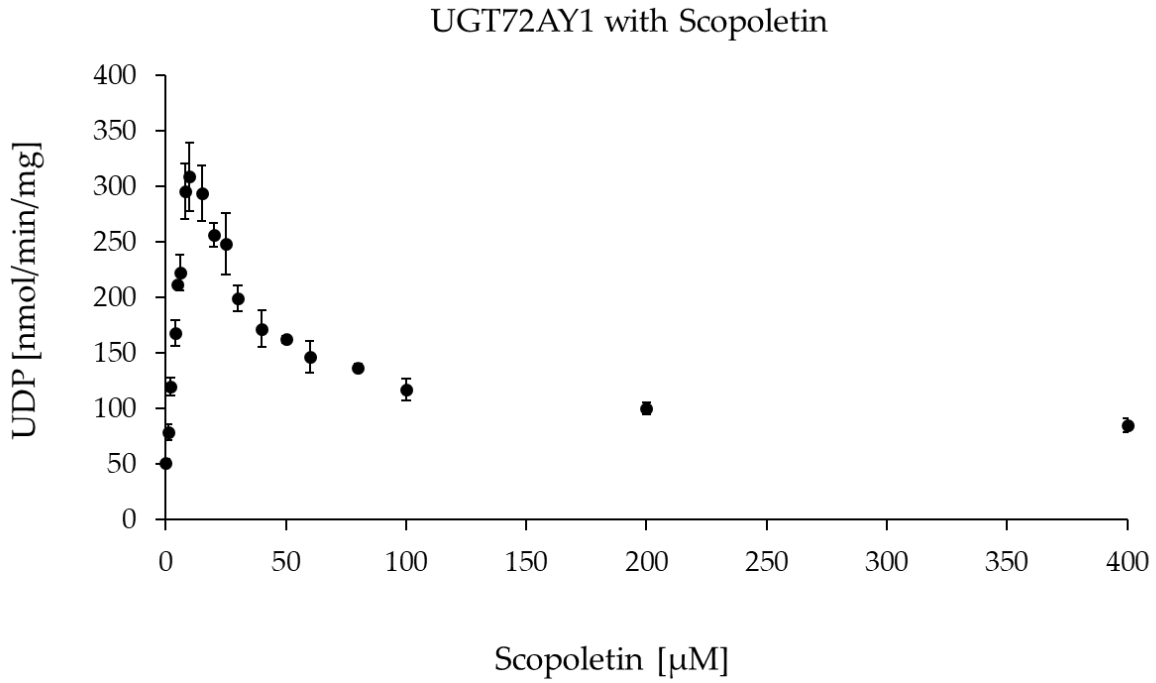

Figure 32. Graphical representation of substrate inhibition with 0.5 μg of UGT72AY1 and increasing concentration of scopoletin (0 – 400 μM). Unpublished data kindly provided from colleague – Dr. Elisabeth Kurze.

Figures 25 D and **26 G**, have initially showed that farnesol and ABA reduce scopoletin glucoside formation with 100 μM of each substrate. **Figure 31 C** illustrates scopoletin glucoside formation at various concentrations 50 μM, 100 μM, and 200 μM along with farnesol from 0 – 200 μM in increments of 50. Lower concentrations of scopoletin substrate resulted in higher peak areas, representing scopoletin substrate inhibition at higher scopoletin concentrations. Therefore, at 50 μM of Scopoletin (blue), upon addition of 50 μM of farnesol the peak area was increased from 30 to 50 mAU. This indicates that farnesol actually had an enhancing effect of scopoletin glucoside formation. As the farnesol concentration was further increased to 100 μM

and 200 μM, the peak area was indeed decreased indicating an inhibitory effect, which is in accordance to **Figure 25 D** (100 μM of scopoletin and 100 μM of farnesol). As the scopoletin substrate concentration was increased to 100 μM (red) and 200 μM (green), farnesol's enhancement effect is not easily evaluated as the scopoletin substrate inhibition is favored and therefore, reducing the effects by approximately 80%. A study utilizing *Fv*UGT1 – a key enzyme for glycosylation of anthocyanidins in strawberry - were able to enhance glucosylation and alleviate pelargonidin substrate inhibition by the addition of calcium/calmodulin [90].

β-Carotene and apocarotenal have shown a significant increase in scopoletin glucoside production **[Figure 26 K and M]**. These intriguing findings have set the stage to further investigate the dependence of substrate concentration present and ultimately the effect of scopoletin substrate inhibition in this case. For both modifiers, they were able to significantly increase scopoletin glucoside production even at higher scopoletin substrate concentrations. The two substrates were able to drive scopoletin glucosylation forward and for the reaction dynamics to overcome substrate inhibition and favor glucoside production. For all scopoletin concentrations – 50 μM, 100 μM, and 200 μM – β-carotene and apocarotenal (concentrations 0 – 200 μM) have shown an enhancement effect on scopoletin glucoside production **[Figure 31 A and B]**. The chemical structures of both (apo)carotenoids are very similar **[Figure 23]** and both play a role as precursors of Vitamin A [132]. Therefore, their mutual enhancement effects on scopoletin glucosylation can be due to their structural similarity and allosteric affinity and competitiveness. These are very important findings as this indicates that certain substrates do exist where *in vitro* one can manipulate the behavior of an enzyme and drive it towards a desirable direction.

V. Conclusions and Outlook

Over the years, GTs along with their promiscuity and broad application spectrum have attracted immense attention in the pharmaceutical, agricultural, cosmeceutical, and nutraceutical industries. Moreover, research has tremendously progressed to attempt and uncover potential GTs along with natural plant secondary metabolites, which could potentially contribute to the discovery of novel applications. This research has allowed for the establishment of two robust and effective HTP methods – UDP Glo™ Activity assay and phosphate GT activity assay – which were tailored to suit the largest plant GT family. These two assays have been utilized in substrate screening, Michaelis-Menten kinetic analyses, substrate inhibition tests, as well as enhancement and inhibition of GT activities. This research has set the stage to further investigate novel GTs in a fast, robust, and cost-effective manner with the potential of uncovering new applications. Interestingly, these HTP methods were able to uncover inherent GT hydrolase activity, which was rarely studied before. As hundreds of GTs across various species and families exist, their inherent hydrolase activity (if at all exists) can be further studied and kinetically quantified. Moreover, initial aglycone screening can be performed along with LC-MS analysis in order to reveal natural plant substrates, which may not be chemically available. Finally, targeted and directed glycosylation (enhancement and inhibition) can be evaluated for other GTs and their behavior *in vitro* can be studied.

Bibliography

1. Morris, J.L., et al., *The timescale of early land plant evolution.* Proceedings of the National Academy of Sciences, 2018. **115**(10): p. E2274.
2. Wang, S., et al., *The Structure and Function of Major Plant Metabolite Modifications.* Molecular Plant, 2019. **12**(7): p. 899-919.
3. Díaz, J., *Information flow in plant signaling pathways.* Plant signaling & behavior, 2011. **6**(3): p. 339-343.
4. Sneppen, K., S. Krishna, and S. Semsey, *Simplified models of biological networks.* Annual Review of Biophysics, 2010. **39**: p. 43-59.
5. Mavituna, F., *Applications of Plant Biotechnology in Industry and Agriculture*, in *Recent Advances in Biotechnology*, F. Vardar-Sukan and Ş.S. Sukan, Editors. 1992, Springer Netherlands: Dordrecht. p. 209-226.
6. Zaynab, M., et al., *Role of secondary metabolites in plant defense against pathogens.* Microbial Pathogenesis, 2018. **124**: p. 198-202.
7. VanEtten, H.D., et al., *Two Classes of Plant Antibiotics: Phytoalexins versus "Phytoanticipins&quot.* The Plant Cell, 1994. **6**(9): p. 1191.
8. T., D., et al., *An Introductory Chapter: Secondary Metabolites, Secondary Metabolites - Sources and Applications*. 2018: IntechOpen.
9. Ni, Y., G. Zhang, and S. Kokot, *Simultaneous spectrophotometric determination of maltol, ethyl maltol, vanillin and ethyl vanillin in foods by multivariate calibration and artificial neural networks.* Food Chemistry, 2005. **89**(3): p. 465-473.
10. Jia, K.P., et al., *Strigolactone Biosynthesis and Signal Transduction*, in *Strigolactones - Biology and Applications*, H. Koltai and C. Prandi, Editors. 2019, Springer International Publishing: Cham. p. 1-45.
11. Wang, J.Y., P.Y. Lin, and S. Al-Babili, *On the biosynthesis and evolution of apocarotenoid plant growth regulators.* Seminars in Cell and Developmental Biology, 2020.

12. Felemban, A., et al., *Apocarotenoids Involved in Plant Development and Stress Response.* Frontiers in Plant Science, 2019. **10**: p. 1168-1168.
13. Verpoorte, R., *Secondary Metabolism*, in *Metabolic Engineering of Plant Secondary Metabolism*, R. Verpoorte and A.W. Alfermann, Editors. 2000, Springer Netherlands: Dordrecht. p. 1-29.
14. Ncube, B. and J. Van Staden, *Tilting Plant Metabolism for Improved Metabolite Biosynthesis and Enhanced Human Benefit.* Molecules (Basel, Switzerland), 2015. **20**(7): p. 12698-12731.
15. Liang, D.M., et al., *Glycosyltransferases: mechanisms and applications in natural product development.* Chemical Society Reviews, 2015. **44**(22): p. 8350-74.
16. Lim, E.K., *Plant glycosyltransferases: their potential as novel biocatalysts.* Chemistry, 2005. **11**(19): p. 5486-94.
17. Li, Y., et al., *High-throughput assays of leloir-glycosyltransferase reactions: The applications of rYND1 in glycotechnology.* Journal of Biotechnology, 2016. **227**: p. 10-18.
18. Campbell, J.A., et al., *A classification of nucleotide-diphospho-sugar glycosyltransferases based on amino acid sequence similarities.* Journal of Biological Chemistry, 1997. **326 (Pt 3)**(Pt 3): p. 929-39.
19. Coutinho, P.M., et al., *An evolving hierarchical family classification for glycosyltransferases.* Journal of Molecular Biology, 2003. **328**(2): p. 307-17.
20. Lombard, V., et al., *The carbohydrate-active enzymes database (CAZy) in 2013.* Nucleic Acids Research, 2014. **42**(Database issue): p. D490-5.
21. Ekstrom, A., et al., *PlantCAZyme: a database for plant carbohydrate-active enzymes.* Database (Oxford), 2014. **2014**.
22. Mackenzie, P.I., et al., *Identification of UDP glycosyltransferase 3A1 as a UDP N-acetylglucosaminyltransferase.* The Journal of biological chemistry, 2008. **283**(52): p. 36205-36210.

23. Han, S.H., et al., *Synthesis of flavonoid O-pentosides by Escherichia coli through engineering of nucleotide sugar pathways and glycosyltransferase.* Applied and Environmental Microbiology, 2014. **80**(9): p. 2754-2762.
24. Shibuya, M., et al., *Identification and characterization of glycosyltransferases involved in the biosynthesis of soyasaponin I in Glycine max.* FEBS Letters, 2010. **584**(11): p. 2258-64.
25. Montefiori, M., et al., *Identification and characterisation of F3GT1 and F3GGT1, two glycosyltransferases responsible for anthocyanin biosynthesis in red-fleshed kiwifruit (Actinidia chinensis).* Plant Journal, 2011. **65**(1): p. 106-118.
26. Singh, S., G.N. Phillips, Jr., and J.S. Thorson, *The structural biology of enzymes involved in natural product glycosylation.* Natural Product Reports, 2012. **29**(10): p. 1201-37.
27. Kikuchi, N., et al., *Comparison of glycosyltransferase families using the profile hidden Markov model.* Biochemical and Biophysical Research Communications, 2003. **310**(2): p. 574-9.
28. Yonekura-Sakakibara, K. and K. Hanada, *An evolutionary view of functional diversity in family 1 glycosyltransferases.* Plant Journal, 2011. **66**(1): p. 182-93.
29. Härtl, K., et al., *Tailoring Natural Products with Glycosyltransferases*, in *Biotechnology of Natural Products*, W. Schwab, B.M. Lange, and M. Wüst, Editors. 2018, Springer International Publishing: Cham. p. 219-263.
30. Busch, C., et al., *A common motif of eukaryotic glycosyltransferases is essential for the enzyme activity of large clostridial cytotoxins.* Journal of Biological Chemistry, 1998. **273**(31): p. 19566-72.
31. Charnock, S.J. and G.J. Davies, *Structure of the nucleotide-diphospho-sugar transferase, SpsA from Bacillus subtilis, in native and nucleotide-complexed forms.* Biochemistry, 1999. **38**(20): p. 6380-5.
32. Vrielink, A., et al., *Crystal structure of the DNA modifying enzyme beta-glucosyltransferase in the presence and absence of the substrate uridine diphosphoglucose.* Embo Journal, 1994. **13**(15): p. 3413-22.

33. Moréra, S., et al., *High resolution crystal structures of T4 phage beta-glucosyltransferase: induced fit and effect of substrate and metal binding.* Journal of Molecular Biology, 2001. **311**(3): p. 569-77.
34. Lovering, A.L., et al., *Structural Insight into the Transglycosylation Step of Bacterial Cell-Wall Biosynthesis.* Science, 2007. **315**(5817): p. 1402.
35. Yuan, Y., et al., *Crystal structure of a peptidoglycan glycosyltransferase suggests a model for processive glycan chain synthesis.* Proceedings of the National Academy of Sciences of the United States of America, 2007. **104**(13): p. 5348-53.
36. Igura, M., et al., *Structure-guided identification of a new catalytic motif of oligosaccharyltransferase.* Embo Journal, 2008. **27**(1): p. 234-43.
37. Zhang, H., et al., *The highly conserved domain of unknown function 1792 has a distinct glycosyltransferase fold.* Nature Communications, 2014. **5**(1): p. 4339.
38. Lairson, L.L., et al., *Glycosyltransferases: structures, functions, and mechanisms.* Annual Review of Biochemistry, 2008. **77**: p. 521-55.
39. Brazier-Hicks, M., et al., *Characterization and engineering of the bifunctional N- and O-glucosyltransferase involved in xenobiotic metabolism in plants.* Proceedings of the National Academy of Sciences of the United States of America, 2007. **104**(51): p. 20238-43.
40. Modolo, L.V., et al., *Crystal structures of glycosyltransferase UGT78G1 reveal the molecular basis for glycosylation and deglycosylation of (iso)flavonoids.* Journal of Molecular Biology, 2009. **392**(5): p. 1292-302.
41. Offen, W., et al., *Structure of a flavonoid glucosyltransferase reveals the basis for plant natural product modification.* Embo Journal, 2006. **25**(6): p. 1396-405.
42. Bowles, D., et al., *Glycosyltransferases of lipophilic small molecules.* Annual Review of Plant Biology, 2006. **57**: p. 567-97.
43. Mackenzie, P.I., et al., *The UDP glycosyltransferase gene superfamily: recommended nomenclature update based on evolutionary divergence.* Pharmacogenetics, 1997. **7**(4): p. 255-69.

44. Gachon, C.M., M. Langlois-Meurinne, and P. Saindrenan, *Plant secondary metabolism glycosyltransferases: the emerging functional analysis.* Trends Plant Science, 2005. **10**(11): p. 542-9.

45. Paquette, S.M., K. Jensen, and S. Bak, *A web-based resource for the Arabidopsis P450, cytochromes b5, NADPH-cytochrome P450 reductases, and family 1 glycosyltransferases (http://www.P450.kvl.dk).* Phytochemistry, 2009. **70**(17-18): p. 1940-7.

46. Hans, J., W. Brandt, and T. Vogt, *Site-directed mutagenesis and protein 3D-homology modelling suggest a catalytic mechanism for UDP-glucose-dependent betanidin 5-O-glucosyltransferase from Dorotheanthus bellidiformis.* Plant Journal, 2004. **39**(3): p. 319-33.

47. Kubo, A., et al., *Alteration of sugar donor specificities of plant glycosyltransferases by a single point mutation.* Archives of Biochemistry and Biophysics, 2004. **429**(2): p. 198-203.

48. Osmani, S.A., S. Bak, and B.L. Møller, *Substrate specificity of plant UDP-dependent glycosyltransferases predicted from crystal structures and homology modeling.* Phytochemistry, 2009. **70**(3): p. 325-347.

49. Bowles, D., et al., *Glycosyltransferases: managers of small molecules.* Current Opinion in Plant Biology, 2005. **8**(3): p. 254-263.

50. Thorson, J.S., et al., *Natures Carbohydrate Chemists The Enzymatic Glycosylation of Bioactive Bacterial Metabolites.* Current Organic Chemistry, 2001. **5**(2): p. 139-167.

51. Palcic, M.M. and K. Sujino, *Assays for Glycosyltransferases.* Trends in Glycoscience and Glycotechnology, 2001. **13**: p. 361-370.

52. Deng, C. and R.R. Chen, *A pH-sensitive assay for galactosyltransferase.* Analytical Biochemistry, 2004. **330**(2): p. 219-26.

53. Khraltsova, L.S., et al., *An enzyme-linked lectin assay for alpha1,3-galactosyltransferase.* Analytical Biochemistry, 2000. **280**(2): p. 250-7.

54. Snow, D.M., et al., *Determination of beta1,4-galactosyltransferase enzymatic activity by capillary electrophoresis and laser-induced fluorescence detection.* Analytical Biochemistry, 1999. **271**(1): p. 36-42.

55. Jobron, L., et al., *Glycosyltransferase assays utilizing N-acetyllactosamine acceptor immobilized on a cellulose membrane.* Analytical Biochemistry, 2003. **323**(1): p. 1-6.

56. Abdul-Rahman, B., et al., *Beta-(1 --> 4)-galactosyltransferase activity in native and engineered insect cells measured with time-resolved europium fluorescence.* Carbohydrate Research, 2002. **337**(21-23): p. 2181-6.

57. Williams, G.J., R.W. Gantt, and J.S. Thorson, *The impact of enzyme engineering upon natural product glycodiversification.* Current Opinion in Chemical Biology, 2008. **12**(5): p. 556-64.

58. Lee, H.S. and J.S. Thorson, *Development of a universal glycosyltransferase assay amenable to high-throughput formats.* Analytical Biochemistry, 2011. **418**(1): p. 85-88.

59. Deng, C. and R.R. Chen, *A pH-sensitive assay for galactosyltransferase.* Analytical Biochemistry, 2004. **330**(2): p. 219-226.

60. Chapman, E. and C.-H. Wong, *A pH sensitive colorometric assay for the high-Throughput screening of enzyme inhibitors and substrates: A case study using kinases.* Bioorganic & Medicinal Chemistry, 2002. **10**(3): p. 551-555.

61. Morís-Varas, F., et al., *Visualization of enzyme-catalyzed reactions using pH indicators: rapid screening of hydrolase libraries and estimation of the enantioselectivity.* Bioorganic & Medicinal Chemistry, 1999. **7**(10): p. 2183-2188.

62. Yao, Y., et al., *Assay for enzyme activity by following the absorbance change of pH-indicators.* Journal of Biochemical and Biophysical Methods, 1998. **36**(2): p. 119-130.

63. Härtl, K., et al., *Glucosylation of Smoke-Derived Volatiles in Grapevine (Vitis vinifera) is Catalyzed by a Promiscuous Resveratrol/Guaiacol Glucosyltransferase.* Journal of Agricultural and Food Chemistry, 2017. **65**(28): p. 5681-5689.

64. McGraphery, K. and W. Schwab, *Comparative Analysis of High-Throughput Assays of Family-1 Plant Glycosyltransferases.* International Journal of Molecular Sciences, 2020. **21**(6).

65. Hicham Zegzouti, L.E., Jacquelyn Hennek, Juliano Alves, Gediminas Vidugiris, and Said Goueli, *Homogeneous Detection of Glycosyltransferase Activities with Universal Bioluminescent Assays*. 2016.

66. Deng, C. and R.R. Chen, *A pH-sensitive assay for galactosyltransferase.* Analytical Biochemistry, 2004. **330**(2): p. 219-226.

67. Persson, M. and M.M. Palcic, *A high-throughput pH indicator assay for screening glycosyltransferase saturation mutagenesis libraries.* Analytical Biochemistry, 2008. **378**(1): p. 1-7.

68. Sheikh, M.O., et al., *Rapid screening of sugar-nucleotide donor specificities of putative glycosyltransferases.* Glycobiology, 2017. **27**(3): p. 206-212.

69. Zegzouti, H., et al. *Homogeneous Detection of Glycosyltransferase Activities with Universal Bioluminescent Assays*. 2016 [cited 2019; Available from: https://www.promega.de/resources/scientific_posters/posters/homogeneous-detection-of-glycosyltransferase-activities-with-universal-bioluminescent-assays-poster/.

70. Das, D., P. Kuzmic, and B. Imperiali, *Analysis of a dual domain phosphoglycosyl transferase reveals a ping-pong mechanism with a covalent enzyme intermediate.* Proceedings of the National Academy of Sciences, 2017. **114**(27): p. 7019-7024.

71. Meng, L., et al., *Enzymatic basis for N-glycan sialylation: structure of rat alpha2,6-sialyltransferase (ST6GAL1) reveals conserved and unique features for glycan sialylation.* Journal of Biological Chemistry, 2013. **288**(48): p. 34680-98.

72. Urbanowicz, B.R., et al., *Two Arabidopsis proteins synthesize acetylated xylan in vitro.* Plant Journal, 2014. **80**(2): p. 197-206.

73. Urbanowicz, B.R., et al., *Structural, mutagenic and in silico studies of xyloglucan fucosylation in Arabidopsis thaliana suggest a water-mediated mechanism.* Plant Journal, 2017. **91**(6): p. 931-949.

74. Wu, Z.L., et al., *Universal phosphatase-coupled glycosyltransferase assay.* Glycobiology, 2011. **21**(6): p. 727-733.
75. Zielinski, T., et al., *Development and Validation of a Universal High-Throughput UDP-Glycosyltransferase Assay with a Time-Resolved FRET Signal.* Assay and Drug Development Technology, 2016. **14**(4): p. 240-51.
76. Wu, Z.L., et al., *Universal phosphatase-coupled glycosyltransferase assay.* Glycobiology, 2011. **21**(6): p. 727-733.
77. Bubner, P., et al., *Comparison of broad-scope assays of nucleotide sugar-dependent glycosyltransferases.* Analytical Biochemistry, 2015. **490**: p. 46-51.
78. Robinson, P.K., *Enzymes: principles and biotechnological applications.* Essays in Biochemistry, 2015. **59**: p. 1-41.
79. Michaelis, L., et al., *The original Michaelis constant: translation of the 1913 Michaelis-Menten paper.* Biochemistry, 2011. **50**(39): p. 8264-9.
80. Johnson, K.A. and R.S. Goody, *The Original Michaelis Constant: Translation of the 1913 Michaelis–Menten Paper.* Biochemistry, 2011. **50**(39): p. 8264-8269.
81. Einav, T., L. Mazutis, and R. Phillips, *.Statistical Mechanics of Allosteric Enzymes.* The Journal of Physical Chemistry, 2016. **120**(26): p. 6021-6037.
82. Kühl, P.W., *Excess-substrate inhibition in enzymology and high-dose inhibition in pharmacology: a reinterpretation [corrected].* Biochemical Journal, 1994. **298 (Pt 1)**(Pt 1): p. 171-80.
83. Hutzler, J.M. and T.S. Tracy, *Atypical kinetic profiles in drug metabolism reactions.* Drug Metabolism and Disposition, 2002. **30**(4): p. 355-62.
84. Korzekwa, K.R., et al., *Evaluation of atypical cytochrome P450 kinetics with two-substrate models: evidence that multiple substrates can simultaneously bind to cytochrome P450 active sites.* Biochemistry, 1998. **37**(12): p. 4137-47.
85. Wiebel, F.J., et al., *Aryl hydrocarbon (benzo[a]pyrene) hydroxylase in microsomes from rat tissues: Differential inhibition and stimulation by benzoflavones and organic solvents.* Archives of Biochemistry and Biophysics, 1971. **144**(1): p. 78-86.

86. Uchaipichat, V., et al., *Kinetic modeling of the interactions between 4-methylumbelliferone, 1-naphthol, and zidovudine glucuronidation by udp-glucuronosyltransferase 2B7 (UGT2B7) provides evidence for multiple substrate binding and effector sites.* Molecular Pharmacology, 2008. **74**(4): p. 1152-62.

87. Reed, M.C., A. Lieb, and H.F. Nijhout, *The biological significance of substrate inhibition: a mechanism with diverse functions.* Bioessays, 2010. **32**(5): p. 422-9.

88. Zhou, J., T.S. Tracy, and R.P. Remmel, *Glucuronidation of dihydrotestosterone and trans-androsterone by recombinant UDP-glucuronosyltransferase (UGT) 1A4: evidence for multiple UGT1A4 aglycone binding sites.* Drug metabolism and disposition: the biological fate of chemicals, 2010. **38**(3): p. 431-440.

89. Kaiser, P.M., *Substrate inhibition as a problem of non-linear steady state kinetics with monomeric enzymes.* Journal of Molecular Catalysis, 1980. **8**(4): p. 431-442.

90. Peng, H., et al., *Calcium/calmodulin alleviates substrate inhibition in a strawberry UDP-glucosyltransferase involved in fruit anthocyanin biosynthesis.* BMC Plant Biology, 2016. **16**(1): p. 197.

91. Winkel-Shirley, B., *Flavonoid Biosynthesis. A Colorful Model for Genetics, Biochemistry, Cell Biology, and Biotechnology.* Plant Physiology, 2001. **126**(2): p. 485.

92. Berli, F.J., et al., *Abscisic acid is involved in the response of grape (Vitis vinifera L.) cv. Malbec leaf tissues to ultraviolet-B radiation by enhancing ultraviolet-absorbing compounds, antioxidant enzymes and membrane sterols.* Plant Cell & Environment, 2010. **33**(1): p. 1-10.

93. Li, J., et al., *Arabidopsis Flavonoid Mutants Are Hypersensitive to UV-B Irradiation.* The Plant cell, 1993. **5**(2): p. 171-179.

94. Mohanta, T.K., et al., *Ginkgo biloba responds to herbivory by activating early signaling and direct defenses.* PLoS One, 2012. **7**(3): p. e32822.

95. He, J. and M.M. Giusti, *Anthocyanins: natural colorants with health-promoting properties.* Annual review of food science and technology, 2010. **1**: p. 163-187.

96. Modolo, L.V., et al., *A functional genomics approach to (iso)flavonoid glycosylation in the model legume Medicago truncatula.* Plant Molecular Biology, 2007. **64**(5): p. 499-518.

97. Kovinich, N., et al., *Functional characterization of a UDP-glucose:flavonoid 3-O-glucosyltransferase from the seed coat of black soybean (Glycine max (L.) Merr.).* Phytochemistry, 2010. **71**(11-12): p. 1253-63.

98. Wu, B., *Substrate inhibition kinetics in drug metabolism reactions.* Drug Metabolism Reviews, 2011. **43**(4): p. 440-56.

99. Yokota, H., et al., *Inhibitory effects of uridine diphosphate on UDP-glucuronosyltransferase.* Life Sciences, 1998. **63**(19): p. 1693-9.

100. Luukkanen, L., et al., *Kinetic characterization of the 1A subfamily of recombinant human UDP-glucuronosyltransferases.* Drug Metabolism and Disposition, 2005. **33**(7): p. 1017-26.

101. Houston, J.B. and K.E. Kenworthy, *In vitro-in vivo scaling of CYP kinetic data not consistent with the classical Michaelis-Menten model.* Drug Metabolism and Disposition, 2000. **28**(3): p. 246-54.

102. Rios, G.R. and T.R. Tephly, *Inhibition and active sites of UDP-glucuronosyltransferases 2B7 and 1A1.* Drug Metabolism and Disposition, 2002. **30**(12): p. 1364-7.

103. Ramakrishnan, B. and P.K. Qasba, *Structure-based design of beta 1,4-galactosyltransferase I (beta 4Gal-T1) with equally efficient N-acetylgalactosaminyltransferase activity: point mutation broadens beta 4Gal-T1 donor specificity.* Journal of Biological Chemistry, 2002. **277**(23): p. 20833-9.

104. Leemhuis, H. and L. Dijkhuizen, *Engineering of Hydrolysis Reaction Specificity in the Transglycosylase Cyclodextrin Glycosyltransferase.* Biocatalysis and Biotransformation, 2003. **21**(4-5): p. 261-270.

105. Sindhuwinata, N., et al., *Binding of an acceptor substrate analog enhances the enzymatic activity of human blood group B galactosyltransferase.* Glycobiology, 2010. **20**(6): p. 718-23.

106. Brockhausen, I., *Crossroads between Bacterial and Mammalian Glycosyltransferases.* Frontiers in Immunology, 2014. **5**: p. 492.

107. Chavaroche, A.A., et al., *Analysis of the polymerization initiation and activity of Pasteurella multocida heparosan synthase PmHS2, an enzyme with glycosyltransferase and UDP-sugar hydrolase activity.* Journal of Biological Chemistry, 2011. **286**(3): p. 1777-85.

108. Just, I., et al., *The enterotoxin from Clostridium difficile (ToxA) monoglucosylates the Rho proteins.* Journal of Biological Chemistry, 1995. **270**(23): p. 13932-6.

109. Ciesla, W.P., Jr. and D.A. Bobak, *Clostridium difficile toxins A and B are cation-dependent UDP-glucose hydrolases with differing catalytic activities.* Journal of Biological Chemistry, 1998. **273**(26): p. 16021-6.

110. D'Urzo, N., et al., *The structure of Clostridium difficile toxin A glucosyltransferase domain bound to Mn2+ and UDP provides insights into glucosyltransferase activity and product release.* The FEBS Journal, 2012. **279**(17): p. 3085-97.

111. Liang, D.-M., et al., *Glycosyltransferases: mechanisms and applications in natural product development.* Chemical Society Reviews, 2015. **44**(22): p. 8350-8374.

112. Williams, G.J. and J.S. Thorson, *Natural Product Glycosyltransferases: Properties and Applications*, in *Advances in Enzymology and Related Areas of Molecular Biology*. 2009, John Wiley & Sons, Inc. p. 55-119.

113. Schwab, W., et al., *Potential applications of glucosyltransferases in terpene glucoside production: impacts on the use of aroma and fragrance.* Applied Microbiology and Biotechnology, 2015. **99**(1): p. 165-174.

114. Ring, L., et al., *Metabolic Interaction between Anthocyanin and Lignin Biosynthesis Is Associated with Peroxidase FaPRX27 in Strawberry Fruit.* Plant Physiology, 2013. **163**(1): p. 43.

115. Breton, C., et al., *Structures and mechanisms of glycosyltransferases.* Glycobiology, 2005. **16**(2): p. 29R-37R.

116. Zhang, J.H., T.D. Chung, and K.R. Oldenburg, *A Simple Statistical Parameter for Use in Evaluation and Validation of High Throughput Screening Assays.* Journal of Biomolecular Screening, 1999. **4**(2): p. 67-73.

117. Sun, G., et al., *Glucosylation of the phytoalexin N-feruloyl tyramine modulates the levels of pathogen-responsive metabolites in Nicotiana benthamiana.* The Plant Journal, 2019. 1**00**(1): p. 20-37.

118. Camacho-Ruiz, M.d.L.A., et al., *A broad pH range indicator-based spectrophotometric assay for true lipases using tributyrin and tricaprylin.* Journal of lipid research, 2015. **56**(5): p. 1057-1067.

119. Simeonov, A., et al., *Fluorescence Spectroscopic Profiling of Compound Libraries.* Journal of Medicinal Chemistry, 2008. **51**(8): p. 2363-2371.

120. Palmier, M.O. and S.R. Van Doren, *Rapid determination of enzyme kinetics from fluorescence: overcoming the inner filter effect.* Analytical Biochemistry, 2007. **371**(1): p. 43-51.

121. Acker, M.G. and D.S. Auld, *Considerations for the design and reporting of enzyme assays in high-throughput screening applications.* Perspectives in Science, 2014. **1**(1): p. 56-73.

122. Maier-Salamon, A., et al., *Hepatic glucuronidation of resveratrol: interspecies comparison of enzyme kinetic profiles in human, mouse, rat, and dog.* Drug Metabolism Pharmacokinetics, 2011. **26**(4): p. 364-73.

123. Lim, E.K., et al., *Evolution of substrate recognition across a multigene family of glycosyltransferases in Arabidopsis.* Glycobiology, 2003. **13**(3): p. 139-45.

124. Lim, E.K., et al., *Arabidopsis glycosyltransferases as biocatalysts in fermentation for regioselective synthesis of diverse quercetin glucosides.* Biotechnology and Bioengineering, 2004. **87**(5): p. 623-31.

125. Lim, E.K. and D.J. Bowles, *A class of plant glycosyltransferases involved in cellular homeostasis.* Embo Journal, 2004. **23**(15): p. 2915-22.

126. Day, A.J., et al., *Conjugation position of quercetin glucuronides and effect on biological activity.* Free Radical Biology and Medicine, 2000. **29**(12): p. 1234-43.

127. Ono, E., et al., *Functional Differentiation of the Glycosyltransferases That Contribute to the Chemical Diversity of Bioactive Flavonol Glycosides in Grapevines (Vitis vinifera).* The Plant Cell, 2010. **22**(8): p. 2856.

128. Hallifax, D., et al., *Prediction of metabolic clearance using cryopreserved human hepatocytes: kinetic characteristics for five benzodiazepines.* Drug Metabolism and Disposition, 2005. **33**(12): p. 1852-8.

129. Sun, H., et al., *A catenary model to study transport and conjugation of baicalein, a bioactive flavonoid, in the Caco-2 cell monolayer: demonstration of substrate inhibition.* Journal of Pharmacology and Experimental Therapeutics, 2008. **326**(1): p. 117-26.

130. Chang, H.J., et al., *Identifying Androsterone (ADT) as a Cognate Substrate for Human Dehydroepiandrosterone Sulfotransferase (DHEA-ST) Important for Steroid Homeostasis: Structure of the Enzyme-ADT Complex.* Journal of Biological Chemistry, 2004. **279**(4): p. 2689-2696.

131. Tang, L., et al., *Structure and concentration changes affect characterization of UGT isoform-specific metabolism of isoflavones.* Molecular Pharmaceutics, 2009. **6**(5): p. 1466-82.

132. Melendez-Martinez, J.A., *An Overview of Carotenoids, Apocarotenoids, and Vitamin A in Agro-Food, Nutrition, Health, and Disease.* Molecular Nutrition & Food Research, 2020. **64**(12): p. 2070024.

Peer-reviewed Publications of the Author

McGraphery, K., Schwab, W. (**2020**). Comparative analysis of high-throughput assays of family-1 plant glycosyltransferases. *International Journal of Molecular Sciences*, 21(6), 2208.

Egorova, O., Lau, H.H.C., **McGraphery, K.**, Sheng, Y. (**2020**). Mdm2 and Mdmx RING domains play distinct roles in the regulation of p53 responses: A comparative study of Mdm2 and Mdmx RING domains in U2OS cells. *International Journal of Molecular Sciences*, 21(4), 1309.

Sun, G., Strebl, M., Merz, M., Blamberg, R., Huang, F.-C., **McGraphery, K.**, Hoffmann, T., Schwab, W. (**2019**). Glucosylation of the phytoalexin N-feruloyl tyramine modulates the levels of pathogen-responsive metabolites in *Nicotiana benthamiana*. *Plant Journal,* 100(1), pp. 20–37.

Song, C., Härtl, K., **McGraphery, K.**, Hoffmann, T., Schwab, W. (**2018**). Attractive but Toxic: Emerging Roles of Glycosidically Bound Volatiles and Glycosyltransferases Involved in Their Formation. *Molecular Plant*, 11(10), pp. 1225–1236.

Härtl, K., **McGraphery, K**., Rüdiger, J., Schwab, W. (**2018**) Tailoring Natural Products with Glycosyltransferases. In: Schwab W., Lange B., Wüst M. (eds) *Biotechnology of Natural Products*. Springer, Cham. DOI: https://doi.org/10.1007/978-3-319-67903-7_9

Scientific Presentations & Posters of the Author

McGraphery, K, Schwab, W.
Poster: Comparative and Functional Analysis of Various High Throughput Glycosyltransferase Assays.
Plant Natural Products Workshop 01.10.2018 – 03.10.2018 in Burg Warberg in collaboration with Technical University of Braunschweig

McGraphery, K, Schwab, W.
Presentation: Comparative and Functional Analysis of Various High Throughput Glycosyltransferase Assays.
Plant Natural Products Workshop 01.10.2018 – 03.10.2018 in Burg Warberg in collaboration with Technical University of Braunschweig

McGraphery, K, Schwab, W.
Presentation: Functional Analysis of Small Molecule Glycosyltransferases from Plants.
Forschungsseminar der Lebensmittelchemie at TUM on 26.06.2017

McGraphery, K, Schwab, W.
Poster: Functional Analysis of Small Molecule Glycosyltransferases from Plants.
Kick-off Seminar at TUM on 05.10.2016 – 07.10.2016

"Science knows no country, because knowledge belongs to humanity, and is the torch which illuminates the world…" – Louis Pasteur

"The important thing is to never stop questioning…" – Albert Einstein

"Nothing in life is to be feared, it is only to be understood. Now is the time to understand more, so that we may fear less..." – Marie Curie